NTIA Report 00-371

Radio Link Performance Prediction via Software Simulation

E.A. Quincy, R.J. Achatz
M.G. Cotton
M.P. Roadifer
J.M. Ratzloff

U.S. DEPARTMENT OF COMMERCE
William M. Daley, Secretary

Bernadette McGuire-Rivera,
Acting Deputy Assistant Secretary
for Communications and Information

October 1999

CONTENTS

RADIO LINK PERFORMANCE PREDICTION VIA SOFTWARE SIMULATION

Edmund A. Quincy[1], Robert J. Achatz[1],
Michael G. Cotton[1], Michael P. Roadifer[2], and Jeanne M. Ratzloff[1]

The subjective quality of speech and image information, transmitted over a high frequency radio link impaired with varying levels of interference, has been evaluated using software simulation. The high frequency radio link was also degraded by frequency-selective multipath and non-Gaussian noise. During radio link signal simulation an error sequence, determined from a comparison of transmitted and received bits, was collected. Next digitized speech and image information was distorted by the error sequence. Last, the quality of the distorted speech and image information was subjectively evaluated. This process was repeated for a large number of interference conditions. The same process can be used to show how multipath and non-Gaussian noise affects speech and image quality. Other wireless applications such as personal communications services and wireless local area networks can be analyzed in the same way using radio channel measurements and models made by the Institute for Telecommunication Sciences.

Keywords: Digital modulation, radio link, radio channel, multipath, non-Gaussian noise, interference, bit error, speech coding, image coding, speech quality, image quality, software simulation.

1. INTRODUCTION

Digitally modulated signals, carrying speech and image information, are often transmitted over radio links whose radio channels are degraded by non-Gaussian noise, time-varying multipath, and interference. These radio channels are found, for example, in applications as diverse as high frequency (HF) radio, land mobile radio (LMR), personal communications services (PCS), and wireless local area networks (WLAN's). In this study, a flexible and efficient two-step software simulation process is described that determines how radio channel impairments affect the quality of speech and image information. As an example, this process is used to evaluate the performance of several HF radio links subjected to varying levels of interference. This process may also be used to evaluate the performance of radio links subjected to varying levels of multipath and non-Gaussian noise.

---

[1]The authors are with the Institute for Telecommunication Sciences, National Telecommunications and Information Administration, U.S. Department of Commerce, Boulder, CO 80303.

[2]The author was with the Institute for Telecommunication Sciences when this work was done.

The Institute for Telecommunication Sciences (ITS) is interested in this type of performance prediction for two reasons. First, ITS has a long history of radio channel measurement and modeling achievement. Radio channel impulse response, noise, and interference measurements have been made at ITS at many frequencies, for many applications, for over 30 years. ITS is interested in using the results of these measurements to develop new signal processing and information coding techniques that use the spectrum more efficiently. Second, the number of radio link software simulation environments (RLSSE's) has increased dramatically. Incorporating the radio channel measurements into these packages is an ideal way for ITS to assist industry and government in designing and acquiring robust, radio products.

Software simulation is ideal for radio link performance prediction because it is repeatable and allows investigation of an isolated radio link parameter. In this study, software simulation is broken into two distinct steps as shown in Figure 1. In the first step, the transmission and reception of a digitally modulated *signal* over an *impaired radio channel* is simulated within the RLSSE. The output of the first step is the *bit error sequence* derived from a comparison between transmitted and received bits. In the second simulation step, the transmission and reception of information *bits* is simulated outside the RLSSE. Here, speech and image information in various *information formats* such as pulse code modulated (PCM) speech, compressed PCM speech, and PCM image is distorted. The distorted information is finally *played back* for *quality assessment*. A quality measure is then used to determine the effect an impaired radio channel parameter has on speech or image quality.

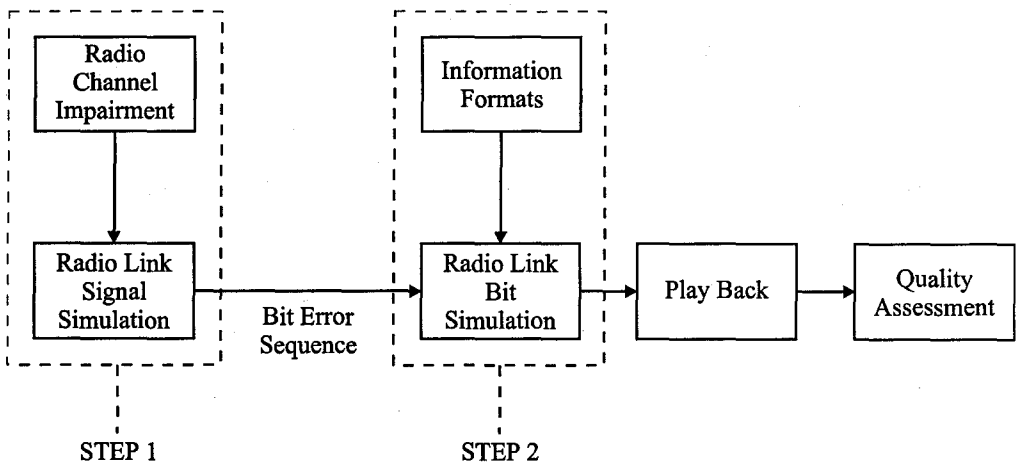

Figure 1. Radio link performance prediction.

Signal distortion during the first simulation step requires a large number of mathematical operations because there are many components (e.g. modulators, filters, detectors) and effects (e.g. multipath, interference, noise) that need to be included and because the signal is sampled at a high rate to minimize distortion. In contrast, information distortion during the second simulation step only requires a single operation executed one time per bit. There is no savings in computation time when the transmission of a single information format is simulated; however, computation time decreases dramatically as the number of information formats increases. The decrease in total computation time, when analyzing the effect of radio channel impairments on numerous information formats, is the primary motivation for breaking the simulation into two steps.

This report is divided into five sections. The first and last are introductory and conclusion sections respectively. The second section discusses radio link modeling. The third section describes the first step where signal distortion is simulated and error sequences are collected. The fourth section describes the second step where speech and image information distortion is simulated and the quality of the received information is evaluated.

2. RADIO LINK MODELING

Figure 2 shows a simplified block diagram of a typical radio link. The blocks of the radio link are broken into three main sections: transmitter, channel, and receiver. The source block (TX BITS) generates the transmitted bit sequence which is then mapped into a sequence of discrete symbol values (BIT-TO-SYM). The modulator (MOD) translates the discrete symbol values to a bandlimited signal which can be transmitted over the radio channel (CHAN). The radio channel adds noise and interference and introduces multipath. The demodulator (DEM) and detector (DET) extract the bandlimited symbols from the received signal. The bandlimited symbols are finally sampled (SMP), quantized (DEC), and converted (SYM-TO-BIT) to the received bit sequence.

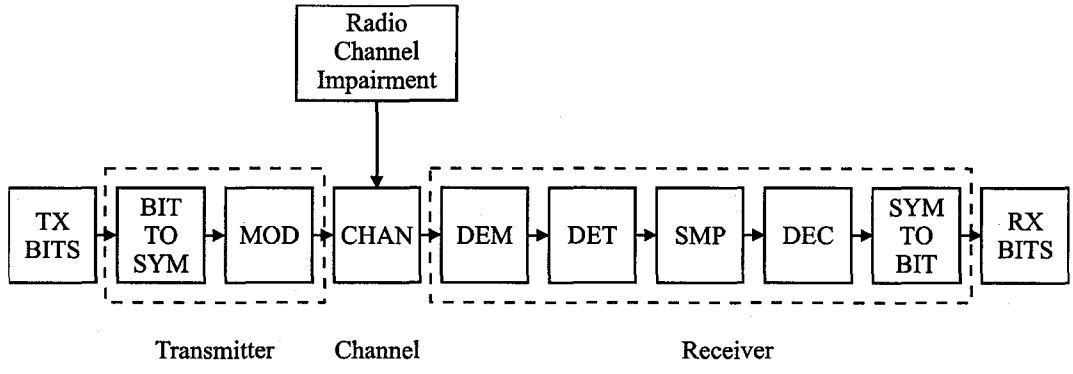

Figure 2. Radio link block diagram.

An HF radio link was simulated for this study. The HF radio channel is characterized by multipath and non-Gaussian noise. High frequency transmitters typically use frequency-shift keying (FSK) and differential phase-shift keying (DPSK) modulation to avoid requiring coherent detection in the receiver. The baud rate is typically low to avoid problems with frequency-selective multipath. Specialized HF radio links included in this study include a voice frequency carrier telegraphy (VFCT) link and a link with interleaving combined with block forward error correction (FEC). Voice frequency carrier telegraphy is a modulation method used in HF radio links to increase the baud rate by increasing the number of simultaneously modulated carrier frequencies. Interleaving combined with FEC can be used to mitigate burst errors introduced by time-varying multipath. Transmitter, channel, and receiver models used in the simulations of the HF radio link are discussed in this section.

2.1 Channel Model

Signals transmitted through the HF radio channel are distorted by multipath, non-Gaussian noise, and interference. The multipath is due to reflections off of ionospheric layers. The non-Gaussian noise is the result of atmospheric lightning and man-made electrical noise. The interference can be caused by intentional jamming or spurious emissions from adjacent bands.

Figure 3 shows a block diagram of the radio channel. The transmitter power amplifier is included in the channel since its main function is to provide gain to overcome channel attenuation. The transmitted signal is convolved with the multipath filter and added to the noise and interference signals.

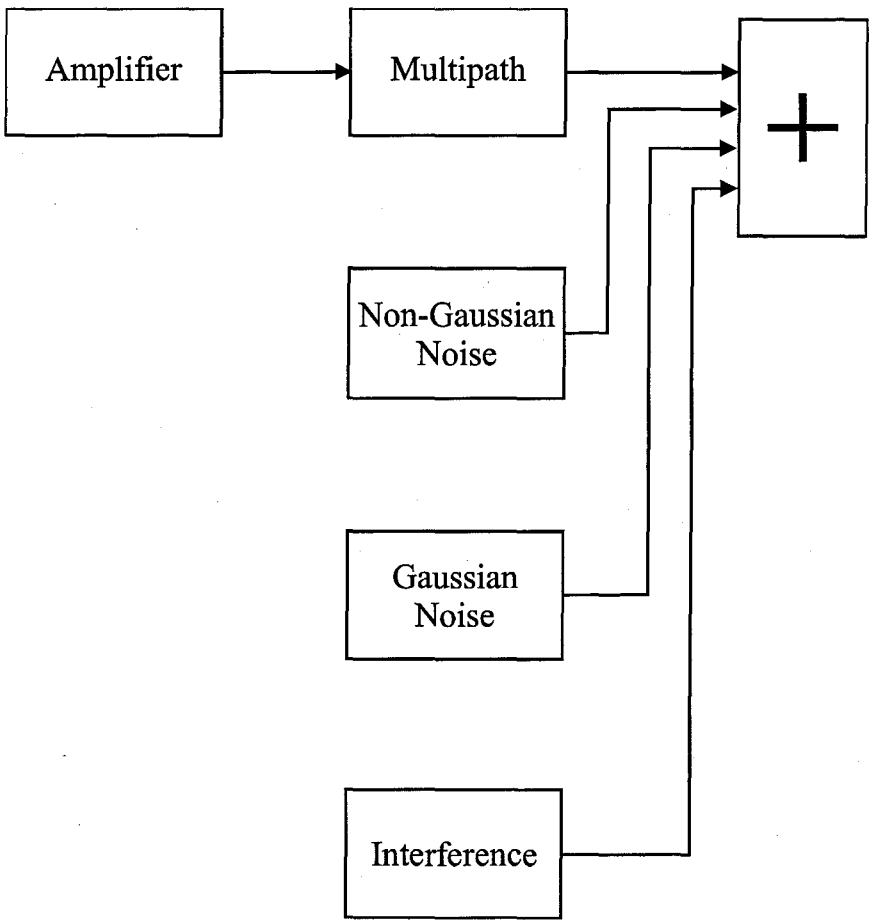

Figure 3. Channel model.

2.1.1 Multipath

The time-varying multipath channel is represented by

$$h(t,\tau) = \sum_{n=1}^{N} \beta_n(t)\,\delta(\tau - \tau_n) \qquad (1)$$

where N is the number of paths, $\beta_n(t)$ is the complex path gain, and τ is the path delay. Implementation of the multipath model is illustrated with the block diagram shown in Figure 4.

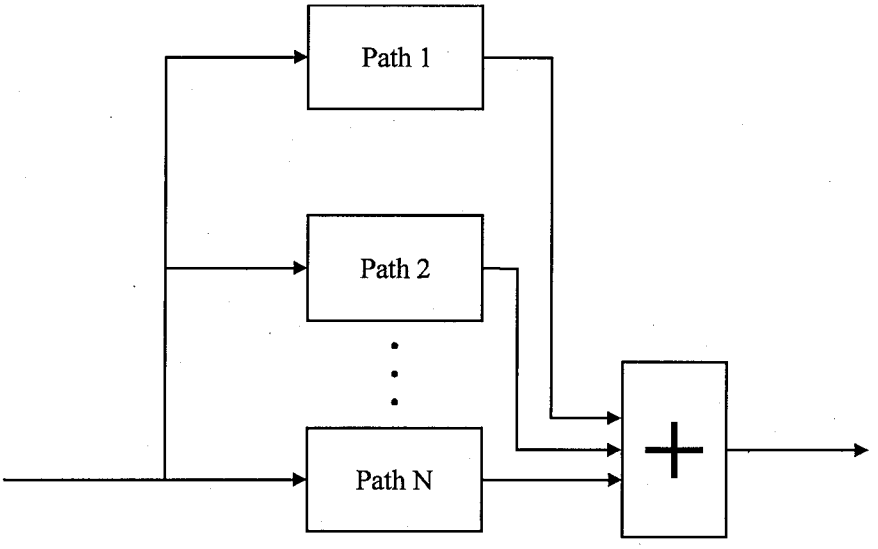

Figure 4. Multipath model.

Figure 5 shows how $\beta_n(t)$ values are generated in the RLSSE. White noise is first generated by a zero mean, unit variance, complex-Gaussian random number generator. This noise, which has Rayleigh distributed amplitudes and uniformly distributed phases, is then amplified and filtered with a 2-pole Butterworth low pass filter

$$\beta_n(t) = A\,b(t) * g(t) \qquad (2)$$

where $b(t)$ is the white noise signal, A is a power scaling factor, and $g(t)$ is the filter impulse response.

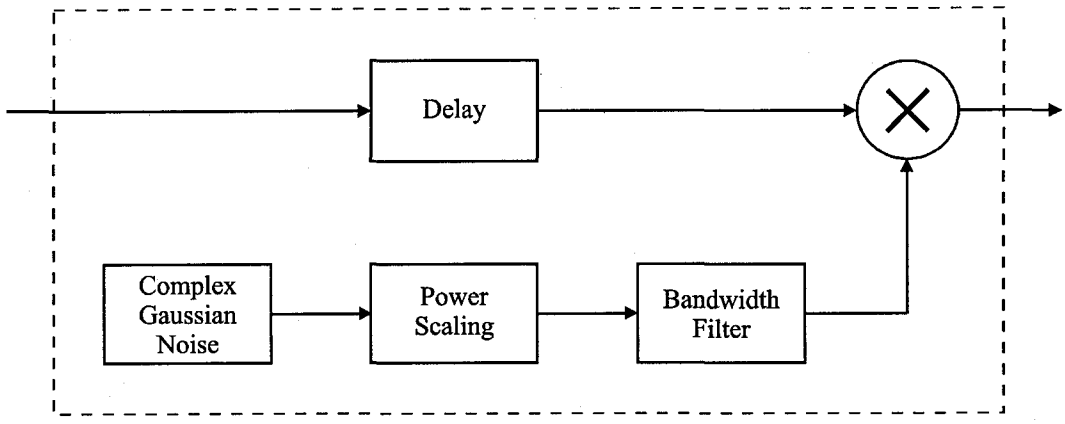

Figure 5. Path model.

The multipath model parameters used in this study are derived from HF radio channel measurements performed by ITS [1]. The measurements were made at 9 MHZ between Boulder, Colorado and Long Branch, Illinois. Three distinct paths were determined from the measurements. These paths correspond to a single hop off the ionospheric E layer (1E), a single hop off the ionospheric F2 layer (1F), and two hops off the F2 layer (2F). The E and F2 layers are 80 and 300 km above the earth surface respectively. The parameters for each path are depicted in Table 1.

Table 1. HF Multipath Parameters

Path	**Relative Delay (us)**	**Relative Power (dB)**	**Bandwidth (Hz)**
1E	40	-1.2	0.0272
1F	290	-7.2	0.144
2F	1140	-13.5	0.344

The relative path delay is the path time delay in excess of the direct (i.e. great circle) path time delay, the relative path power is the ratio of the average power in a single path to the average power in all paths, and the path bandwidth is the 3-dB bandwidth of the path power spectral density. Referring to Equation 1, τ corresponds to the path delay, the variance of $\beta_n(t)$ corresponds to path power, and the 3-dB bandwidth of $g(t)$ corresponds to the path bandwidth.

2.1.2 Gaussian Noise

The Gaussian noise, *n(t)*, is modeled as a signal whose amplitude is Rayleigh distributed

$$f(n) = \frac{2n}{n_0^2} e^{(-\frac{n}{n_0})^2} \quad (3)$$

where n_0^2 is the average Gaussian noise power equal to kT_0b where k is the Boltzman constant, T_0 is the temperature in K, and b is the noise equivalent bandwidth, and whose phase is uniformly distributed

$$f(\theta) = \frac{1}{2\pi} \quad (4)$$

where θ is the phase in radians.

2.1.3 Non-Gaussian Noise

The non-Gaussian noise is modeled as identically distributed and independent wideband pulses with random amplitudes, phases, and time intervals [2]. This type of non-Gaussian noise is often called impulsive noise. The pulse amplitude is described by the Power-Rayleigh distribution

$$f(r) = \frac{\alpha r^{\alpha-1}}{r_0^{\alpha}} e^{(-\frac{r}{r_0})^{\alpha}} \quad (5)$$

where r is the pulse amplitude, r_0 is a number that adjusts the average non-Gaussian noise power, and α controls the shape of the amplitude distribution. Setting α to 1.0 yields an exponential amplitude probability density function (PDF) whereas setting α to 2.0 yields a Rayleigh amplitude PDF. The phase of the pulse is uniformly distributed.

The time interval between pulses is determined by the Poisson distribution which describes the probability of k pulses occurring in t seconds

$$f_k(t) = \frac{e^{-\lambda t}}{k!}(\lambda t)^k \quad (6)$$

where λ is the average pulse rate. The corresponding probability of a single pulse occurring in a simulation time increment is

$$f_{k=1}(\Delta t) = \lambda \Delta t \quad (7)$$

where Δt represents the simulation time increment.

Non-Gaussian HF noise parameters are derived from HF noise measurements performed by ITS and published in CCIR Report 322 [3]. The measurements indicated that hourly median environmental noise power (on a winter day, between 8 and 12 a.m., in Illinois) at 9 MHZ was 30 dB above kT_0b. Second-order statistics describing the time interval between impulses were not measured. Parameters used in this study to simulate the non-Gaussian noise are shown in Table 2.

Table 2. HF Non-Gaussian Noise Parameters

Non-Gaussian noise power	30 dB above kT_0b
Power-Rayleigh distribution α	1.0
Poisson distribution λ	$1/\Delta t$ pulses/second

2.1.4 Interference

The interfering signal, unless otherwise noted, has the same modulation, baud rate, and symbol timing as the desired signal. The interfering signal data sequence is not correlated with the desired signal data sequence and the interfering signal is not distorted by the ionospheric radio channel.

2.2 Transmitter and Receiver Models

Simulated radio links include 2-, 4-, and 8-FSK, 2-, 4-, and 8-DPSK, 2-FSK with FEC and interleaving, and 6-tone, 2-FSK VFCT. Table 3 summarizes the radio links and their corresponding baud and effective bit rates. The baud rate, R, is the symbol transmission rate and the effective bit rate is the information transmission rate. Forward error correction decreases the effective bit rate in comparison to R by introducing parity bits. Four and eight-level modulations increase the effective bit rate in comparison to R by transmitting more than one bit per symbol. Voice frequency carrier telegraphy increases the effective bit rate in comparison to R by transmitting symbols on several carrier frequencies simultaneously.

Table 3. HF Radio Link Rates

HF Radio Link	R (symbols/second)	Effective Bit Rate (bits/second)
2-FSK	100	100
2-FSK with FEC	100	47
4-FSK	100	200
8-FSK	100	300
2-DPSK	100	100
4-DPSK	100	200
8-DPSK	100	300
2-FSK VFCT	100	600

2.2.1 Frequency-Shift Keying

Simulations of 2-, 4-, and 8-FSK were executed with a non-coherent, matched filter receiver. Frequency-shift keying is represented in complex baseband notation by

$$s(t) = A \sum_{m=0}^{\infty} p(t - mT) e^{j2\pi m_f (d(t) - (M-1)/2)t} \quad (8)$$

where A is the signal amplitude, $p(t)$ is the pulse shape, m_f is the frequency modulation coefficient, $d(t)$ is the pulse amplitude modulated (PAM) data sequence, and M is the alphabet size of 2, 4, or 8.

For FSK simulations in this study $p(t)$ is rectangular, m_f is 100 Hz/V, and $d(t)$ is defined by

$$d(t) = a_m \Pi(t - mT - T/2) \quad (9)$$

where a_m is the symbol value 0,1,...,M-1 and $\Pi(t)$ is the rectangular function that is 1 from -T/2 to T/2 and 0 otherwise.

2.2.2 Frequency-Shift Keying with Forward Error Correction and Interleaving

Simulations of 2-FSK were also conducted with FEC and interleaving. It has been demonstrated that a combination of Bose-Chaudhuri-Hocquenghem (BCH) FEC and interleaving is effective in mitigating the effects of time-varying HF radio link multipath [4]. A BCH (15,7) FEC capable of correcting 2 errors in each 15-bit codeword and a block interleaver with 32 rows and 15 columns is

used. In theory, this combination of FEC and interleaving could negate the effects of an isolated 64 symbol error burst.

At the transmitter the symbols are FEC coded and interleaved while at the receiver the symbols are deinterleaved and corrected. The interleaver reads the bits in row-by-row and reads them out column-by-column. The deinterleaver reverses this process, that is, the received bits are read into the deinterleaver column-by-column and read out row-by-row. The symbol rate is not increased to compensate for the 7/15 code rate. Consequently the effective bit rate is reduced to approximately 47 bits/second.

2.2.3 Differential Phase-Shift Keying

Simulations of 2-, 4-, and 8-DPSK were executed with a differentially-coherent, matched filter receiver. DPSK is represented in complex baseband notation as

$$s(t) = A \sum_{m=0}^{\infty} p(t - mT) e^{j m_p d(t)} \tag{10}$$

where m_p is the phase modulation constant. To differentially encode, the phase of the current symbol is added to the phase of the previous symbol. To differentially decode, the phase of the previous symbol is subtracted from the phase of the current symbol. For DPSK simulations in this study *p(t)* is rectangular and m_p is $2\pi/M$.

2.2.4 Voice-Frequency Carrier-Telegraphy

Voice-frequency carrier-telegraphy [5] is implemented with six, 2-FSK signals operating simultaneously at evenly spaced carrier frequencies (or tones). Each 2-FSK signal is operated at 100 baud; therefore the effective bit rate is 600 bits/second.

The spacing between the 2-FSK signals is 400 Hz. Four pole, Chebychev filters with a 400 Hz bandwidth and 1-dB passband ripple are used to reduce interference between adjacent 2-FSK signals. The interfering signal is provided by a broadband noise generator that transmits a complex impulse with unit amplitude and a phase that randomly flips between 0 and 180 degrees every simulation time increment.

3. EFFECT OF RADIO LINK ON BIT ERRORS

The first simulation step works at the signal level as shown in Figure 1. Components such as modulators, filters, and detectors and effects such as multipath, non-Gaussian noise, and interference are accounted for during signal simulation. Signal simulation is run once for each radio link and channel impairment condition. In this study, each interference level corresponds to a unique channel impairment condition.

Radio link signal simulation is performed with a commercial, off-the-shelf RLSSE. This tool allows the user to manipulate transmitter, channel, and receiver models using a graphical user interface. The RLSSE provides useful graphical information including in-phase and quadrature-phase (I/Q) constellation diagrams, spectrum magnitude plots, and signal eye diagrams. Figure 6 shows the computer screen of the RLSSE when 2-FSK performance is limited by interference. The interference is added after the block representing the HF radio channel (labeled "hfchan04"). The interference causes spectrum distortion and additional discrete eye diagram traces. Figure 7 shows the RLSSE screen when 2-FSK is limited by non-Gaussian noise. The noise severely distorts the spectrum and causes a confusion of eye-diagram traces.

In Figures 6 and 7, frequency is normalized by the symbol rate yielding units of cycles/symbol while time is normalized by symbol period yielding units of symbols. Conversion to SI units is possible by multiplying normalized frequency by symbol rate and multiplying normalized time by symbol period. Signal-to-noise ratio (SNR) represents the ratio of average signal power to average Gaussian noise power. Non-Gaussian noise power is not included in SNR. Signal-to-interference ratio (SIR) represents the ratio of the average desired signal power to average interfering signal power.

The bit error sequence is determined in the RLSSE by

$$e = d_t \oplus d_r \tag{11}$$

where $\oplus$ is the "exclusive or" logical operation, d_t represents the transmitted bits, and d_r represents the received bits. Figure 8 illustrates the radio link signal simulation process that generates the bit error sequences. The delay block represents the delay involved in transmitting, propagating, and receiving the transmitted bit sequence. Figure 9 shows how a bit error sequence is generated from transmitted and received bit streams. Correct bit detection results in a 0 while incorrect bit detection results in a 1.

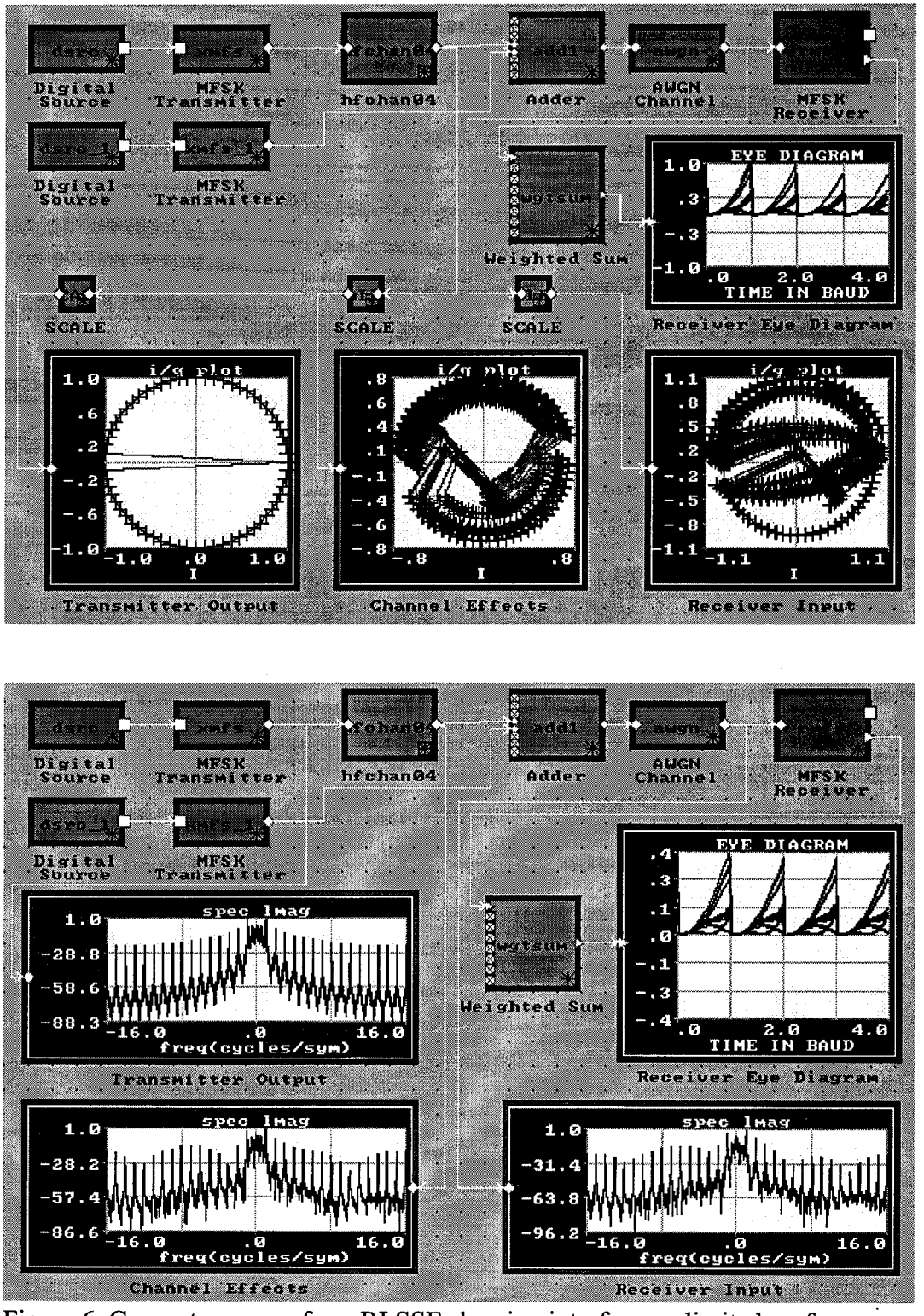

Figure 6. Computer screen from RLSSE showing interference limited performance for 2-FSK. Top figure shows eye diagram and I/Q plots while bottom screen shows eye diagram and spectrum magnitude (in dB) plots. Simulation parameters are SNR=80 dB, SIR=10 dB, and BER=6.5e-2.

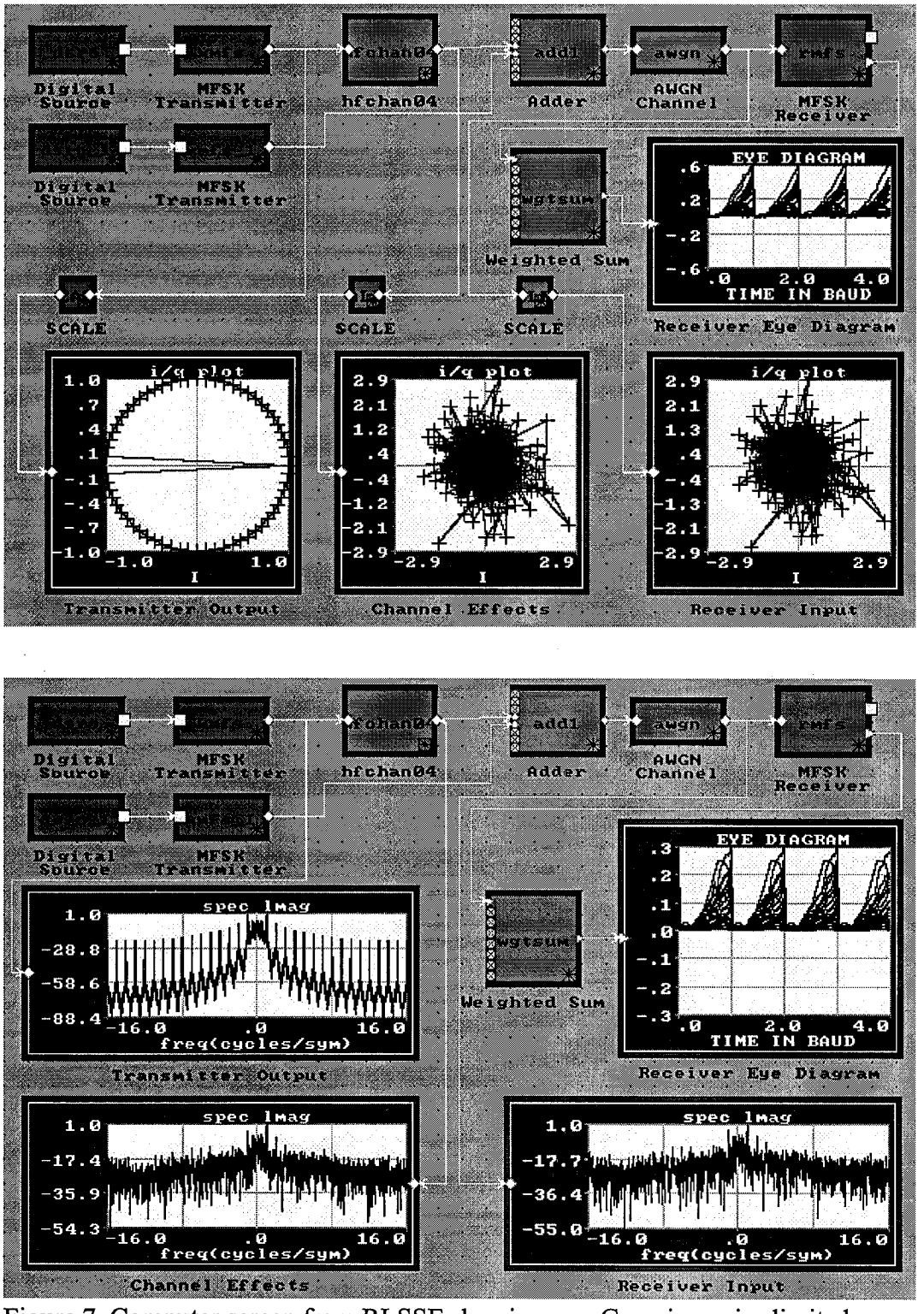

Figure 7. Computer screen from RLSSE showing non-Gaussian noise limited performance for 2-FSK. Top figure shows eye diagram and I/Q plots while bottom screen shows eye diagram and spectrum magnitude (in dB) plots. Simulation parameters are SNR=30 dB, SIR=50 dB, and BER=2.4e-2.

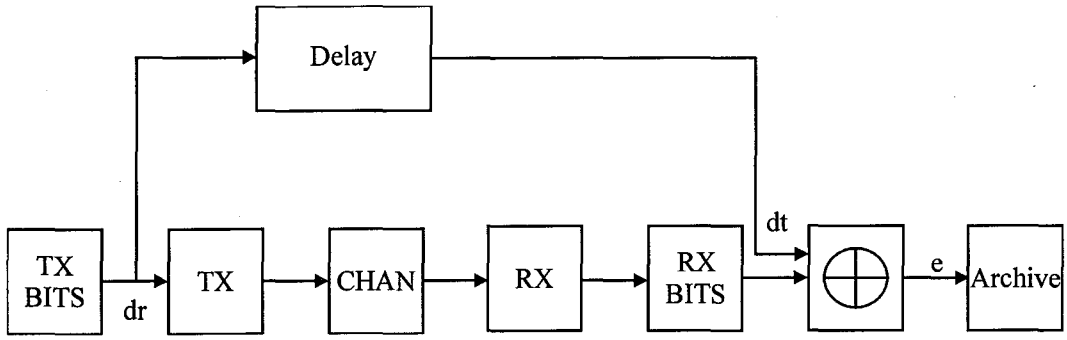

Figure 8. Radio link signal simulation and bit error sequence collection.

4. EFFECT OF BIT ERRORS ON SPEECH AND IMAGE INFORMATION

The second simulation step works at the bit level as shown in Figure 1. Bit level simulation can be performed directly from simulated bit error sequences or from a statistical bit error model (which can be derived from simulated bit error sequences). The Gilbert model [6] is an example of a statistical bit error model. Both approaches should yield the same first and second order statistics. First order statistics include the average bit error rate while second order statistics include the probability of consecutive bit errors. In this study the bit error sequences collected during the first simulation step are used.

Bit level simulations need to be run once for every information format. The bit error sequence distorts the speech and image information by

$$i_r = i_t \oplus e \tag{12}$$

where i_t is the undistorted information and i_r is the distorted information predicted to be present at the output of the receiver. This process is shown diagrammatically in Figure 10.

4.1 Information Formats

A speech sample from the TIMIT standard source, distributed by the National Institute for Standards and Technology, is used to evaluate speech quality. The 3.4 second sample, recorded at 16 kilo-samples per second (ksps) with 16-bit resolution, contains the sentence "Rob sat by the pond and sketched stray geese." The sample was decimated to 8 ksps and 8-bit resolution to produce "toll quality" 64 kilo-bits per second (kbps) PCM speech. The 64-kbps PCM speech was also compressed by the U.S. Federal Standard 1016, 4.8-kbps code excited linear prediction (CELP) vocoder [7] algorithm. Corresponding file sizes are 27.2 kilobytes (kB) for 64-kbps speech and 2 kB for compressed PCM speech.

A U.S. Geological Survey topographic map, "scanned" into the computer and saved in bit-map file format (filename.bmp), was used to evaluate image quality. Bit-map file formatting information,

sometimes referred to as "header" information, was assumed to be transmitted error free. The image has easily identifiable features such as shading, sharp lines, symbols, and text. The resulting PCM image sample is 320 pixels/line by 200 lines. Each pixel had one of 16 possible gray shades represented by 4 bits. The PCM image file size is 32 kB.

4.2 Subjective Quality Rating

Speech and image quality ratings presented in this study are based on the opinions of two people. These subjective quality ratings are expressed in terms of the typical opinion class scale ranging from 1 to 5. Class 1 is completely undecipherable, class 2 is marginally useful, and class 5 is free from distortion. Speech degradation is characterized by "pops", "hisses", "burps", and "warbles" while image degradation is characterized by "dots", "snow", "dashes", and "streaks."

PCM speech quality was evaluated by playing the distorted speech file through an 8-bit personal computer sound card. Compressed PCM speech was converted to PCM speech before its quality was evaluated. Auxiliary sound card software was used to display the time-varying voltage associated with each speech "waveform." The speech waveform is useful for qualitative comparisons of degraded and clear speech.

Figures 11 and 12 show "marginal" and "best" speech waveforms for PCM speech and compressed PCM speech, respectively. The top waveform of each figure represents class 2 while the bottom waveforms represent approximately class 4. The ordinate of the speech waveforms, corresponding to the amplitude of the demodulated signal, extends from -127 to 127 analog-to-digital conversion units. The speech waveforms show approximately 1.5 seconds of the speech segment. Although both class 2 examples are intelligible, their speech waveforms show clear qualitative differences. PCM speech errors in these waveforms have a much larger amplitude variation than compressed PCM speech errors. Also compressed PCM speech errors occur in bursts while PCM speech errors appear to be more randomly distributed in time.

PCM image quality was evaluated on a high resolution computer screen. Figure 13 shows marginal and best images. The top image represents class 2 while the bottom image represents approximately class 4. The class 2 image text is illegible; however, map shading and contour lines are still decipherable. Examples of "marginal" and "best" speech and image transmission for all radio links and information formats are included in the Appendix.

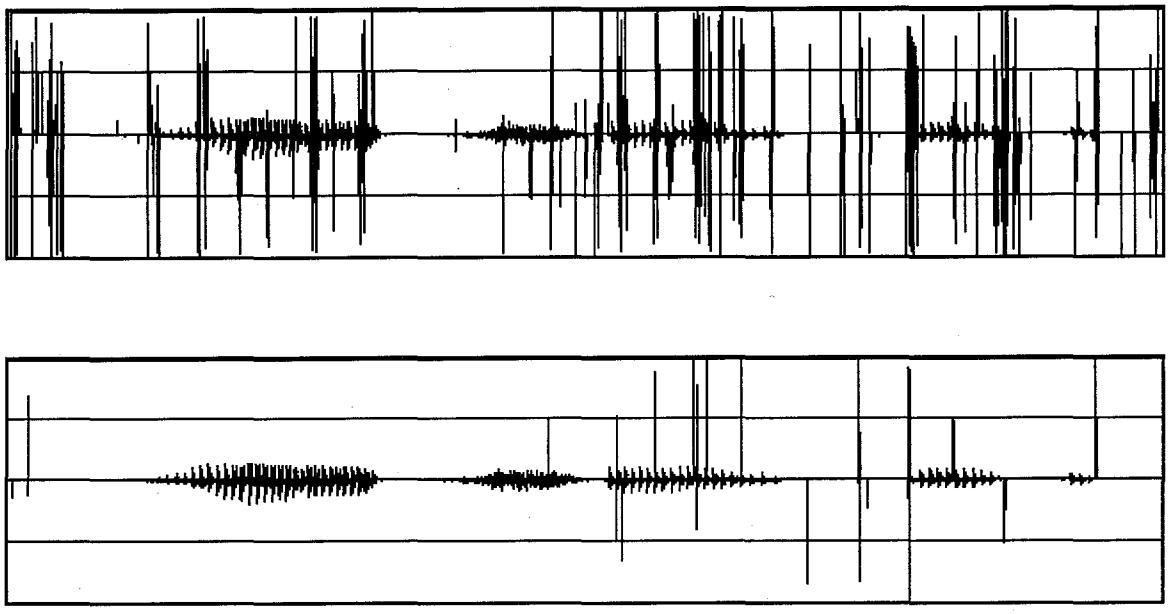

Figure 11. PCM speech waveform for 2-FSK. Top waveform represents class 2.0 [SNR=30 dB, SIR=20 dB, BER=2.6e-2] and bottom waveform represents class 3.8 [SNR=70 dB, SIR=30 dB, BER=3.6e-3].

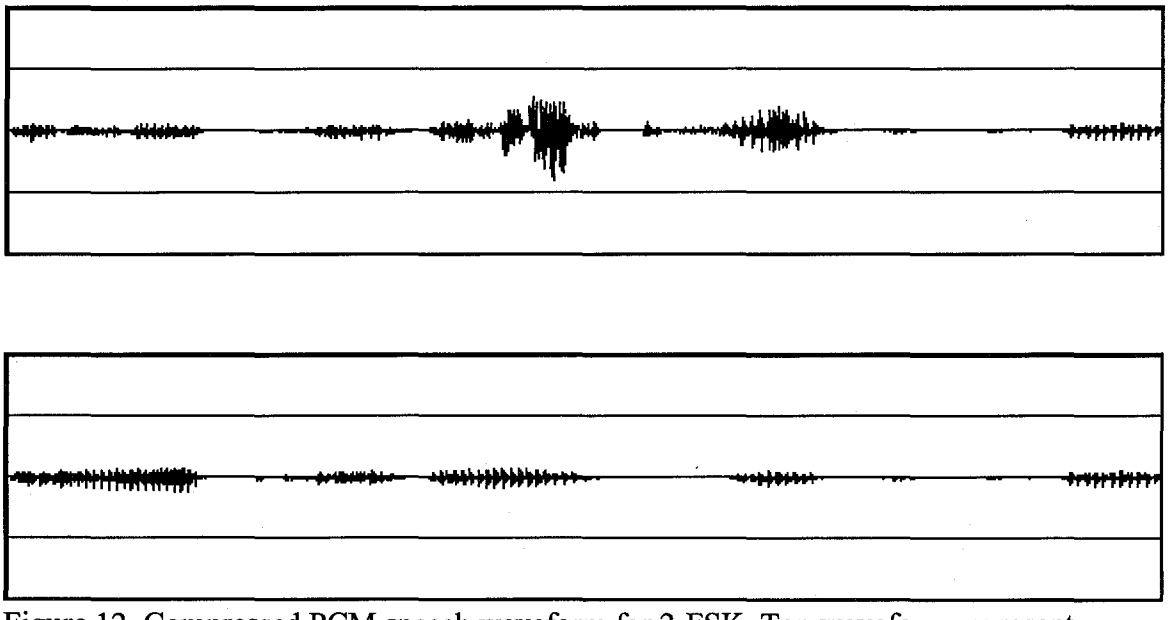

Figure 12. Compressed PCM speech waveform for 2-FSK. Top waveform represents class 2.0 [SNR=30 dB, SIR=10 dB, BER=7.0e-2] and bottom waveform represents class 4.0 [SNR=80 dB, SIR=30 dB, BER=1.2e-3].

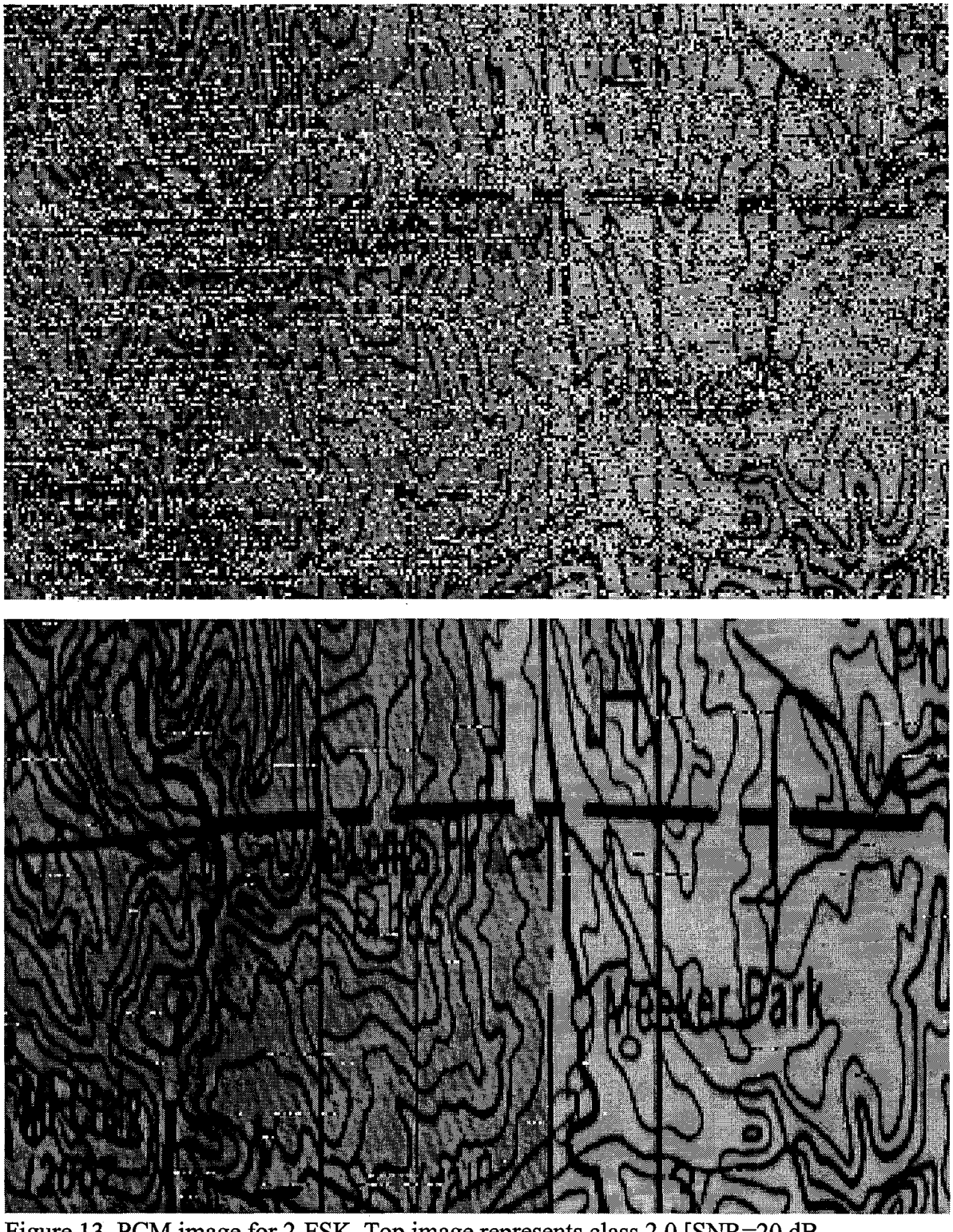

Figure 13. PCM image for 2-FSK. Top image represents class 2.0 [SNR=20 dB, SIR=10 dB, BER=1.7e-1] and bottom image represents class 4.5 [SNR=80 dB, SIR=50 dB, BER=3.6e-3].

4.3. Effect of Signal-to-Interference Ratio on Speech and Image Quality

Speech and image quality for a 2-FSK HF radio link subjected to interference are shown in Figures 14-16. Each graph represents a different information format and each curve in the graph represents a distinct interference level. Interference levels identified in the graph legend are in units of jamming-to-signal ratio (JSR) in dB. The JSR is the inverse of SIR which makes JSR in dB the negative of SIR in dB. The ordinate is in units of symbol error rate (SER) and the abscissa is in units of SNR in dB (non-Gaussian noise power is not included in SNR). Subjective quality regions are represented by different shades of gray and identified with circled numbers. For comparison, results for 2-FSK in Gaussian noise alone are displayed by the curve labeled "2FSKRGN." Similar speech and image quality graphs for all radio links and information formats are included in the Appendix.

Data contained in the quality graphs can be used to answer questions concerning the robustness of radio link and information format combinations. This is most easily accomplished by comparing radio channel impairment levels for several radio links at a fixed SNR and quality classification. For example, Table 4 shows the lowest SIR necessary for class 3 quality when the SNR is fixed at 80 dB. The values in the table are estimated from the speech and image quality graphs in the Appendix.

Table 4. Minimum SIR for Class 3 quality when SNR is 80 dB.

HF Radio Link	PCM Speech SIR (dB)	Compressed PCM Speech SIR (dB)	PCM Image SIR (dB)
2-FSK	30	20	15
2-FSK with FEC	25	15	15
4-FSK	30	20	20
8-FSK	30	20	20
2-DPSK	30	20	15
4-DPSK	30	20	20
8-DPSK	40	30	30
VFCT	30	20	10

Table 4 indicates that for all radio links PCM speech needs 10 dB more SIR for class 3 quality than compressed PCM speech. Thus compressed PCM speech is more robust than PCM speech in the HF radio channel. The error correction in the CELP speech compression algorithm may partially explain this performance improvement. Most radio links required 30 dB SIR for PCM speech and 20 dB for compressed PCM speech. Exceptions were 2-FSK with FEC, which performed 5 dB better, and 8-DPSK, which performed 10 dB worse.

The PCM image information format required the lowest SIR values. However, it also had the most variation from radio link to radio link. The performance improvement may be due to differences in perception between the ear and the eye. A comparison between compressed PCM image quality and PCM image quality, not included in this study, would be more relevant.

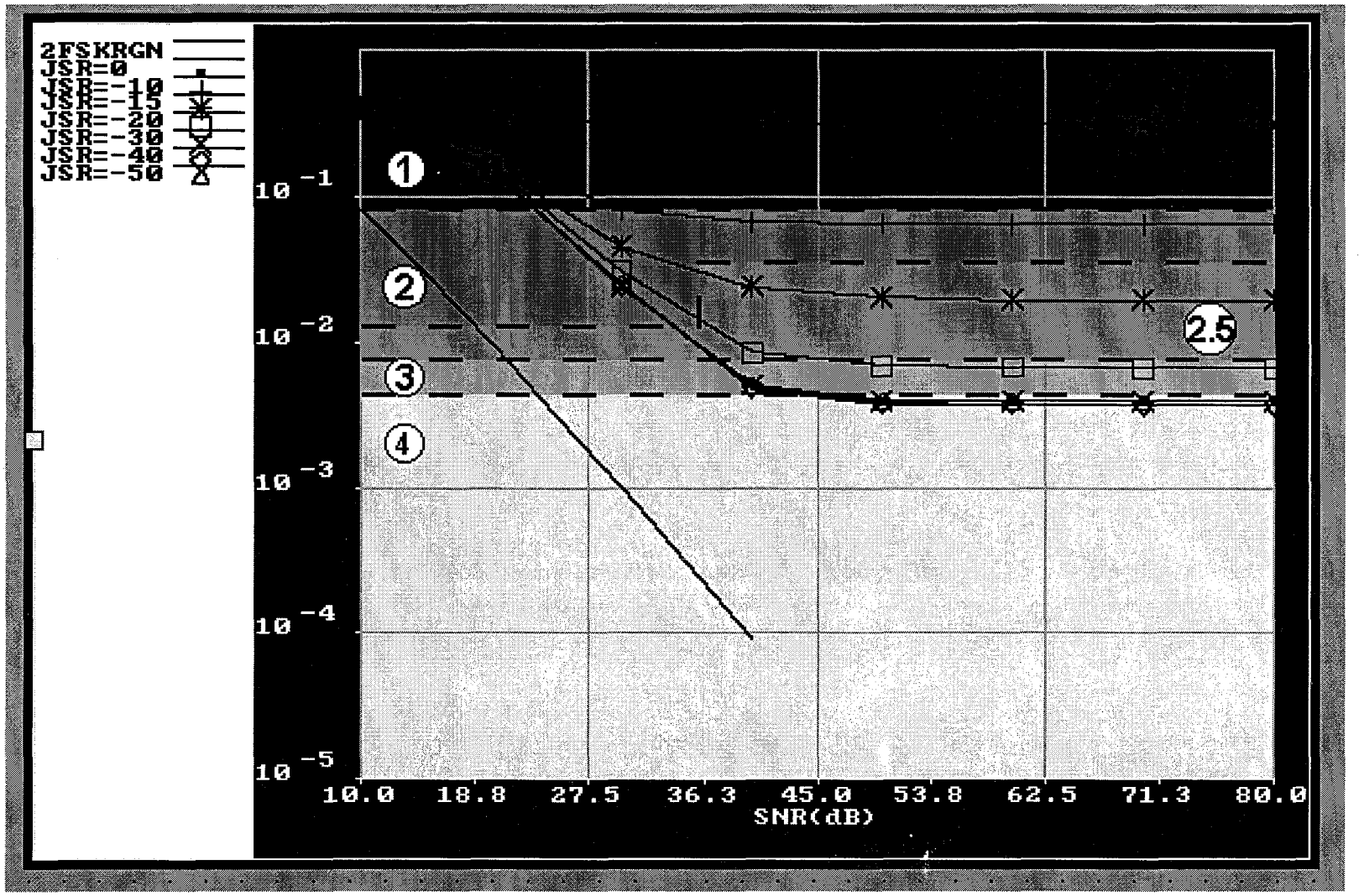

Figure 14. PCM speech quality for 2-FSK. Circled numbers represent quality class and ordinate is in units of SER.

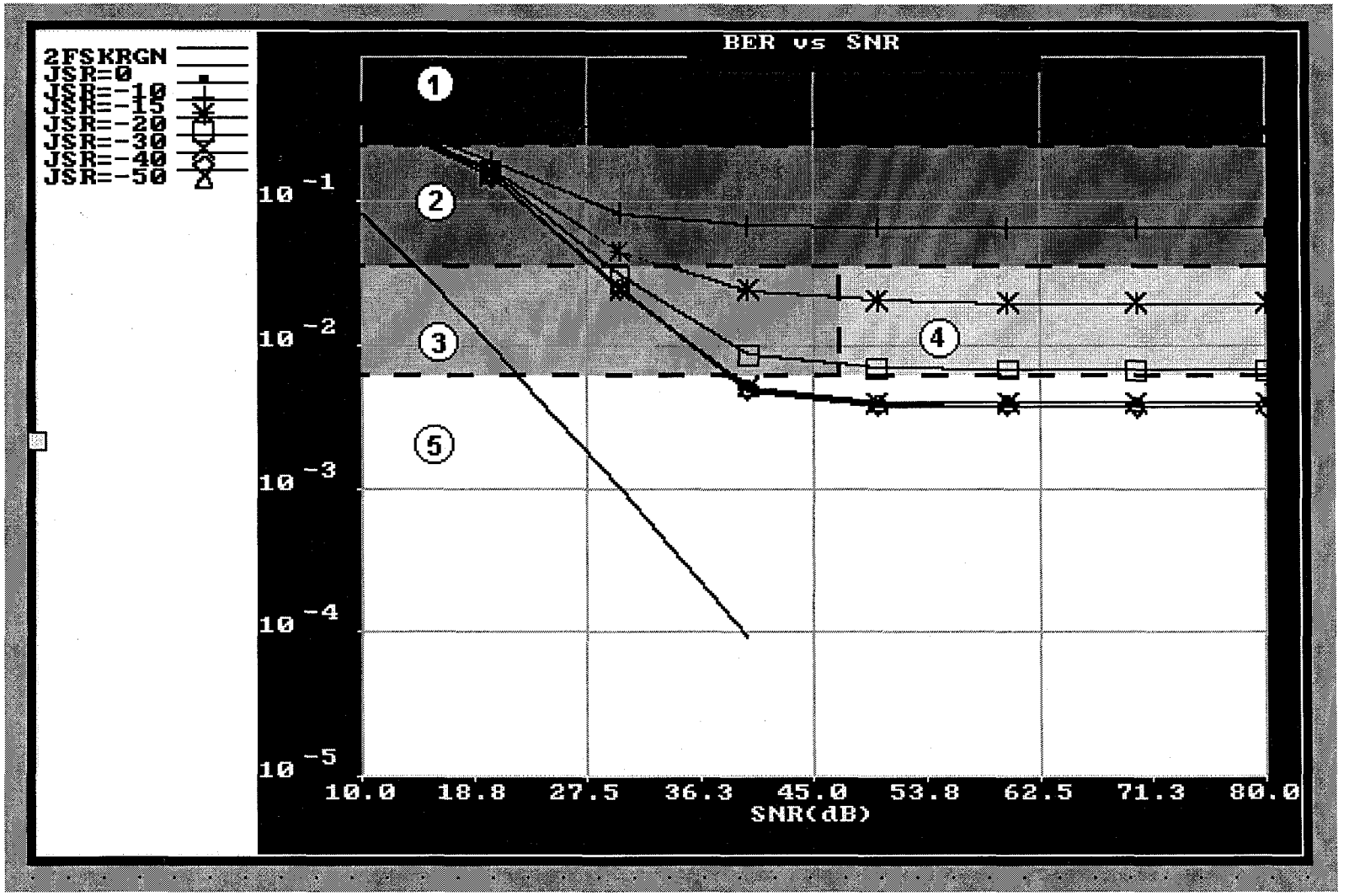

Figure 15. Compressed PCM speech quality for 2-FSK. Circled numbers represent quality class and ordinate is in units of SER.

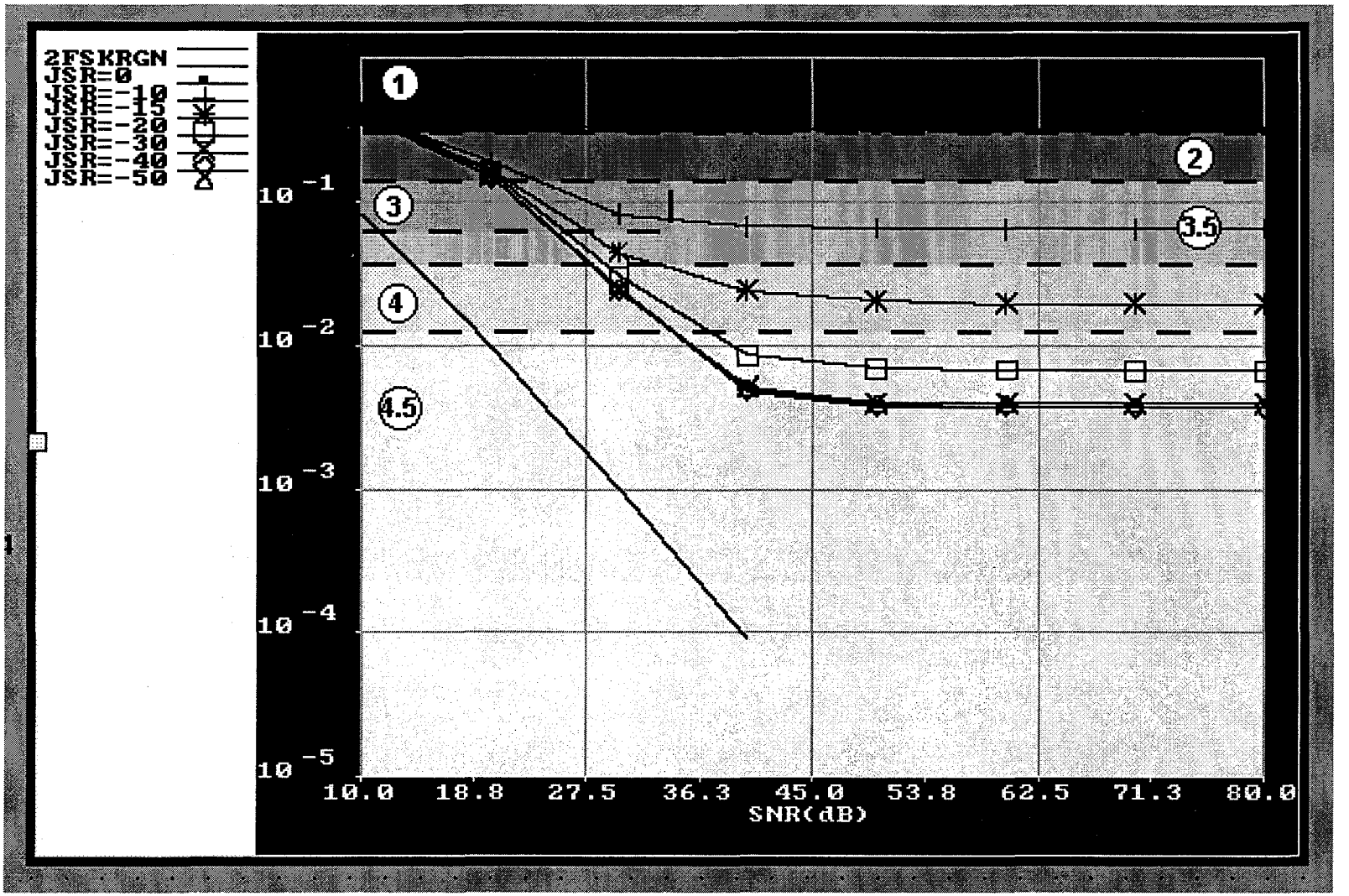

Figure 16. PCM image quality for 2-FSK. Circled numbers represent quality class and ordinate is in units of SER.

5. CONCLUSION

This study has demonstrated how software simulation can be used to predict wireless speech and image quality degradation caused by an impaired radio channel. This performance prediction capability will become increasingly important as multimedia wireless applications increase in number. The software simulation process is composed of two steps. In the first step the radio link is simulated at the signal level while in the second step the radio link is simulated at the bit level. Division of the simulation process, in this way, makes comparison of numerous speech and image formats very efficient.

Eight different HF radio links were simulated to illustrate this performance prediction method. Speech in PCM and compressed PCM formats and an image in PCM format were transmitted over a radio channel impaired by multipath, non-Gaussian noise, and varying levels of interference. Quality degradation was shown in three ways. First, example speech waveforms and images at specific SNR and SIR conditions exhibiting "marginal" and "best" quality were presented. Second, graphs showing quality as a function of SNR and SIR were presented. Last, the minimum SIR necessary for class 3 quality at a high SNR was tabulated. These tabulated results, found in Section 4, Table 4, indicate that PCM speech was more sensitive to interference than compressed PCM speech for all HF radio links. PCM image transmission allowed the lowest SIR of the three information formats. These results highlight the fact that quality can be dependent upon the choice of information format as much as the type of modulation.

This type of performance prediction can be extended to include more radio links, radio channels, and information formats. Radio links for applications such as PCS and WLAN are currently of much interest. These applications are dominated by the same type of multipath as that found in HF radio links. ITS multipath measurements in PCS and WLAN frequency bands are currently available for signal level simulations [8,9]. PCS and WLAN applications also use digital facsimile (FAX) [10] and compressed PCM image formats such as the JPEG [11] and MPEG [12]. These formats can be easily added to bit level simulations.

The performance prediction method can be improved by using objective quality measures and modeling the bit error sequences. ITS has been developing objective speech and image quality measurement software in support of various standards groups for a number of years [13]. This work has been directed towards fixed radio channels such as cable and line-of-sight microwave. Recently ITS has turned its attention towards the mobile radio channel. In the future, performance prediction can be improved by using objective quality measures instead of subjective panel quality measures. Lastly, for this study, bit-level simulation was performed with bit error sequences collected during signal simulations. It may be possible to reduce signal simulation time by modeling the bit error sequences from shorter signal simulations and using the model to generate bit error sequences of any length. This approach will result in lower overall computation times when larger speech or image files are distorted.

6. REFERENCES

[1] C.C. Watterson, J.R. Juroshek, and W.D. Bensema, "Experimental confirmation of an HF channel model," *IEEE Trans. on Comm. Tech.*, pp. 792 - 803, Dec. 1970.

[2] J.W. Modestino and K.R. Matis, "Interactive simulation of digital communication systems," *IEEE Journal on Selected Areas in Comm.*, pp. 51-76, Jan. 1984.

[3] CCIR Report 322, "World distribution and characteristics of atmospheric radio noise."

[4] K. Brayer, "The improvement of digital HF communication through coding: I - interleaved cyclic coding," *IEEE Trans. on Comm. Tech.*, pp. 771-778, Dec. 1968.

[5] CCIR Report 864-1, "Data transmission at 2400/1200/600/300/150/75 bits/s over HF circuits using multi-channel voice-frequency telegraphy and phase-shift keying."

[6] M.C. Jeruchim, P. Balaban, and K.S. Shanmugan, *Simulation of Communication Systems*, New York: Plenum Press, 1992, pp. 386-396.

[7] J.P. Campbell, Jr., T.E. Tremain, and V.C. Welch, "An expandable error-protected 4800 bps CELP coder (U.S. Federal Standard 4800 BPS Voice coder)," *Proc. of 1989 ICASSP.*, 1989, pp. 735-738.

[8] P.B. Papazian, Y. Lo, E.E. Pol, M.P. Roadifer, T.G. Hoople, and R.J. Achatz, "Wideband propagation measurements for wireless indoor communications," NTIA Report 93-292, Jan. 1993.

[9] J.A. Wepman, J.R. Hoffman, and L.H. Loew, "Impulse response measurements in the 1850-1990 MHz band in large outdoor cells," NTIA Report 94-309, Jun. 1994.

[10] K.R. McConnell, *FAX: Digital Facsimile Technology & Applications*, Artech House, 1990.

[11] G.K. Wallace, "The JPEG still picture compression standard," *Communications of the ACM*, pp. 31-44, Apr. 1991.

[12] D. Le Gall, "MPEG: a video compression standard for multimedia communications," *Communications of the ACM*, pp. 47-58, Apr. 1991.

[13] N.B. Seitz, S. Wolf, S. Voran, and R. Bloomfield, "User-oriented measures of telecommunications quality," *IEEE Comm. Magazine*, pp. 56-67, Jan. 1994.

APPENDIX

This Appendix includes performance prediction results for the radio links and information formats described in the main text. Speech and image quality and symbol error rate (SER) as a function of SNR and SIR are shown graphically in Figures A.1.1 to A.3.8. Each graph represents a unique radio link and information format combination and each graph curve represents a distinct interference level. Interference levels identified in the graph legend are in units of jamming-to-signal ratio (JSR) in dB. The JSR is the inverse of SIR which makes JSR in dB the negative of SIR in dB. The graph ordinate is in units of SER and the abscissa is in units of SNR in dB. Non-Gaussian noise power is not included in SNR. Subjective quality regions are represented by different shades of gray and identified with circled numbers. For comparison, results for 2-FSK and 2-DPSK in Gaussian noise alone are displayed by the curve labeled "RGN." Quality measures range from 1 to 5 with 1 being undecipherable, 2 marginally useful, and 5 excellent. Figures A.4.1 to A.6.8 show examples of "marginal" and "best" speech and image transmission. Marginal performance corresponds approximately to class 2 quality. Best performance may be anywhere from class 3 to class 5 depending on the radio link.

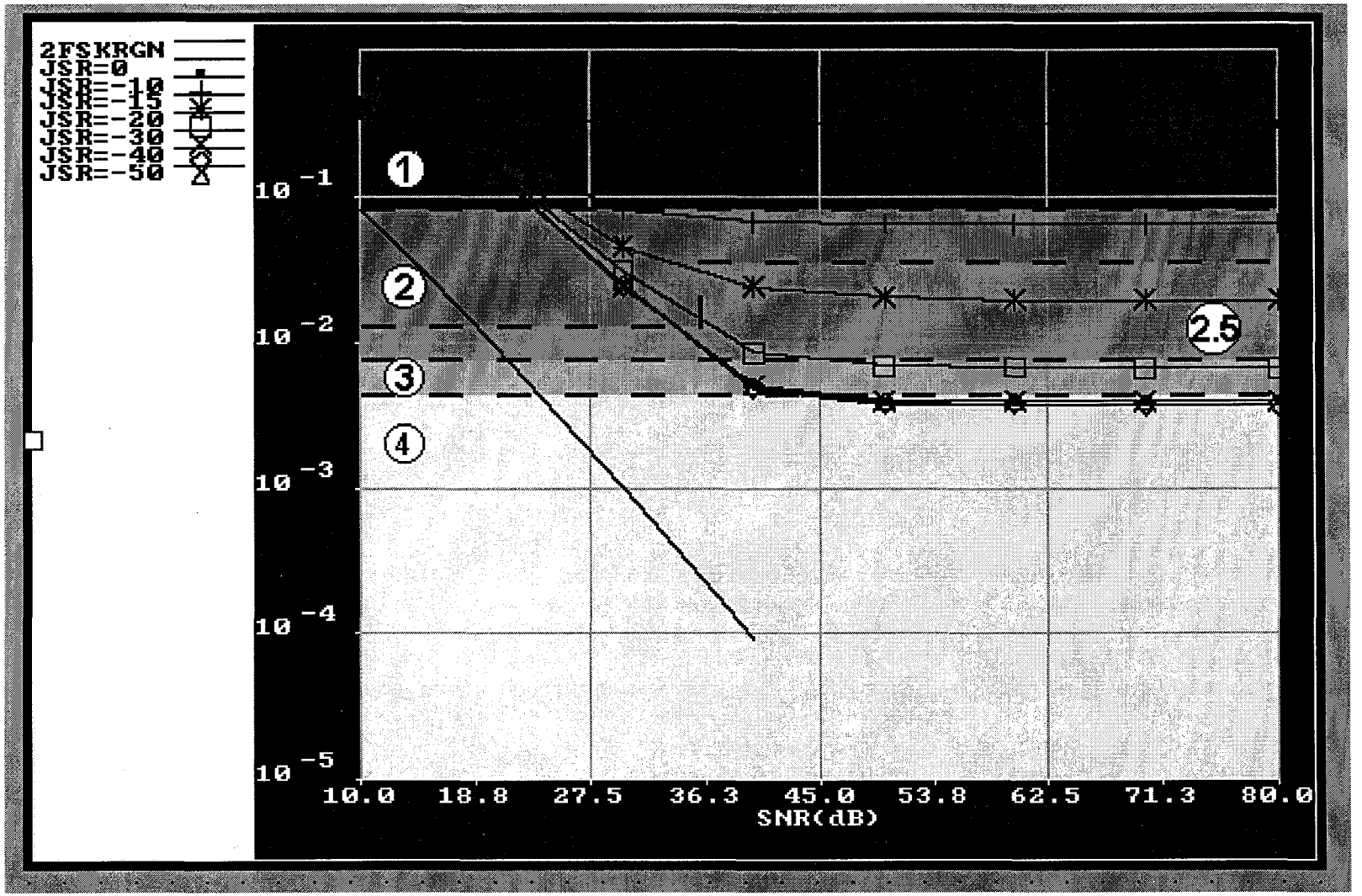

Figure A.1.1. PCM speech quality for 2-FSK. Circled numbers represent quality class and ordinate is in units of SER.

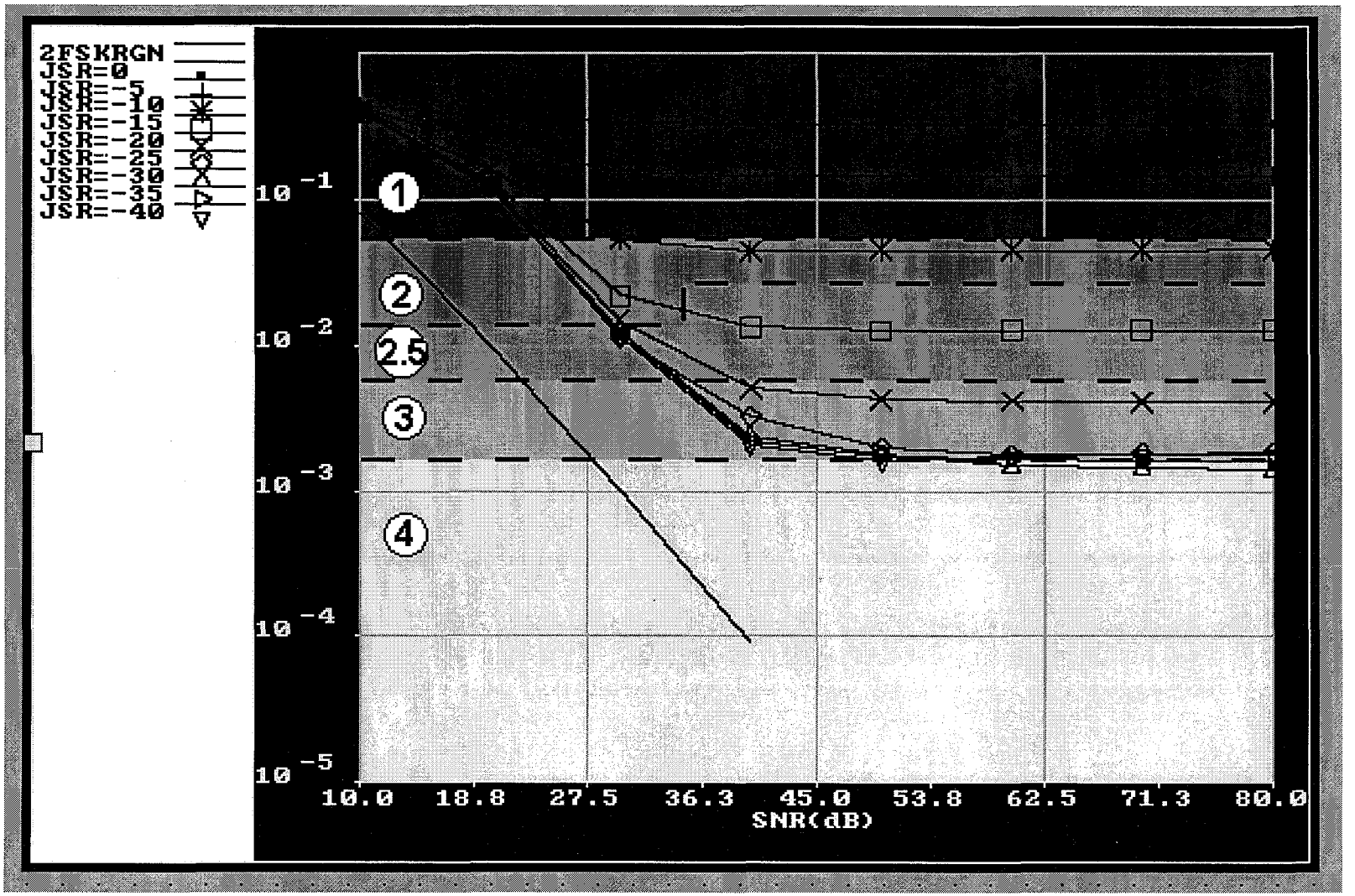

Figure A.1.2. PCM speech quality for 2-FSK with FEC and interleaving. Circled numbers represent quality class and ordinate is in units of SER.

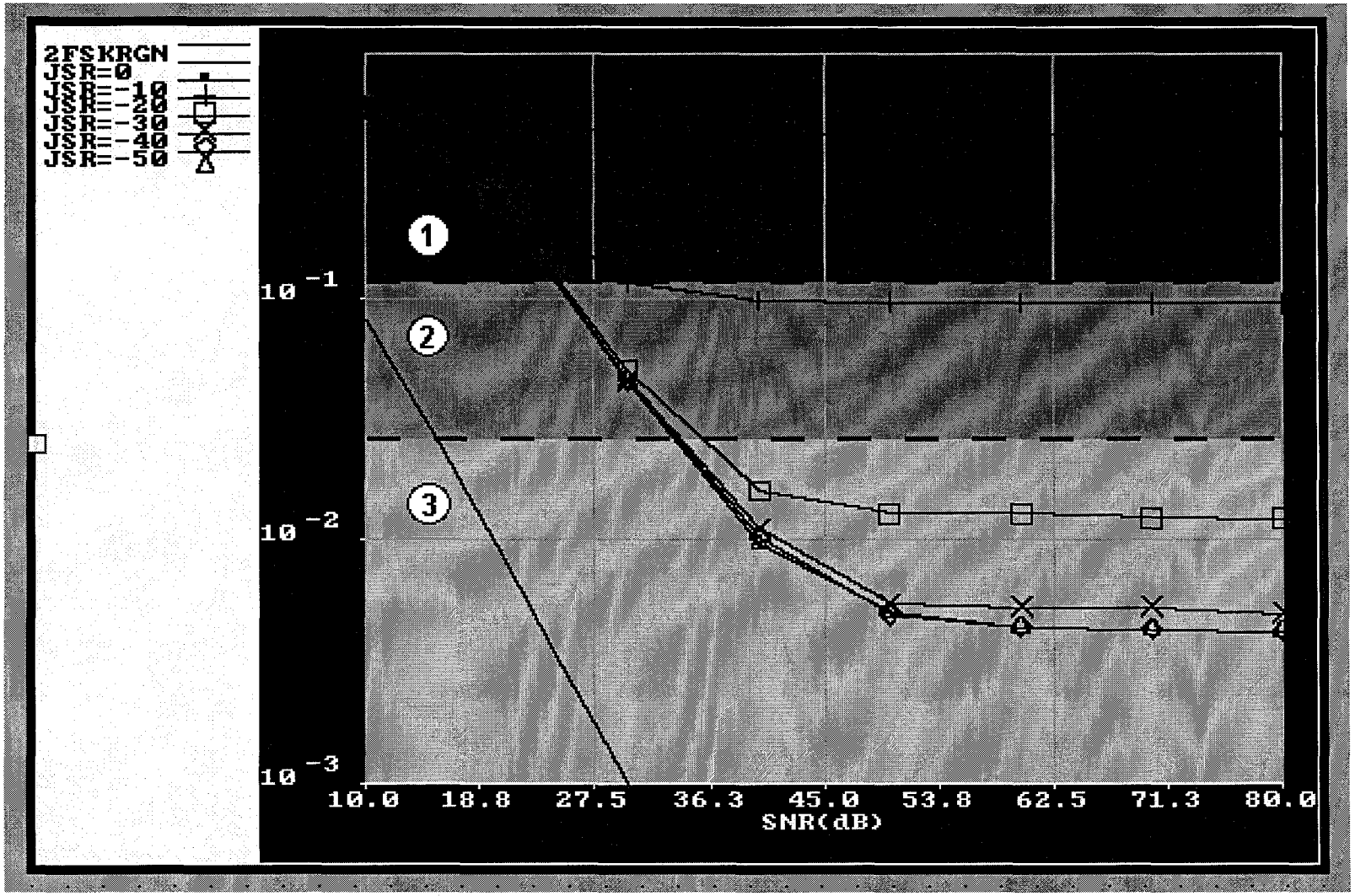

Figure A.1.3. PCM speech quality for 4-FSK. Circled numbers represent quality class and ordinate is in units of SER.

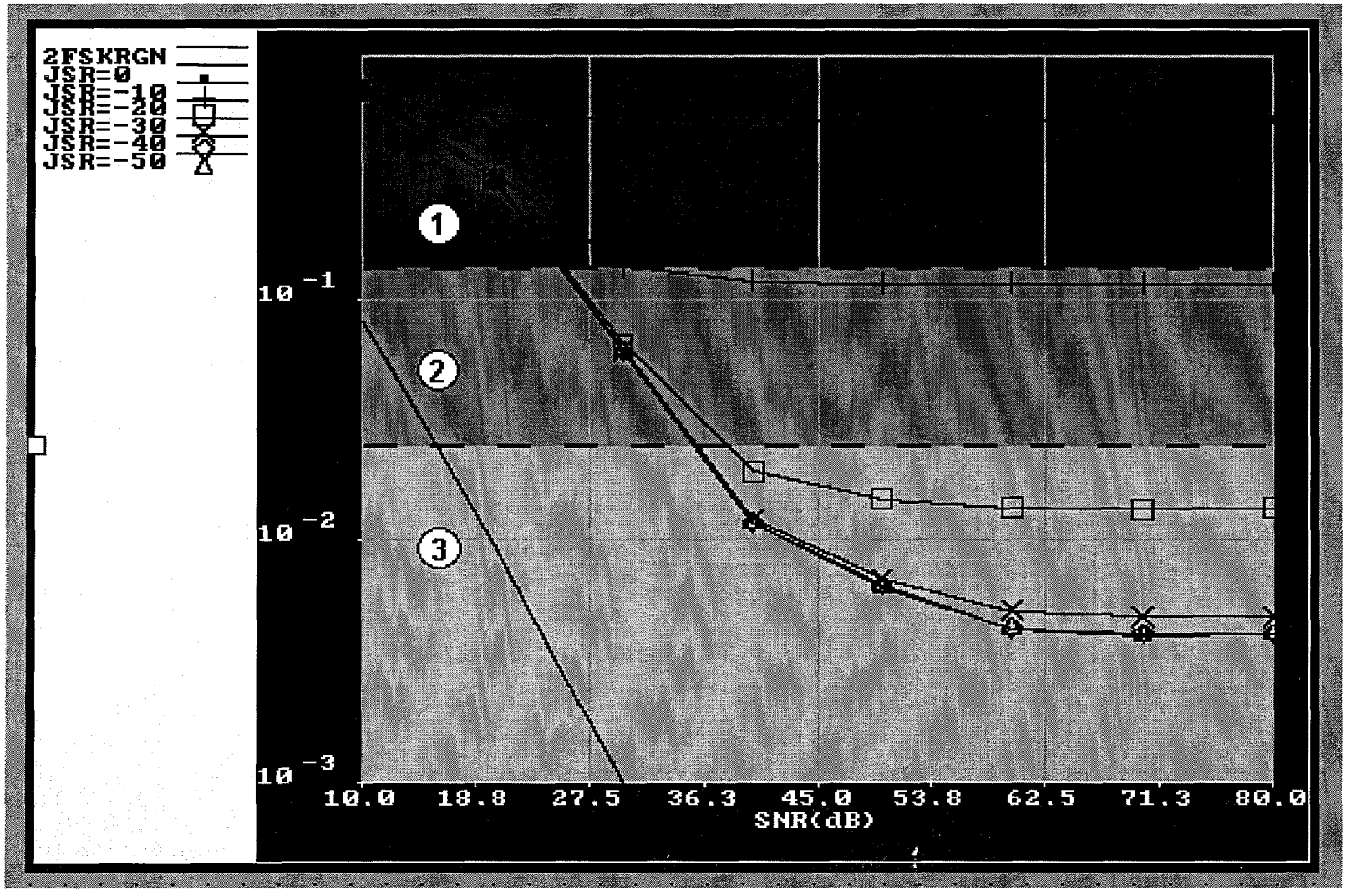

Figure A.1.4. PCM speech quality for 8-FSK. Circled numbers represent quality class and ordinate is in units of SER.

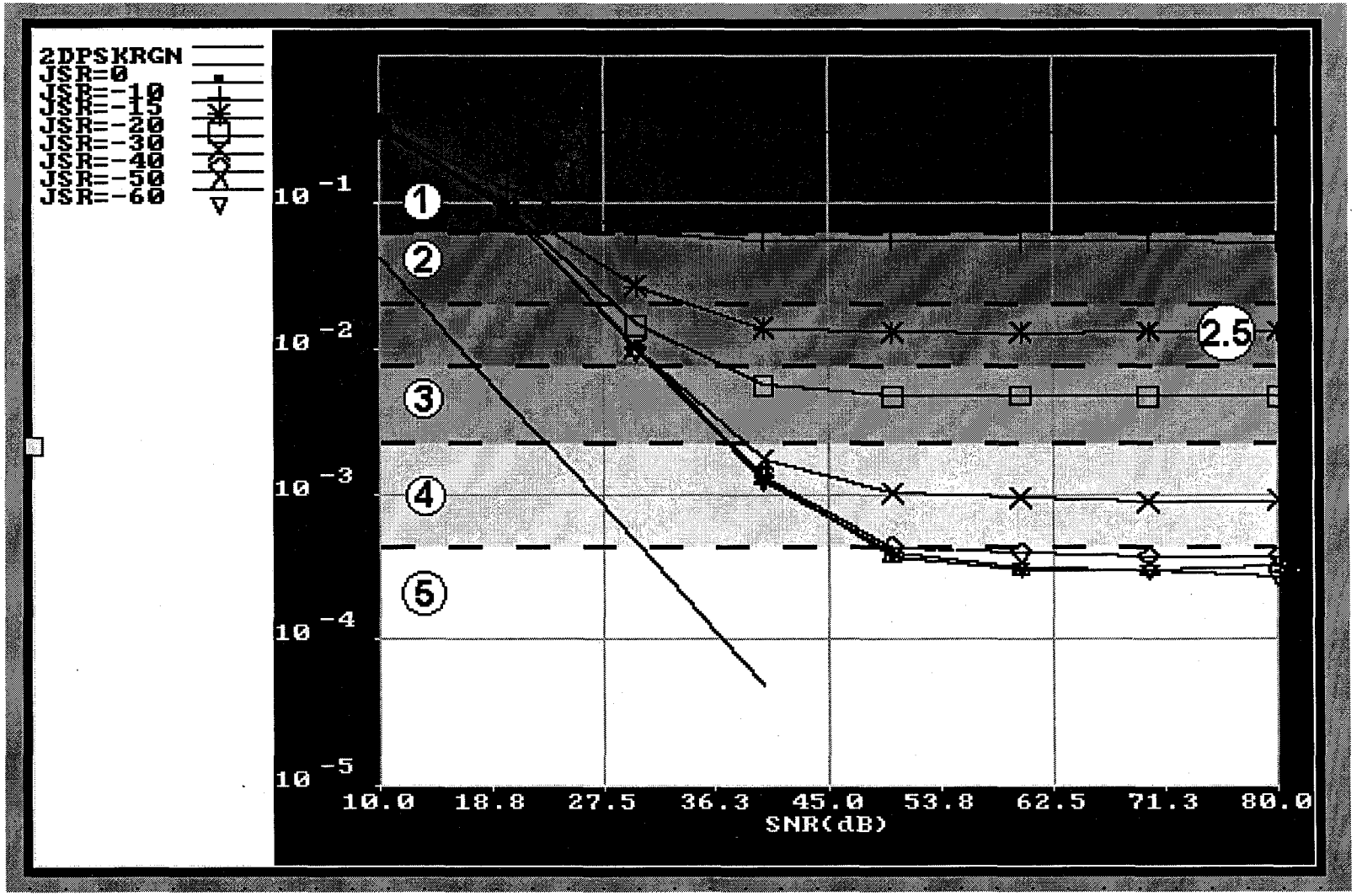

Figure A.1.5. PCM speech quality for 2-DPSK. Circled numbers represent quality class and ordinate is in units of SER.

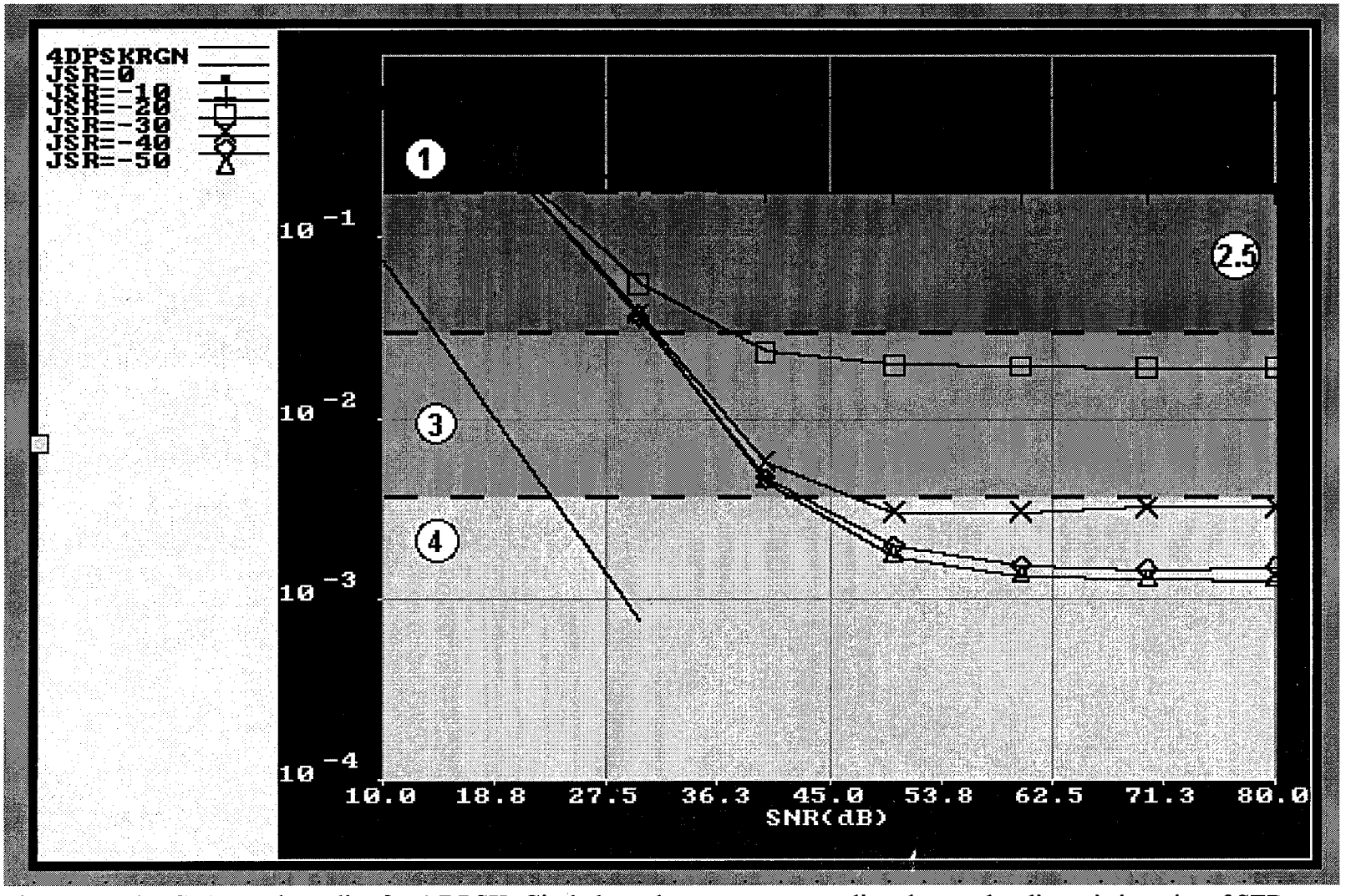

Figure A.1.6. PCM speech quality for 4-DPSK. Circled numbers represent quality class and ordinate is in units of SER.

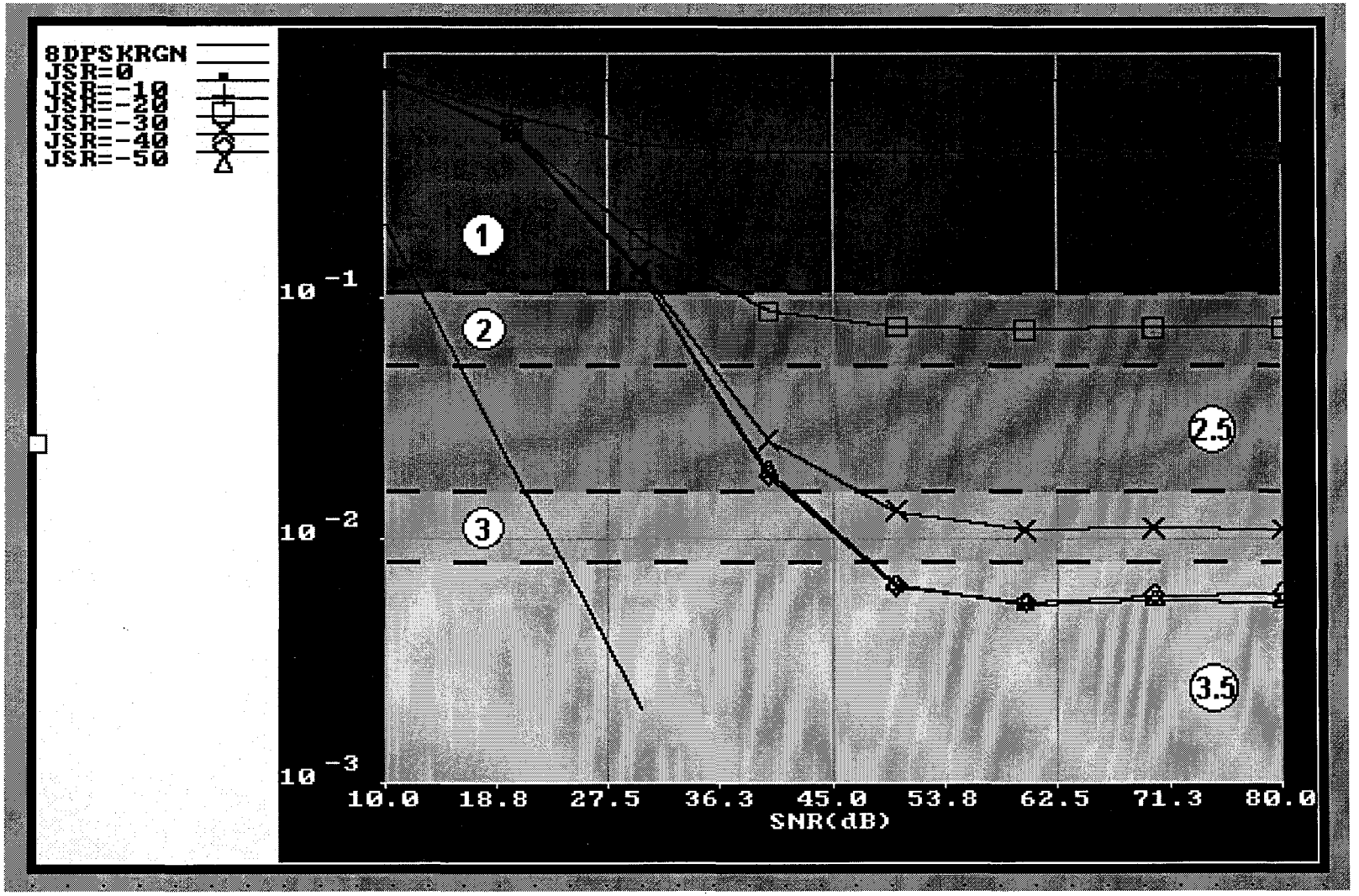

Figure A.1.7. PCM speech quality for 8-DPSK. Circled numbers represent quality class and ordinate is in units of SER.

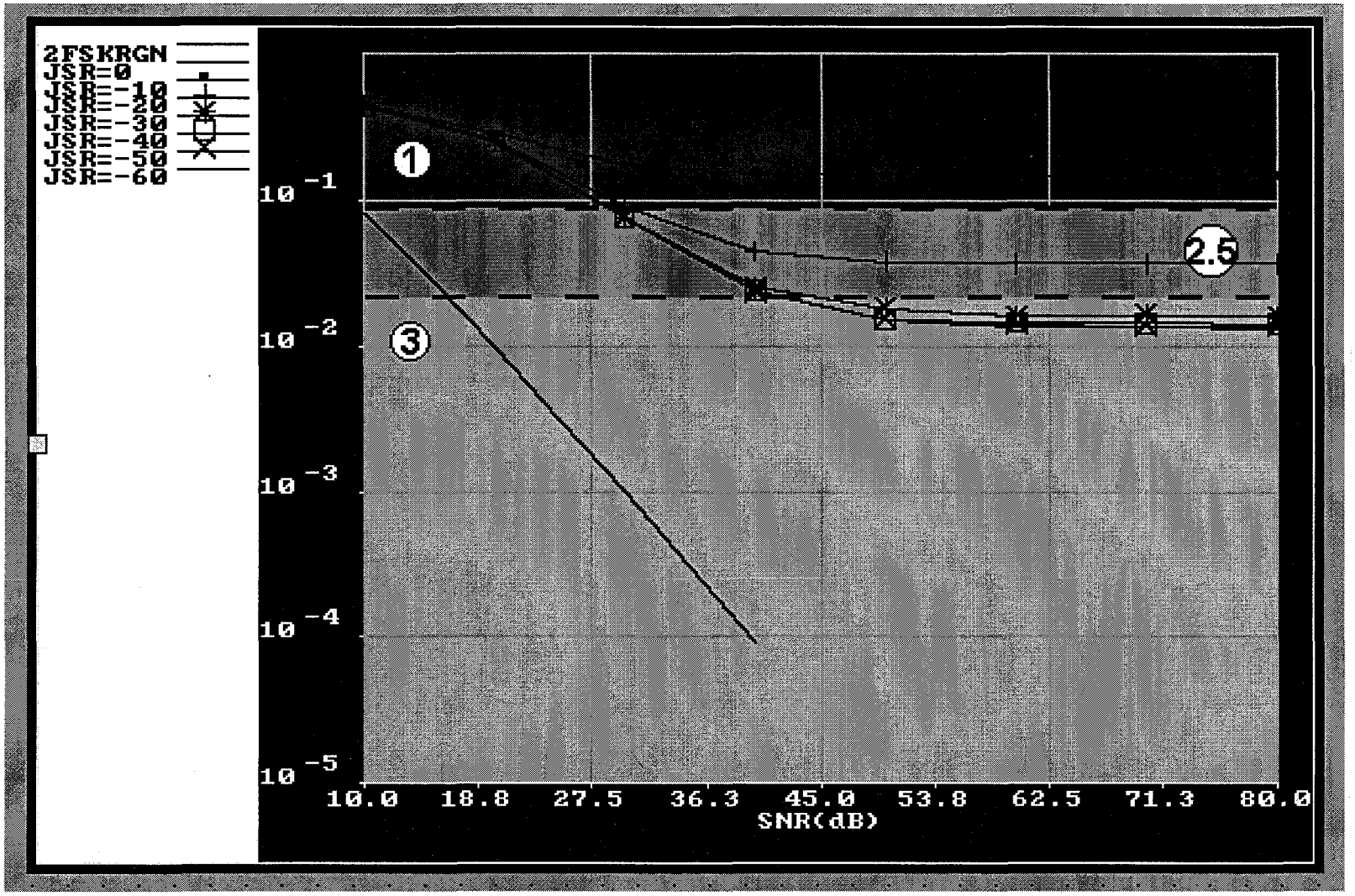

Figure A.1.8. PCM speech quality for 6-tone 2-FSK VFCT. Circled numbers represent quality class and ordinate is in units of SER.

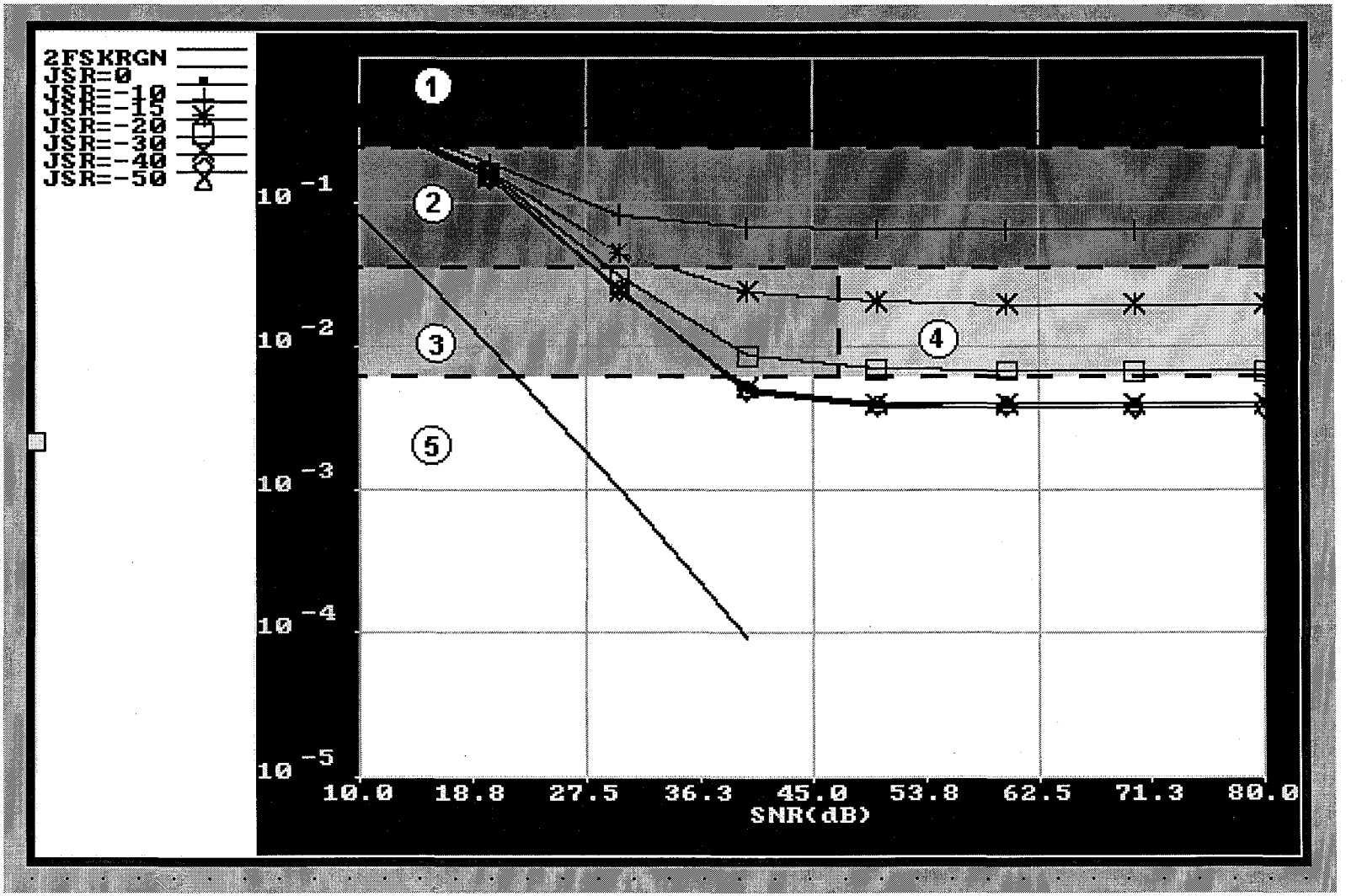

Figure A.2.1. Compressed PCM speech quality for 2-FSK. Circled numbers represent quality class and ordinate is in units of SER.

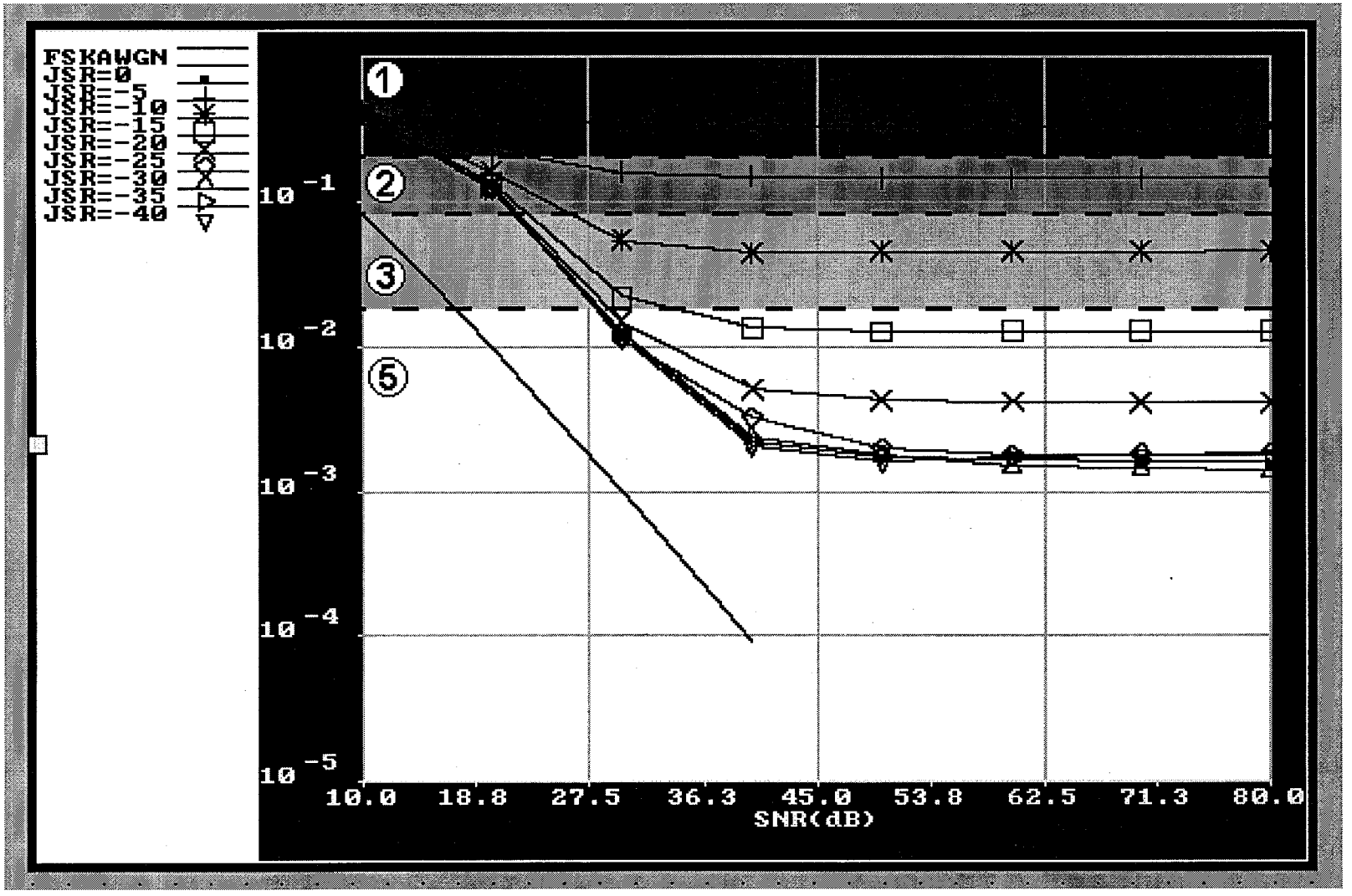

Figure A.2.2. Compressed PCM speech quality for 2-FSK with FEC and interleaving. Circled numbers represent quality class and ordinate is in units of SER.

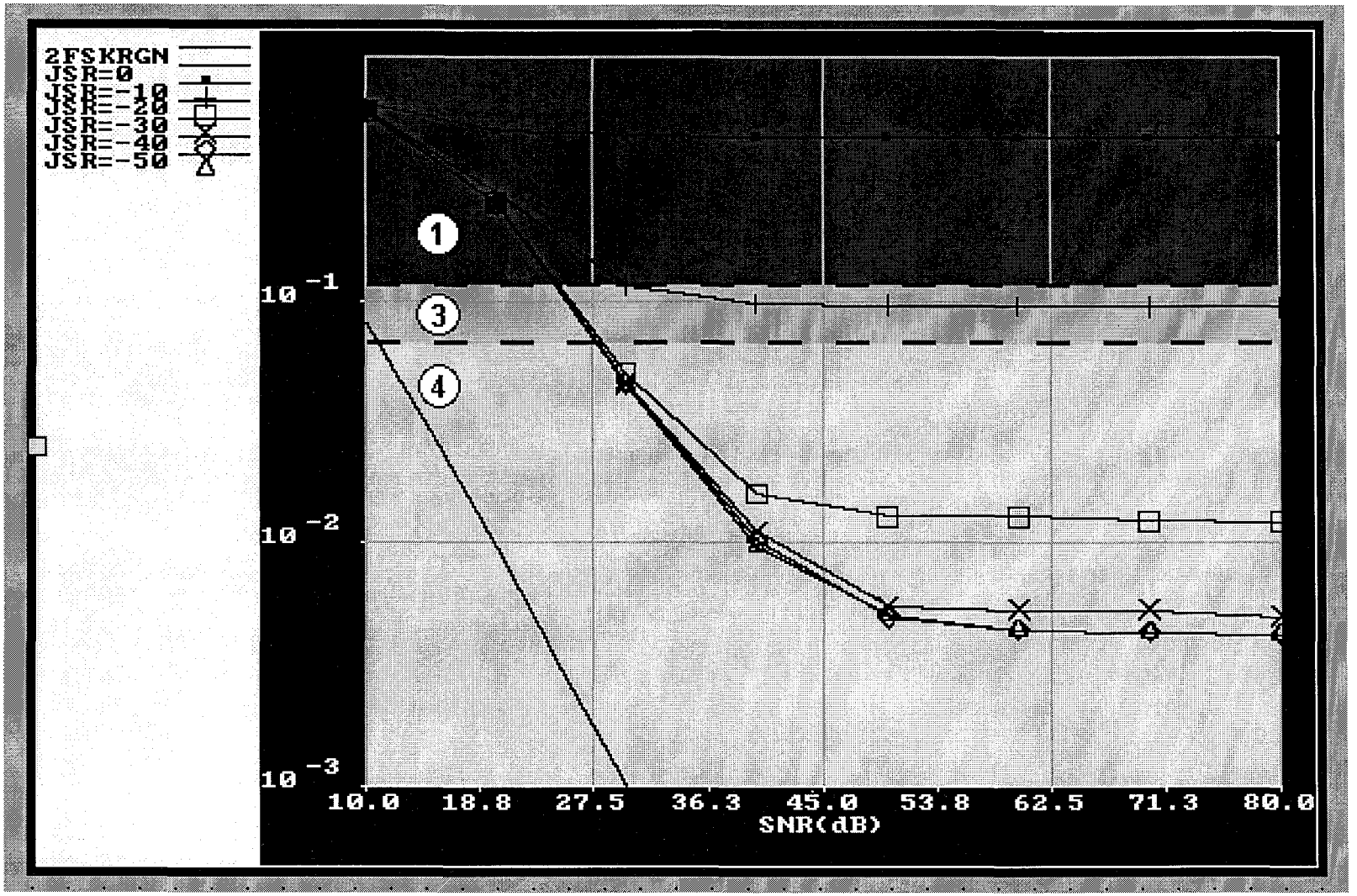

Figure A.2.3. Compressed PCM speech quality for 4-FSK. Circled numbers represent quality class and ordinate is in units of SER.

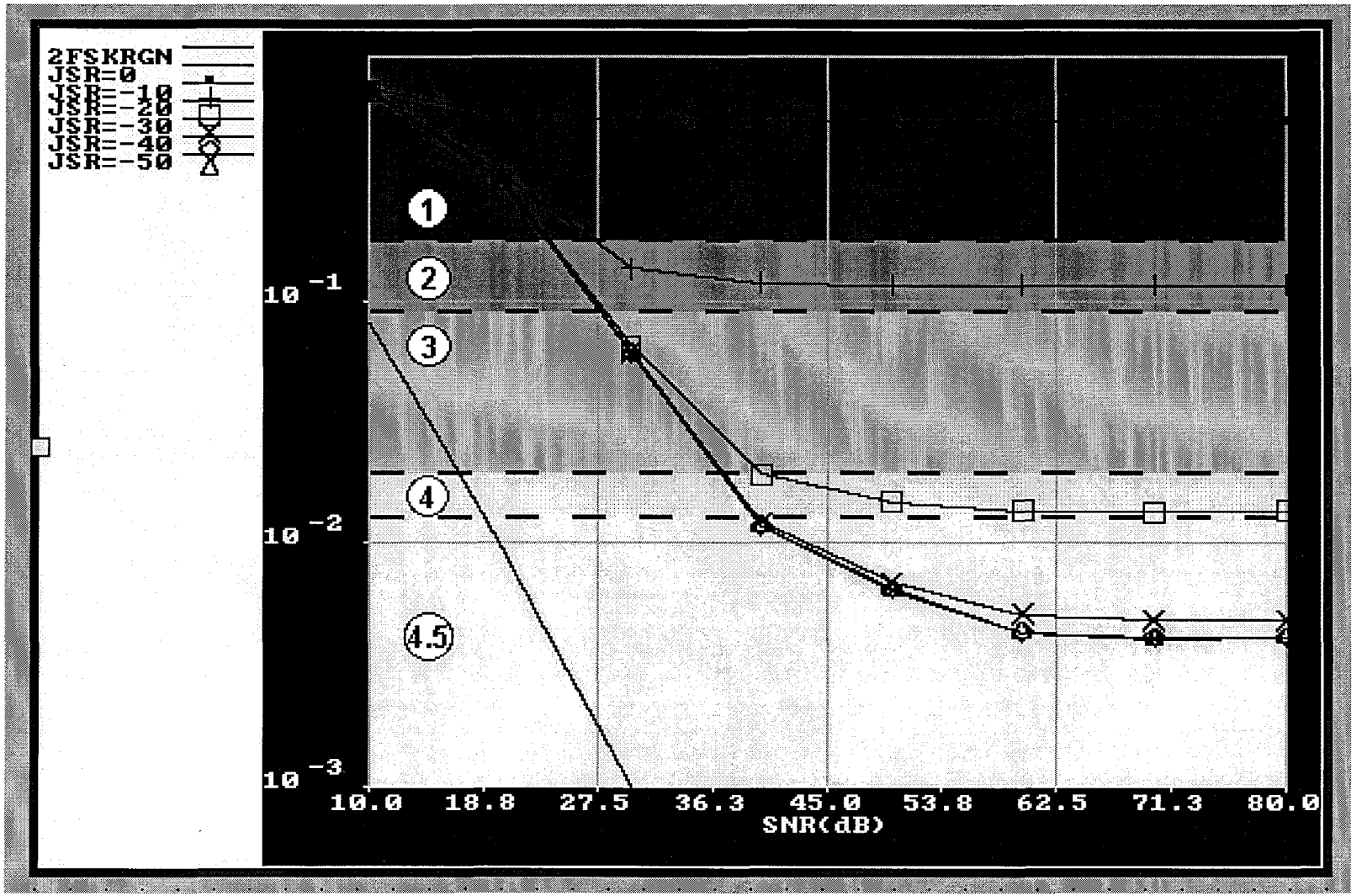

Figure A.2.4. Compressed PCM speech quality for 8-FSK. Circled numbers represent quality class and ordinate is in units of SER.

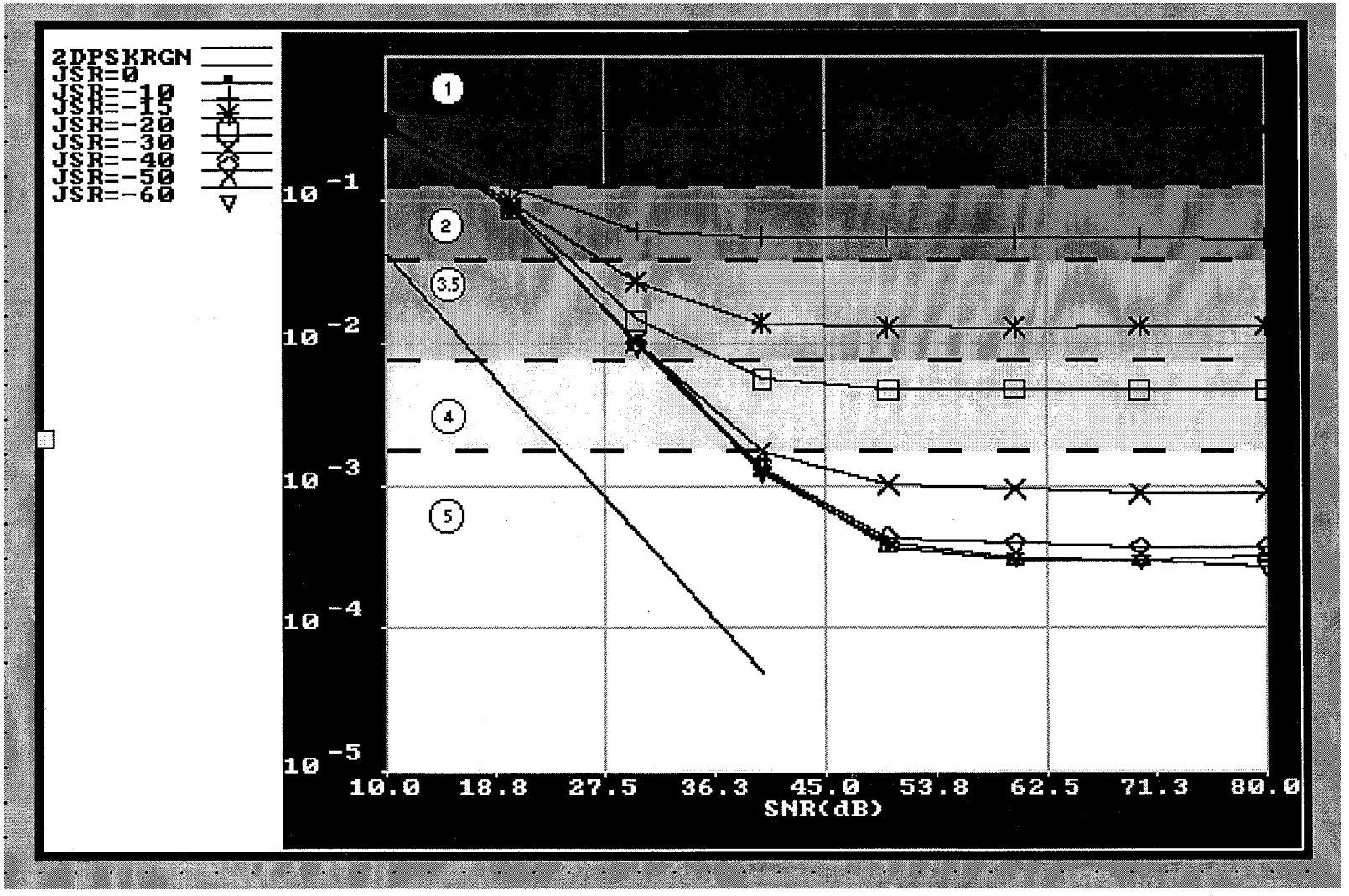

Figure A.2.5. Compressed PCM speech quality for 2-DPSK. Circled numbers represent quality class and ordinate is in units of SER.

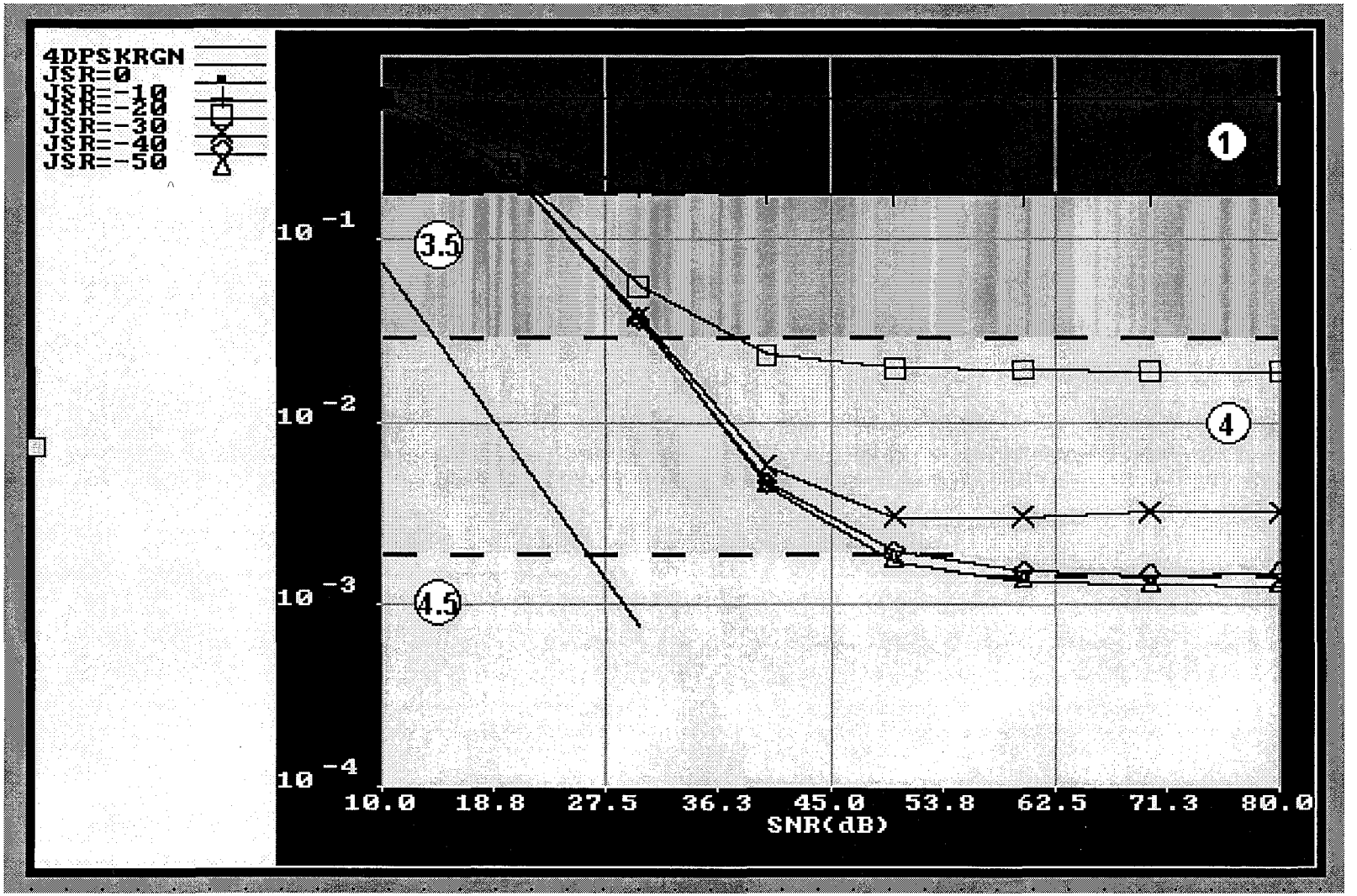

Figure A.2.6. Compressed PCM speech quality for 4-DPSK. Circled numbers represent quality class and ordinate is in units of SER.

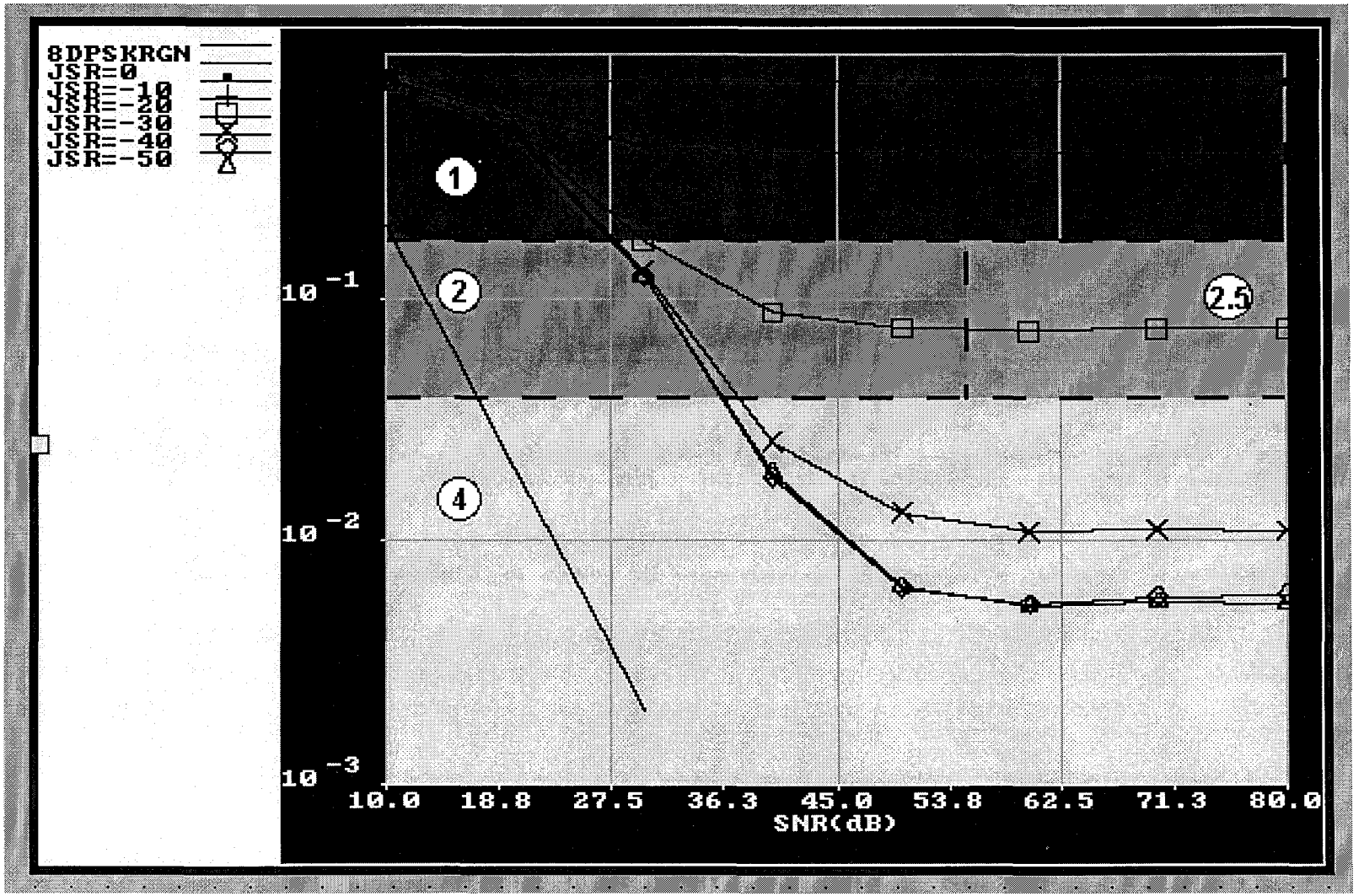

Figure A.2.7. Compressed PCM speech quality for 8-DPSK. Circled numbers represent quality class and ordinate is in units of SER.

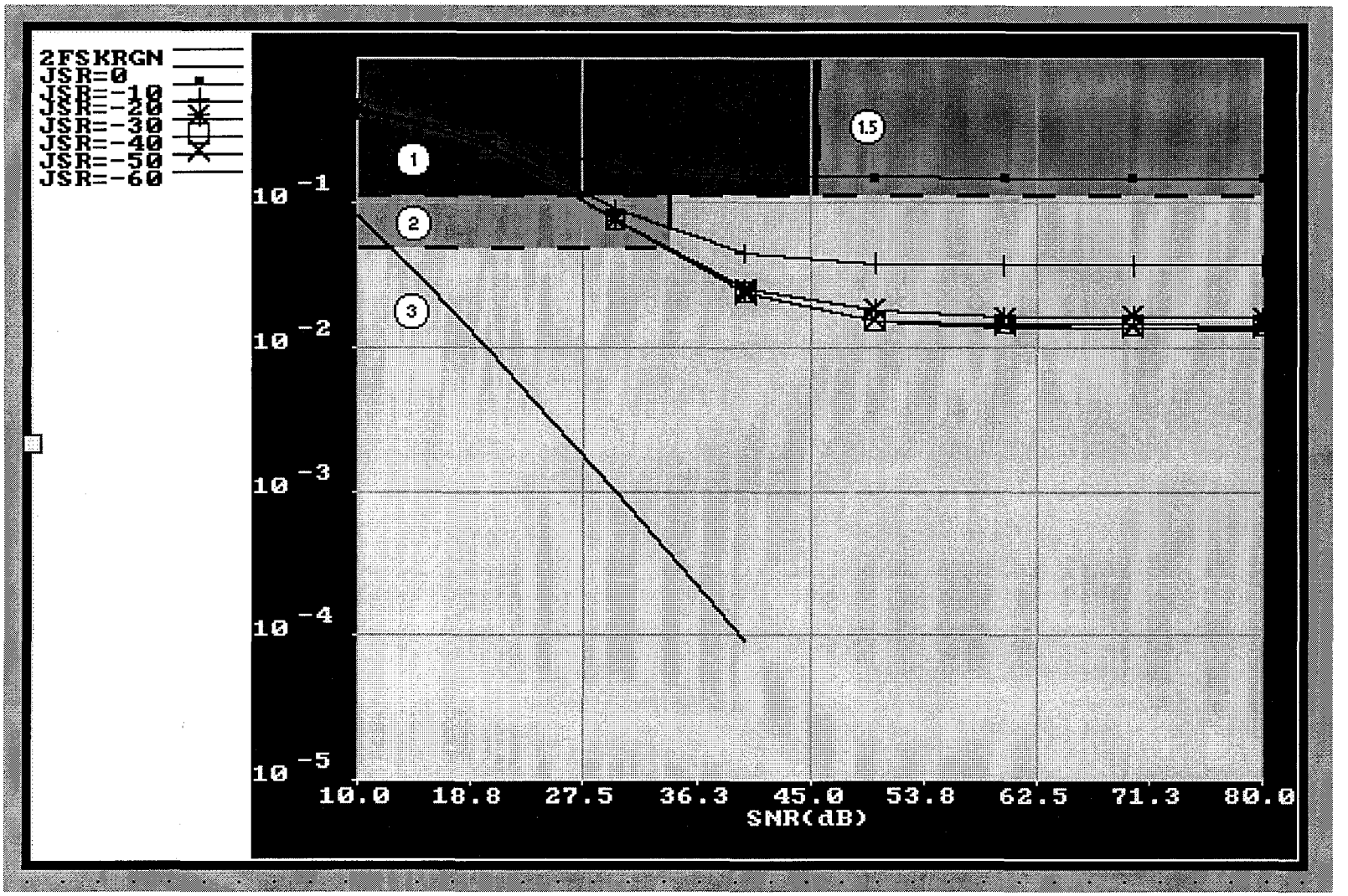

Figure A.2.8. Compressed PCM speech quality for 6-tone, 2-FSK VFCT. Circled numbers represent quality class and ordinate is in units of SER.

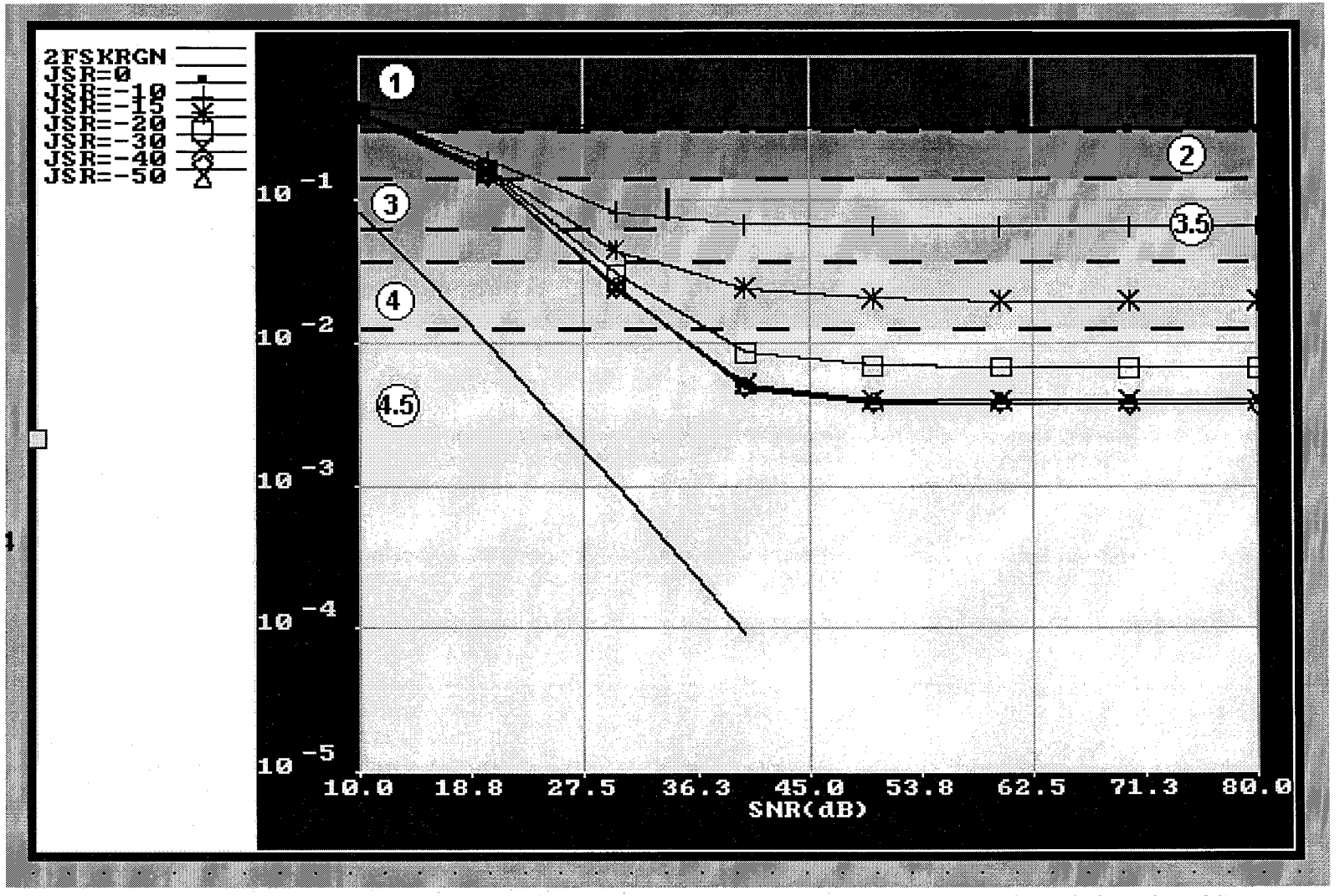

Figure A.3.1. PCM image quality for 2-FSK. Circled numbers represent quality class and ordinate is in units of SER.

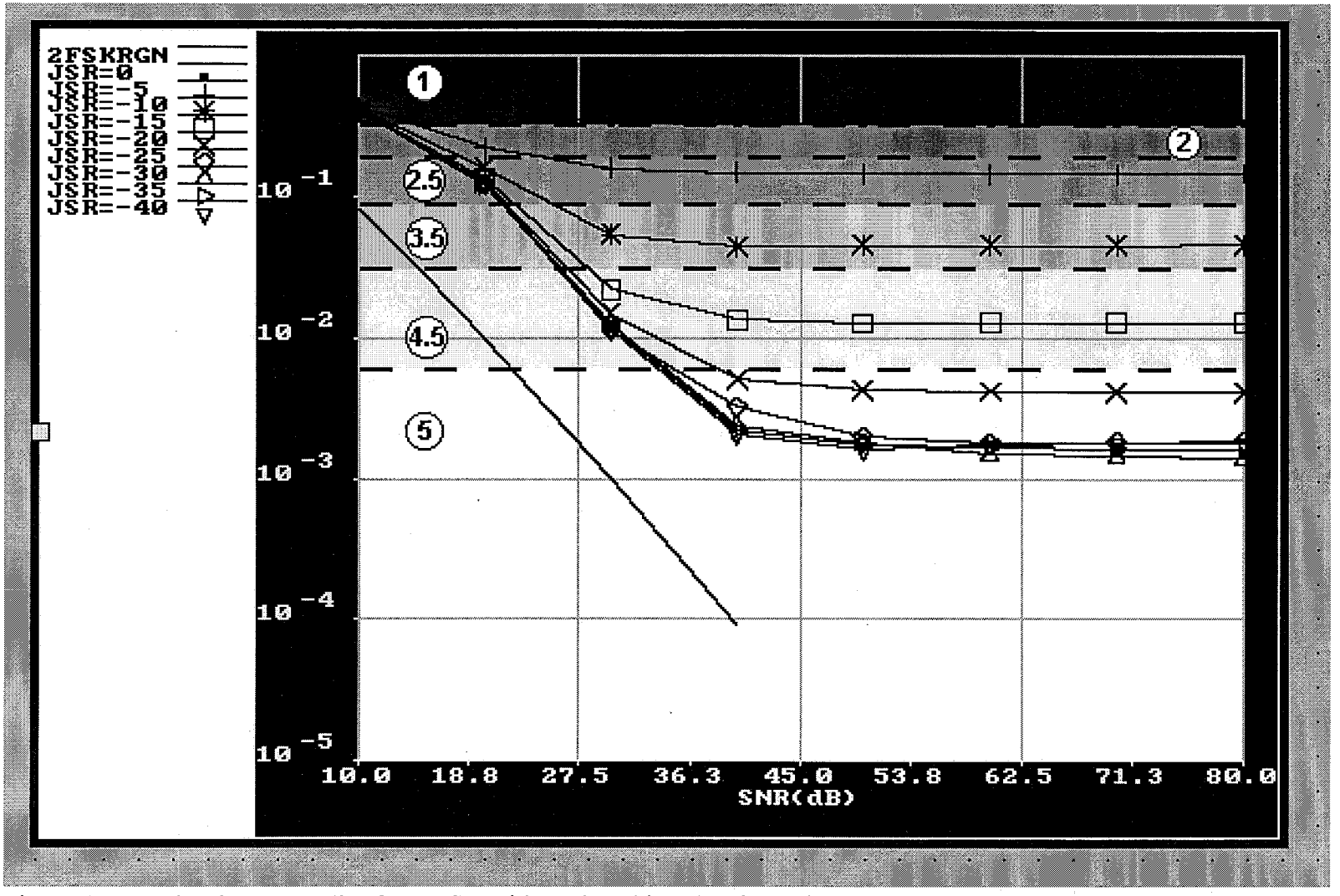

Figure A.3.2. PCM image quality for 2-FSK with FEC and interleaving. Circled numbers represent quality class and ordinate is in units of SER.

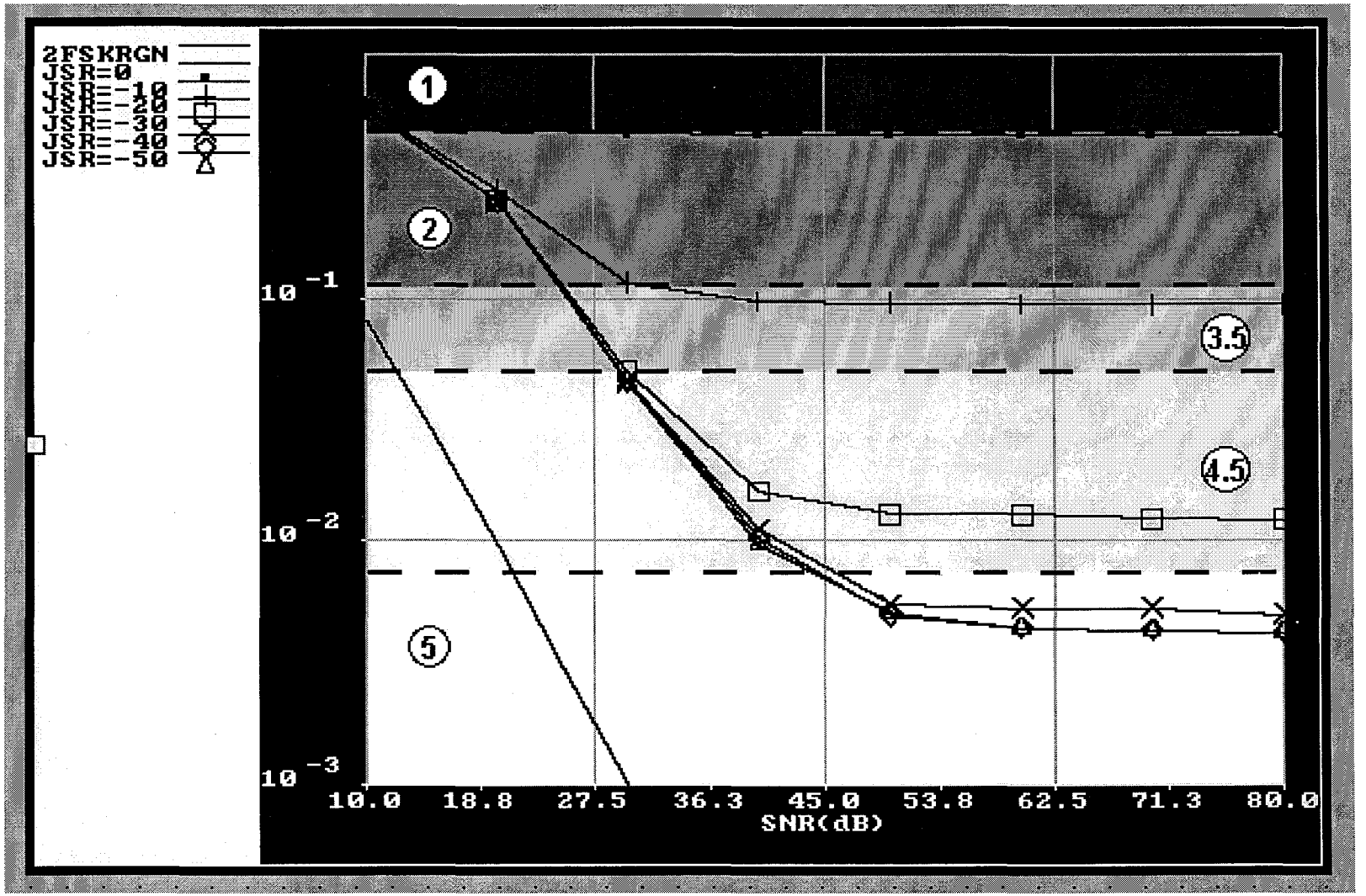

Figure A.3.3. PCM image quality for 4-FSK. Circled numbers represent quality class and ordinate is in units of SER.

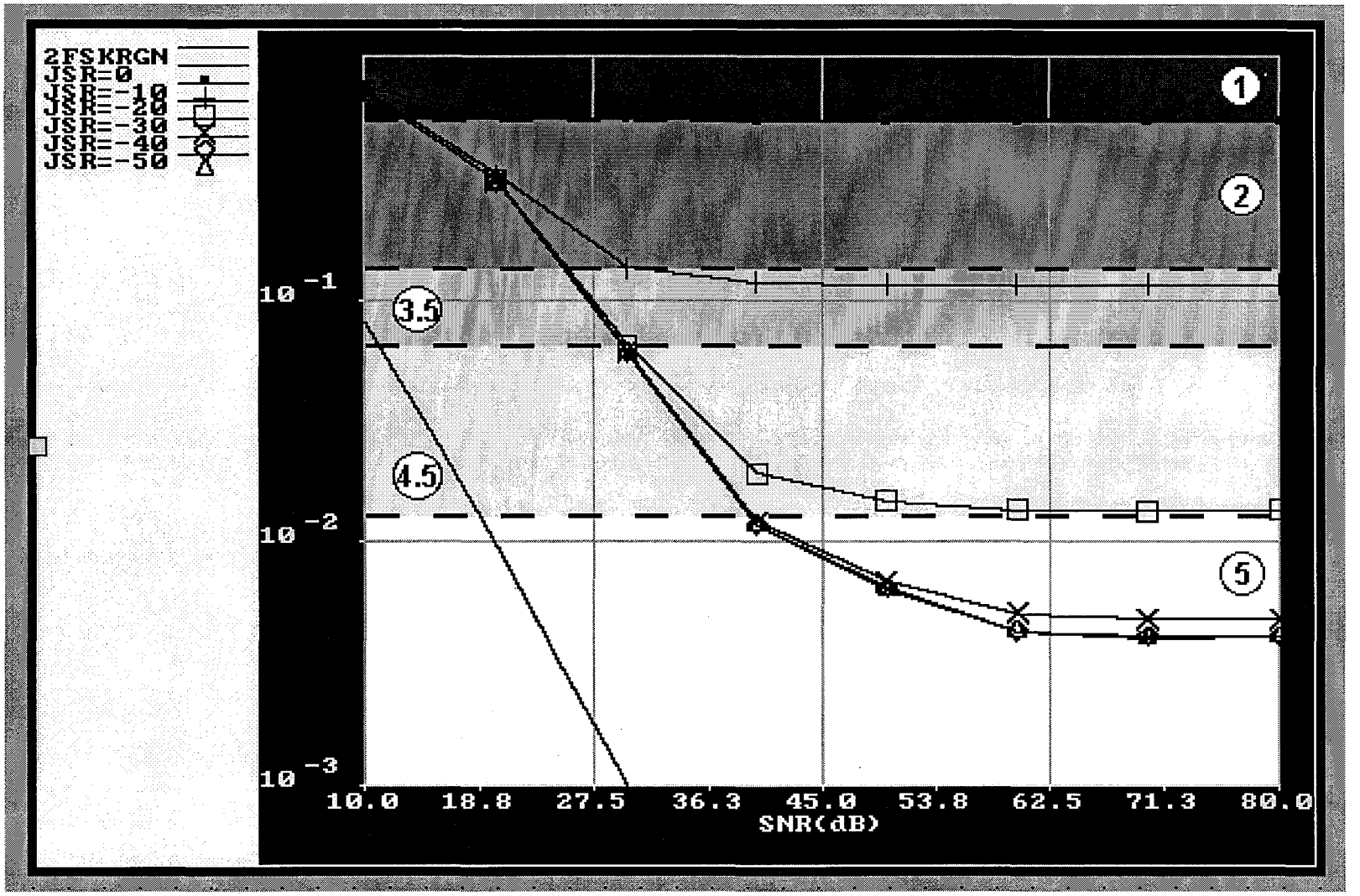

Figure A.3.4. PCM image quality for 8-FSK. Circled numbers represent quality class and ordinate is in units of SER.

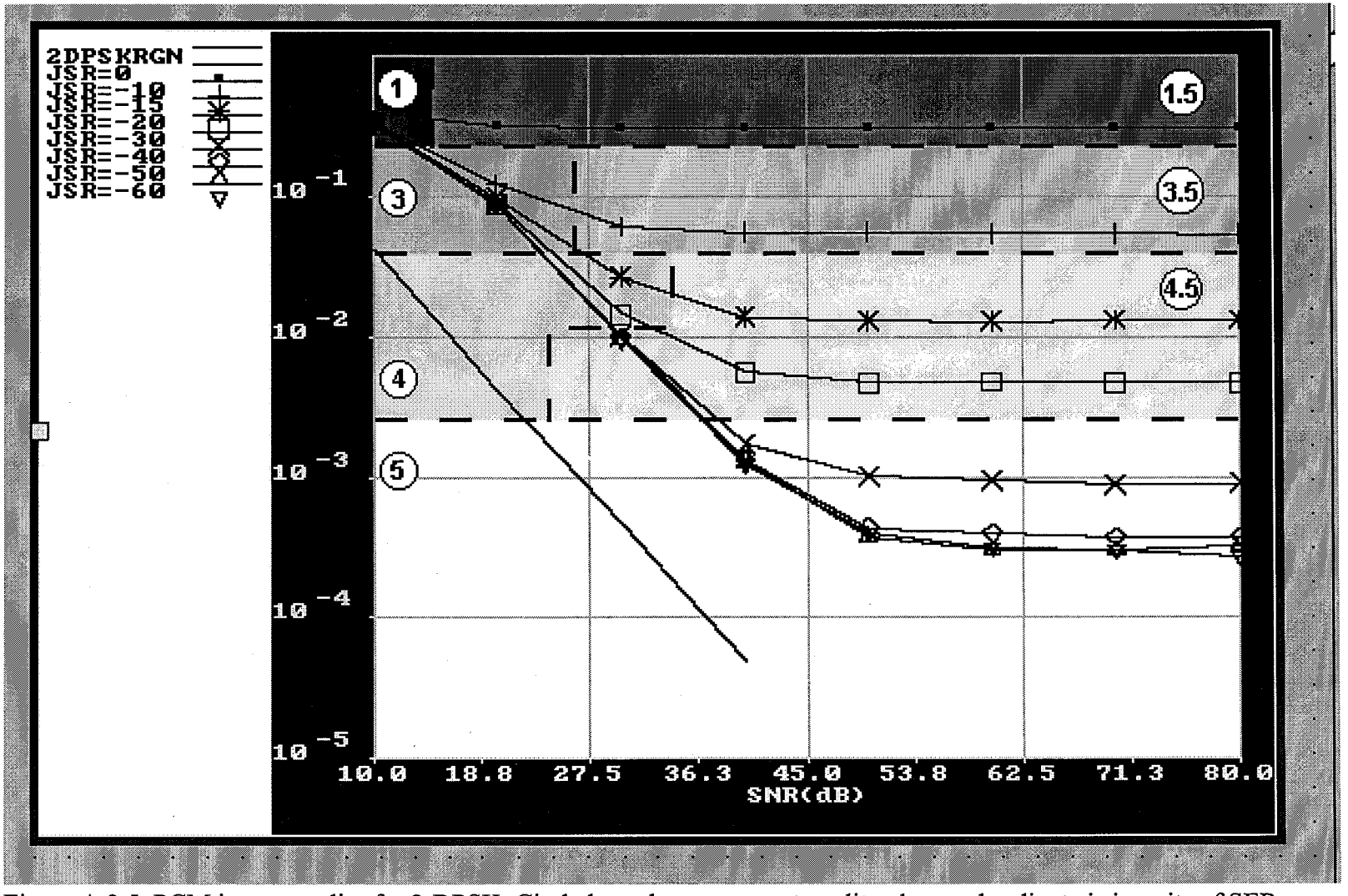

Figure A.3.5. PCM image quality for 2-DPSK. Circled numbers represent quality class and ordinate is in units of SER.

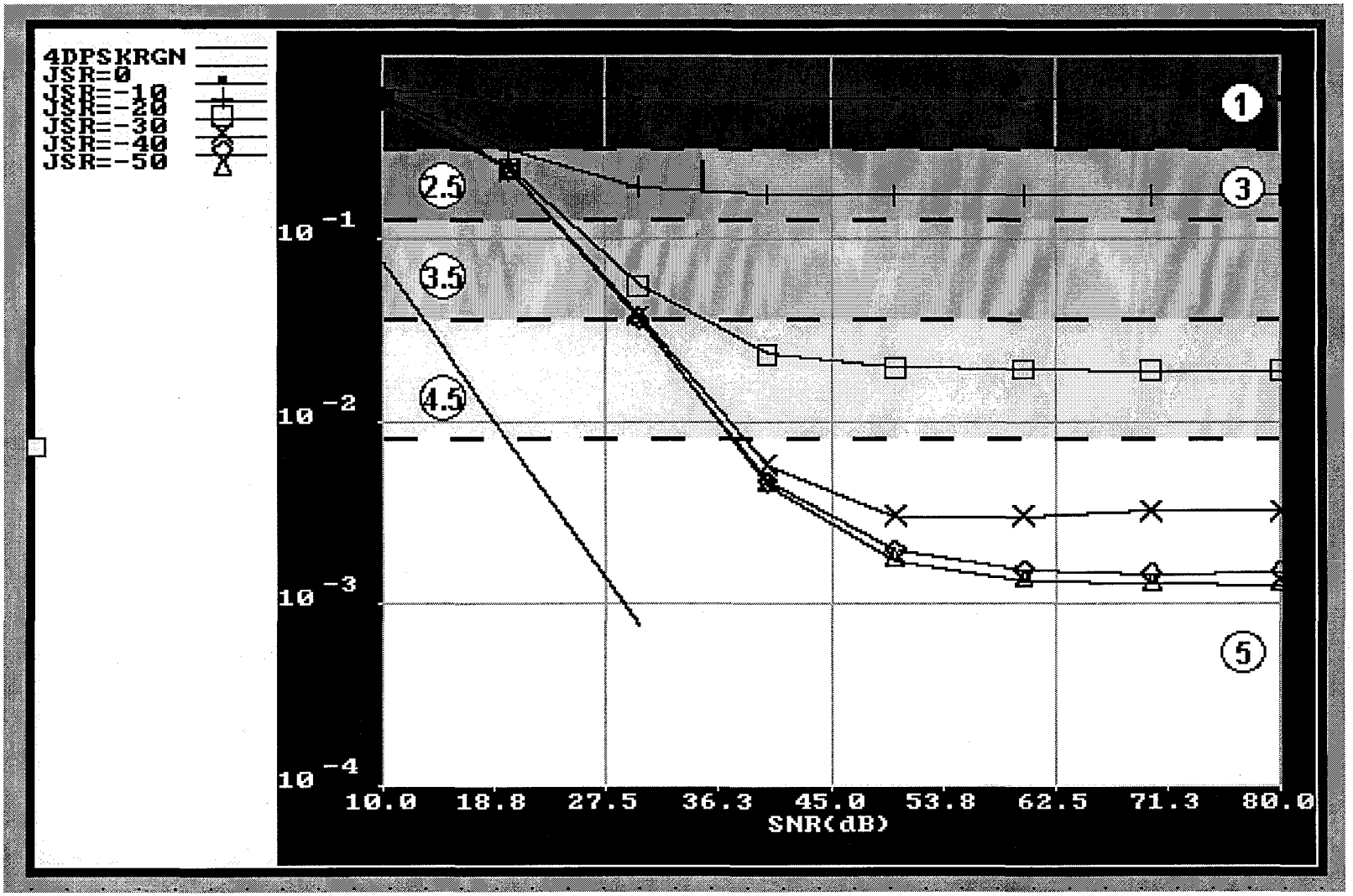

Figure A.3.6. PCM image quality for 4-DPSK. Circled numbers represent quality class and ordinate is in units of SER.

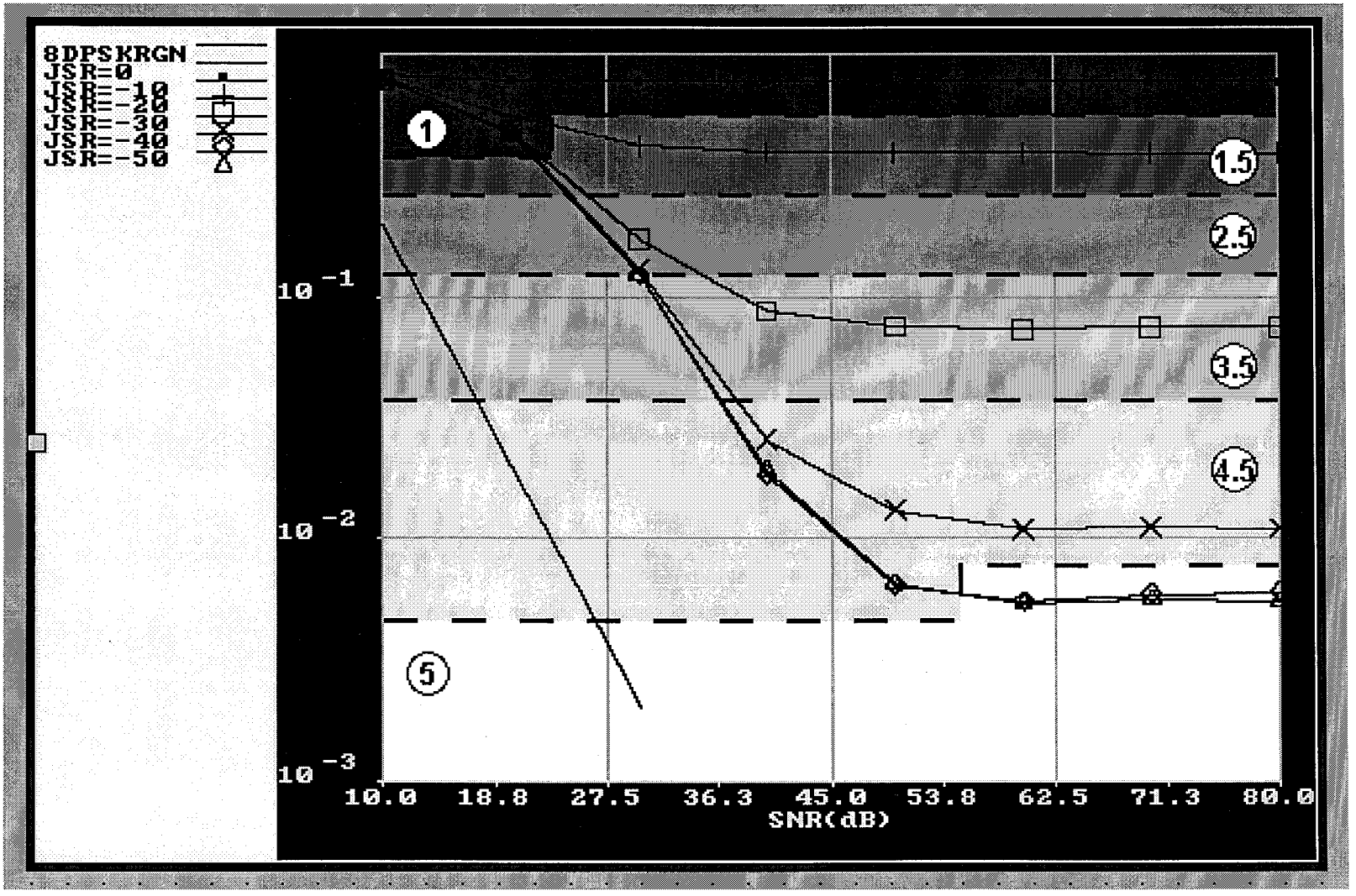

Figure A.3.7. PCM image quality for 8-DPSK. Circled numbers represent quality class and ordinate is in units of SER.

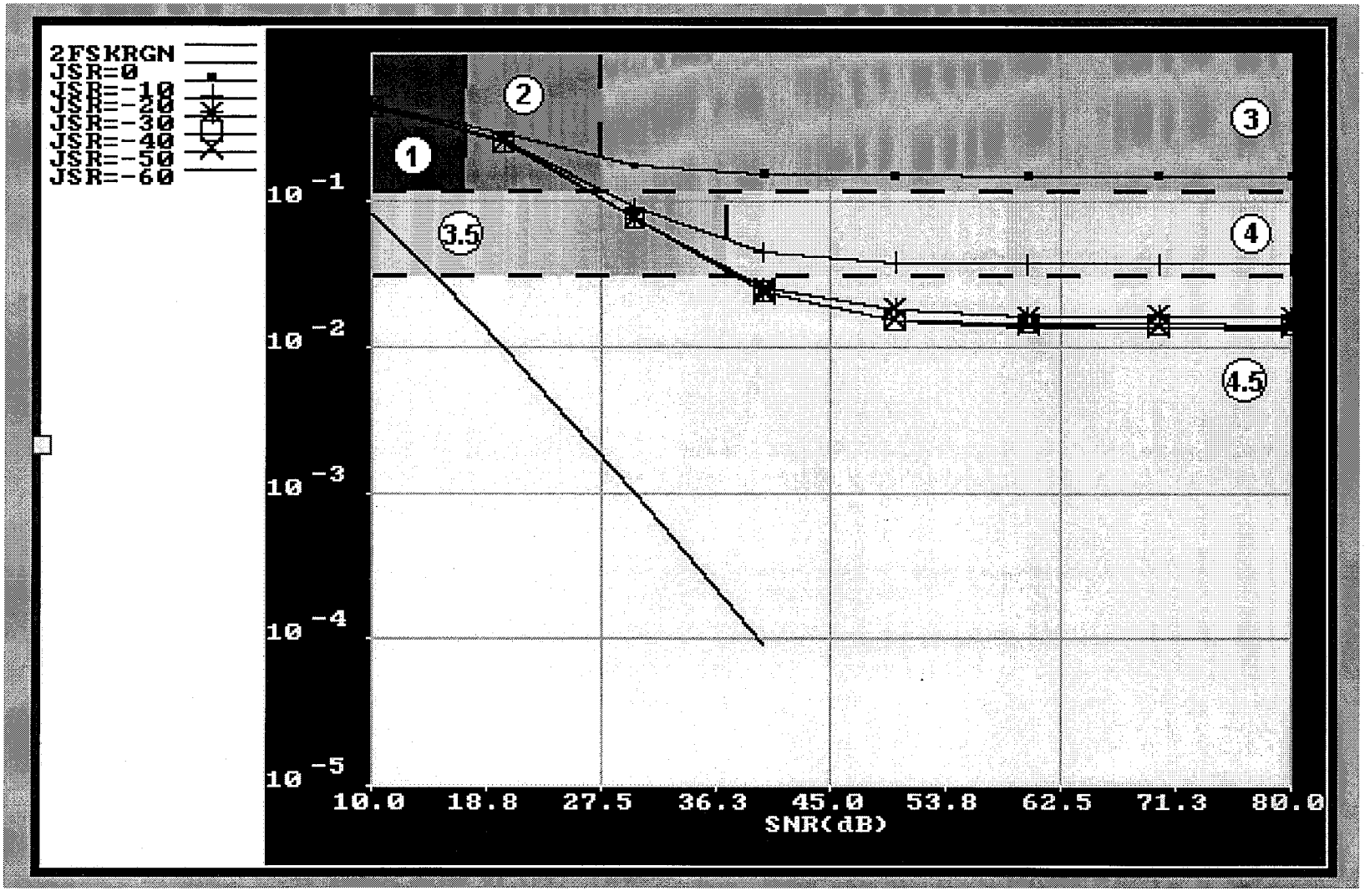

Figure A.3.8. PCM image quality for 6-tone, 2-FSK VFCT. Circled numbers represent quality class and ordinate is in units of SER.

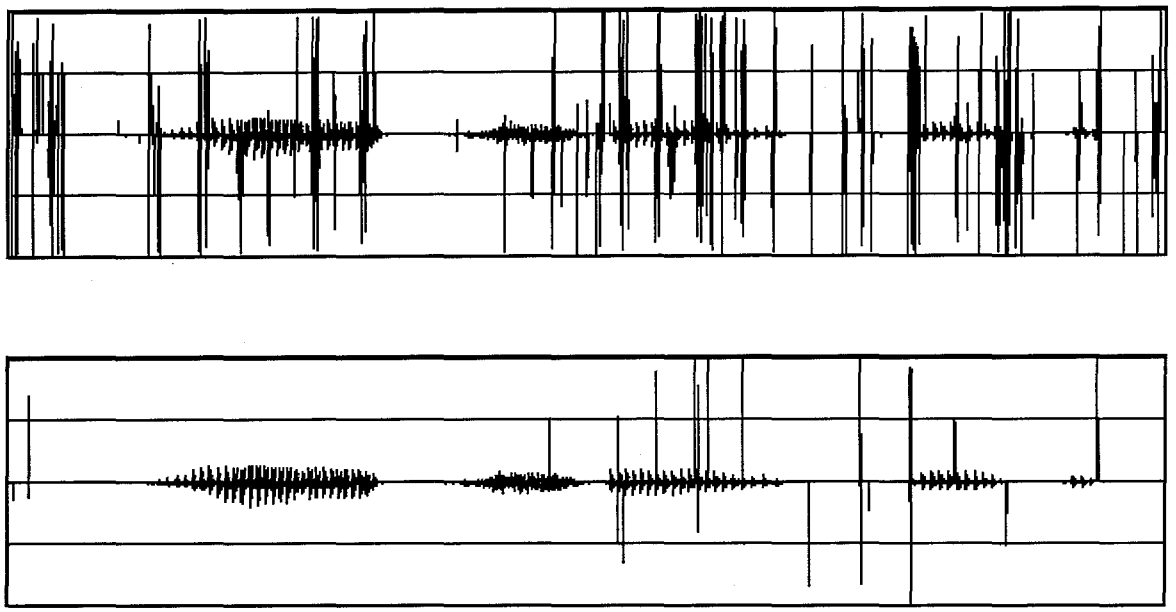

Figure A.4.1. PCM speech waveform for 2-FSK. Top waveform represents class 2.0 [SNR=30 dB, SIR=20 dB, BER=2.6e-2] and bottom waveform represents class 3.8 [SNR=70 dB, SIR=30 dB, BER=3.6e-3].

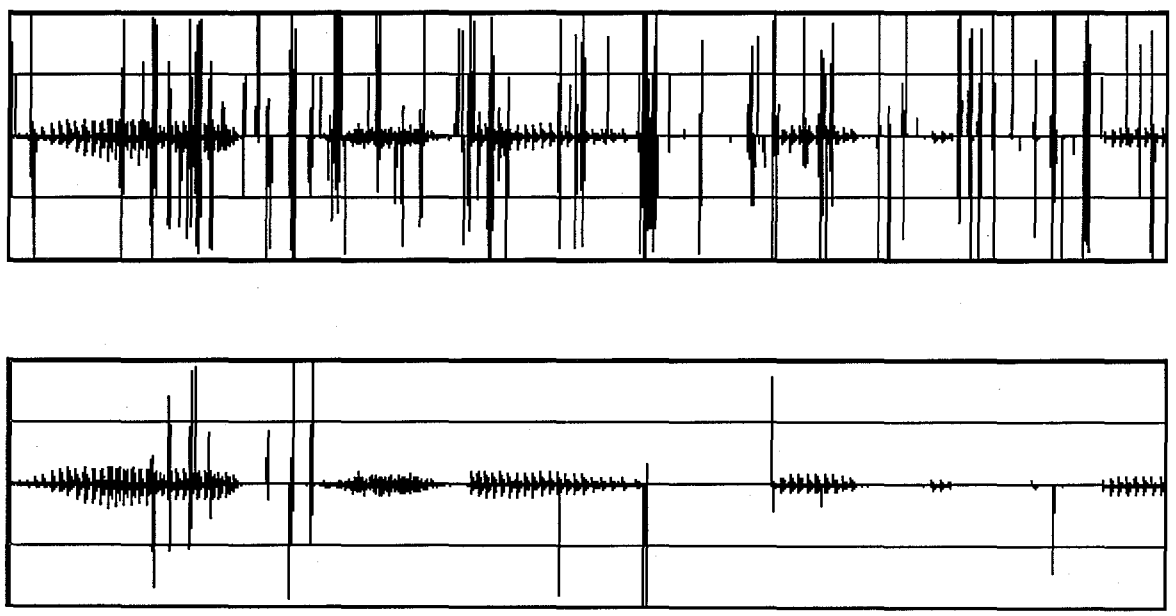

Figure A.4.2. PCM speech waveform for 2-FSK with FEC and interleaving. Top waveform represents class 2.0 [SNR=30 dB, SIR=15 dB, BER=2.1e-2 and bottom waveform represents class 3.8 [SNR=80 dB, SIR=30 dB, BER=1.3e-3].

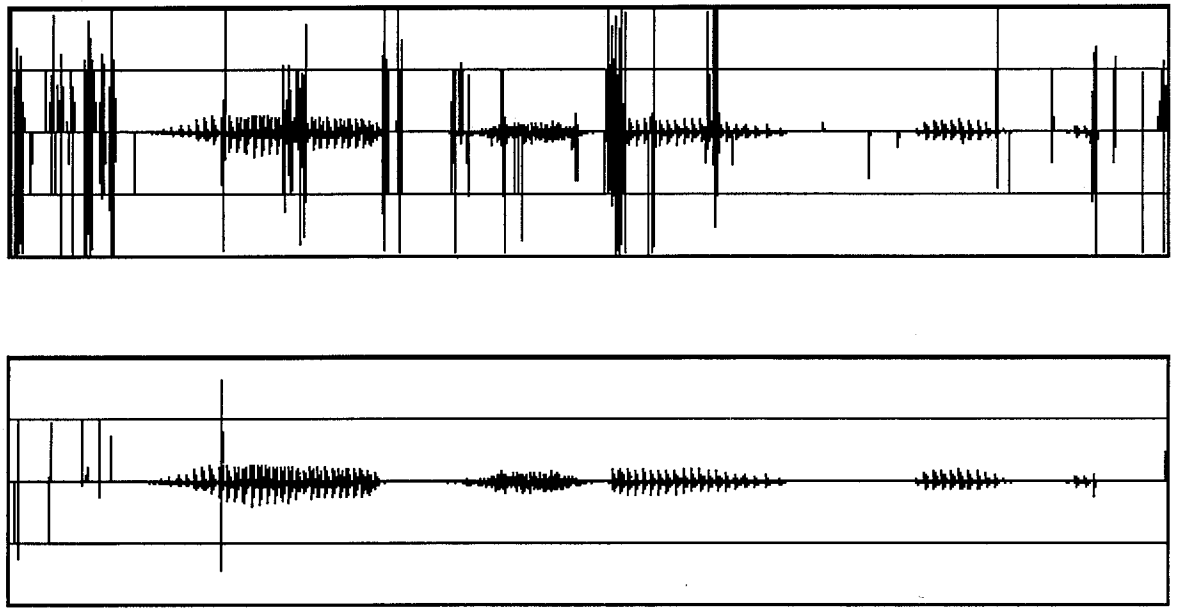

Figure A.4.3. PCM speech waveform for 4-FSK. Top waveform represents class 2.0 [SNR=30 dB, SIR=20 dB, SER=5.0e-2, BER=2.9e-2] and bottom waveform represents class 3.2 [SNR=80 dB, SIR=40 dB, SER=4.2e-3, BER=2.5e-3].

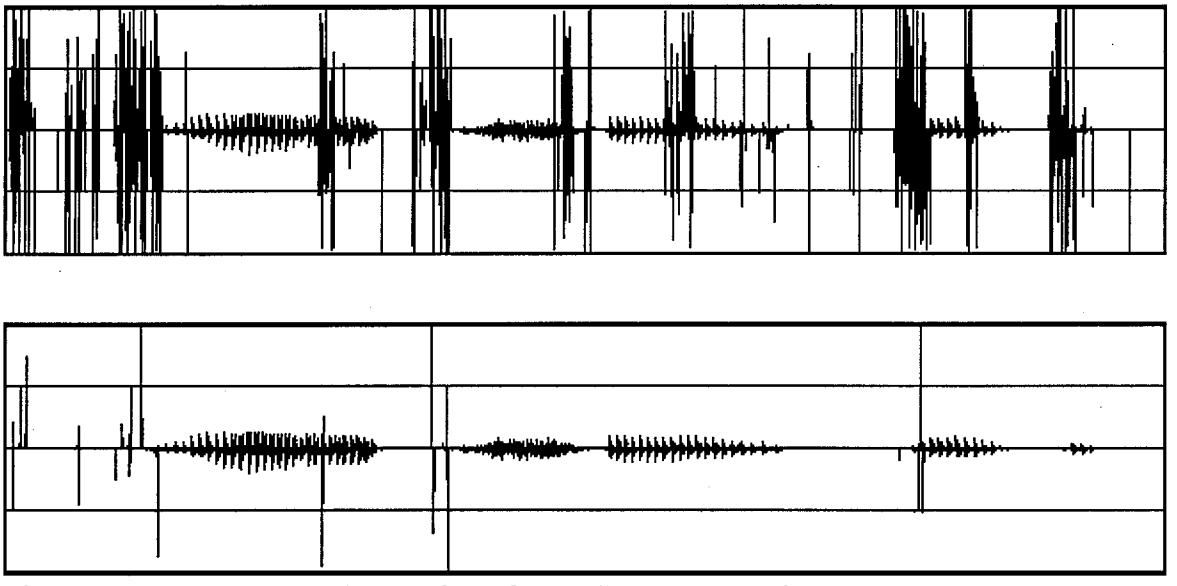

Figure A.4.4. PCM speech waveform for 8-FSK. Top waveform represents class 2.0 [SNR=30 dB, SIR=20 dB, SER=6.5e-2, BER=2.8e-2] and bottom waveform represents class 3.0 [SNR=70 dB, SIR=40 dB, SER=4.1e-3, BER=1.7e-3].

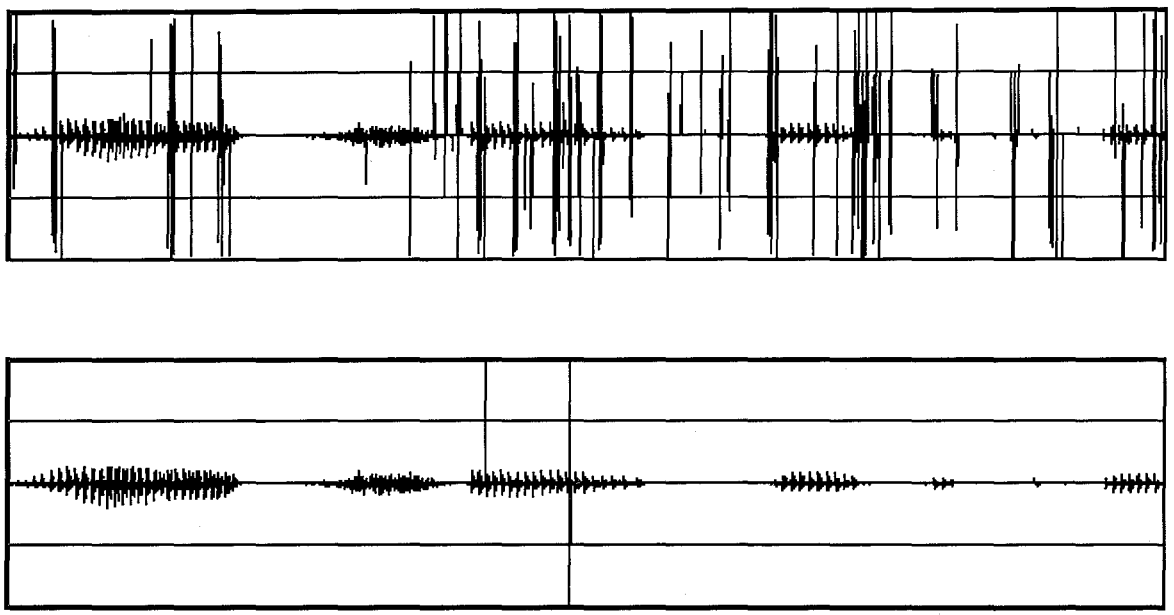

Figure A.4.5. PCM speech waveform for 2-DPSK. Top waveform represents class 2.0 [SNR=30 dB, SIR=15 dB, BER=2.5e-2] and bottom waveform represents class 5.0 [SNR=80 dB, SIR=40 dB, BER=5.0e-4].

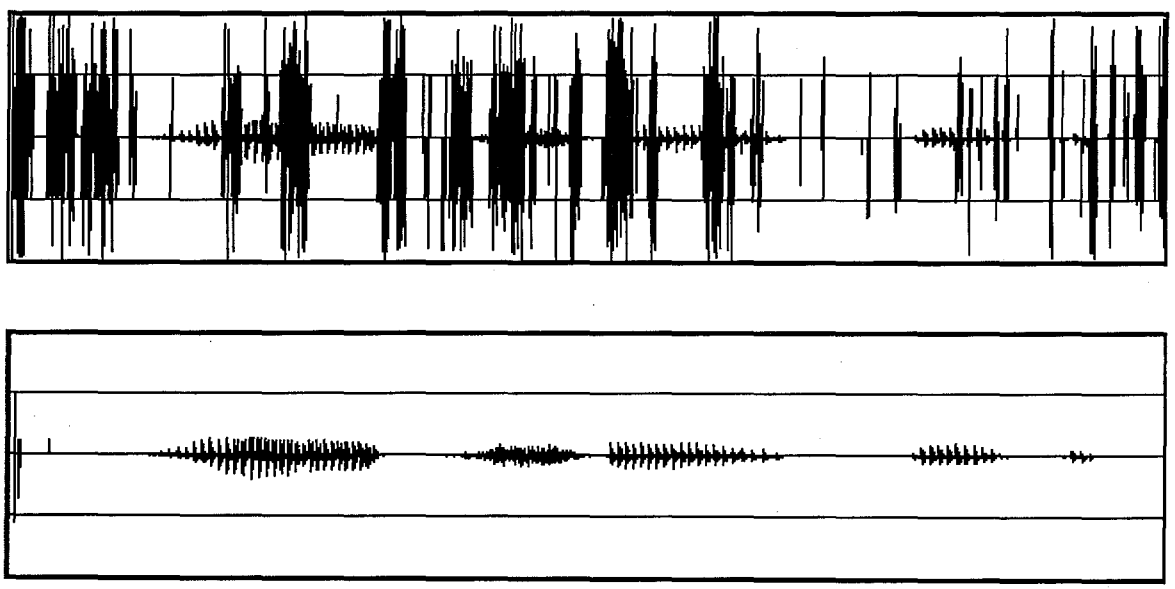

Figure A.4.6. PCM speech waveform for 4-DPSK. Top waveform represents class 1.3 [SNR=70 dB, SIR=10 dB, SER=1.7e-1, BER=1.2e-1] and bottom waveform represents class 4.0 [SNR=80 dB, SIR=50 dB, SER=1.2e-3, BER=1.0e-3].

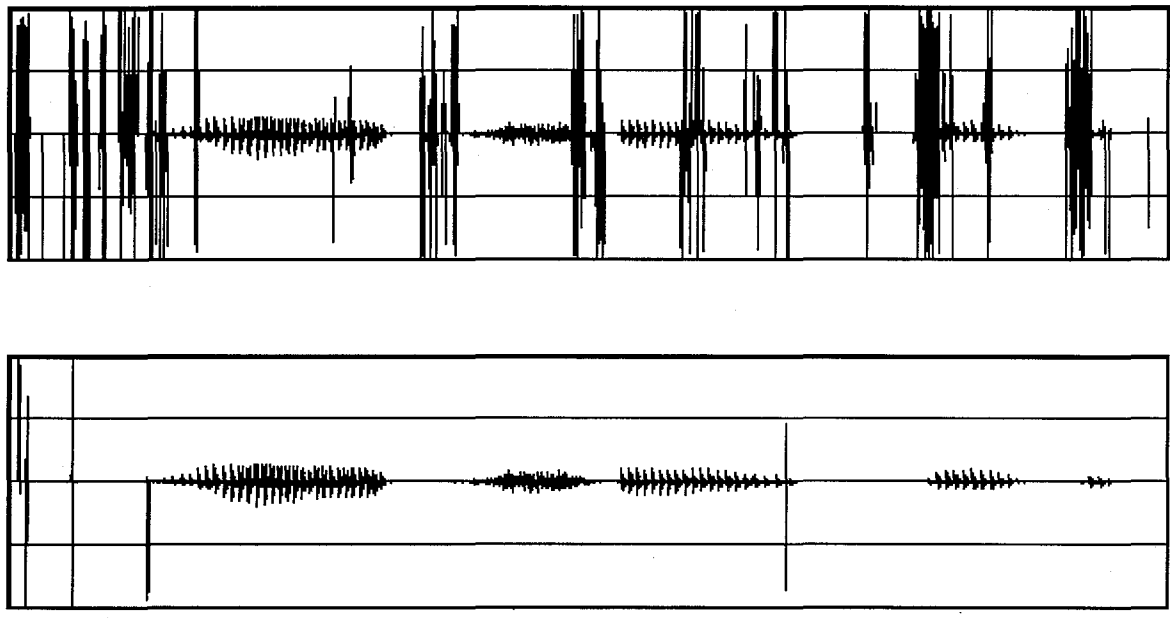

Figure A.4.7. PCM speech waveform for 8-DPSK. Top waveform represents class 2.0 [SNR=60 dB, SIR=20 dB, SER=7.4e-2, BER=3.9e-2] and bottom waveform represents class 3.5 [SNR=80 dB, SIR=50 dB, SER=5.5e-3, BER=3.1e-3].

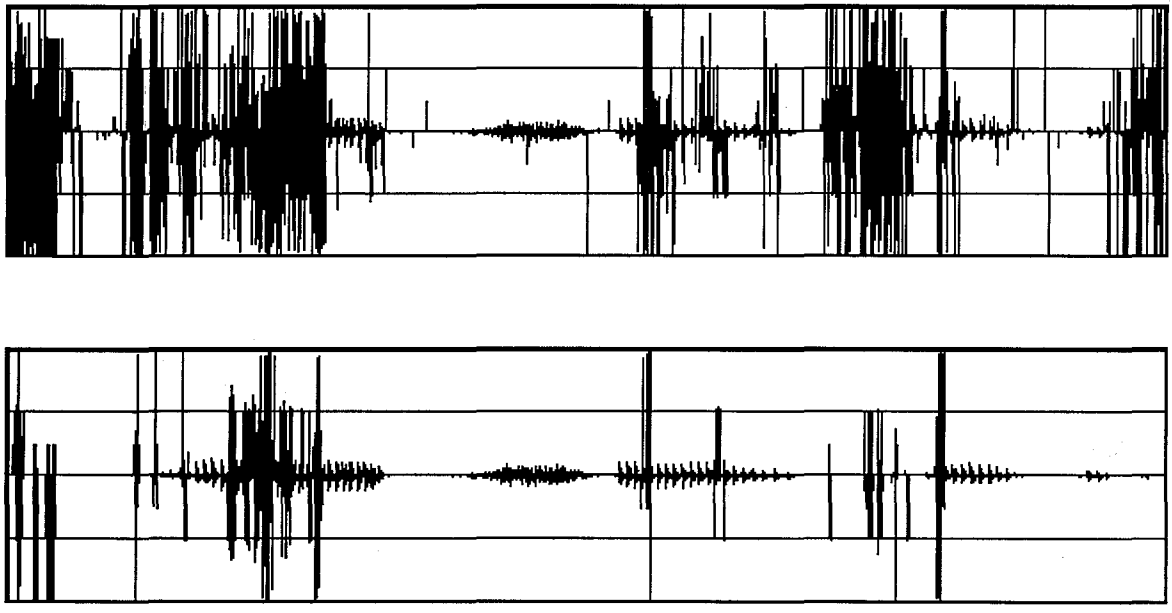

Figure A.4.8. PCM speech waveform for 6-tone 2-FSK VFCT. Top waveform represents class 1.7 [SNR=30 dB, SIR=10 dB, BER=3.7e-2] and bottom waveform represents class 3.0 [SNR=80 dB, SIR=50 dB, BER=7.5e-3].

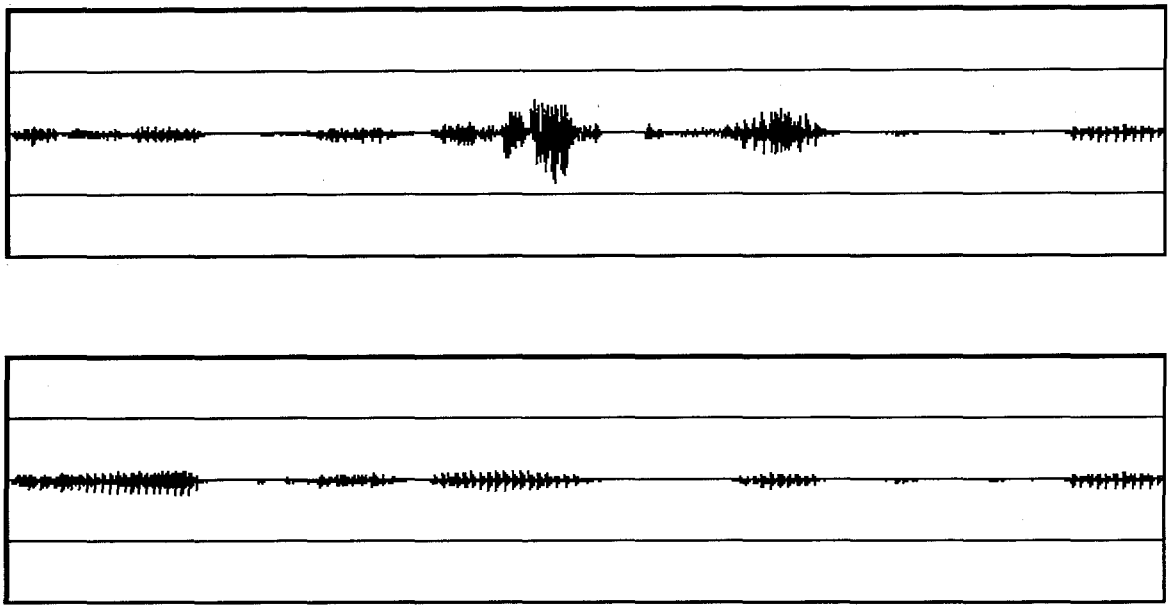

Figure A.5.1. Compressed PCM speech waveform for 2-FSK. Top waveform represents class 2.0 [SNR=30 dB, SIR=10 dB, BER=7.0e-2] and bottom waveform represents class 4.0 [SNR=80 dB, SIR=30 dB, BER=1.2e-3].

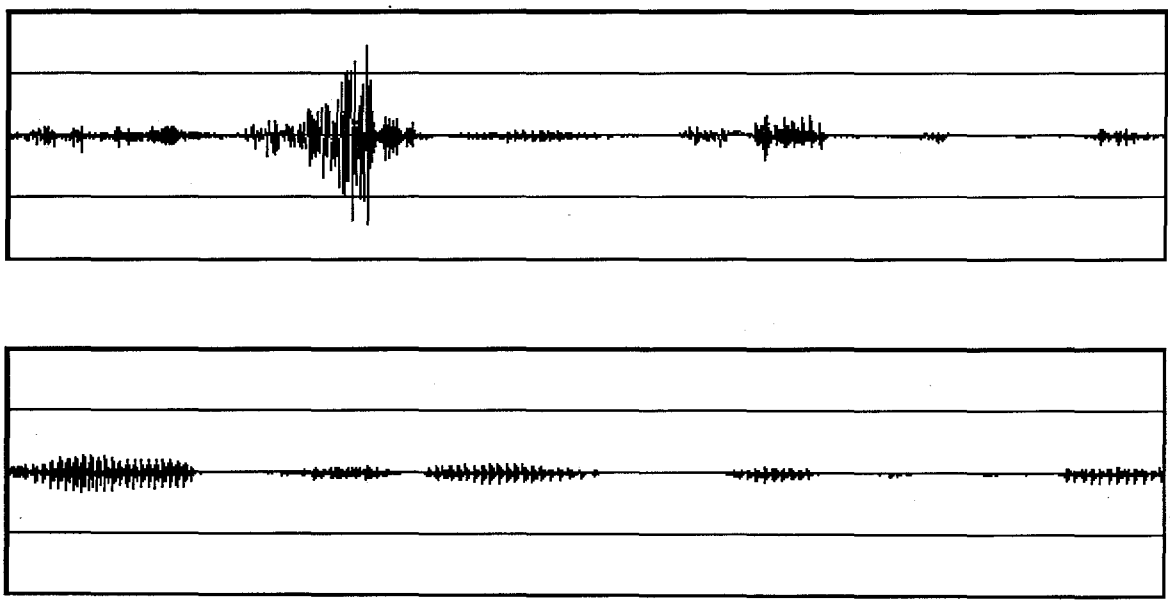

Figure A.5.2. Compressed PCM speech waveform for 2-FSK with FEC and interleaving. Top waveform represents class 2.0 [SNR=20 dB, SIR=10 dB, BER=1.2e-1] and bottom waveform represents class 5.0 [SNR=70 dB, SIR=30 dB, BER=0.0e-0].

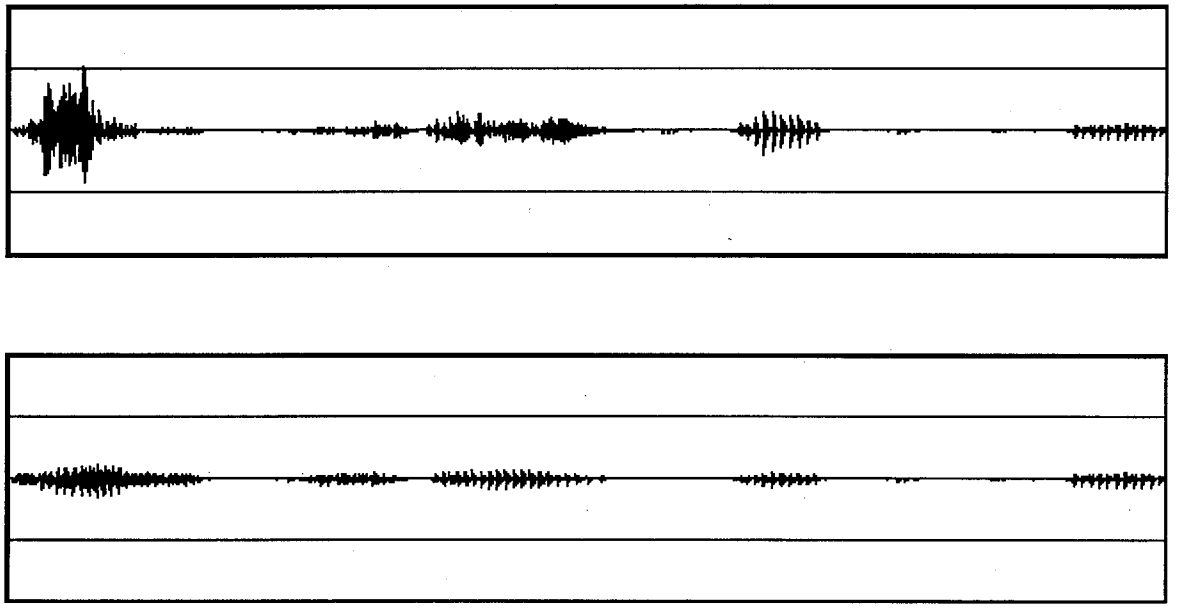

Figure A.5.3. Compressed PCM speech waveform for 4-FSK. Top waveform represents class 1.5 [SNR=30 dB, SIR=10 dB, SER=1.2e-1, BER=7.2e-2] and bottom waveform represents class 4.0 [SNR=80 dB, SIR=40 dB, SER=4.2e-3, BER=3.0e-3].

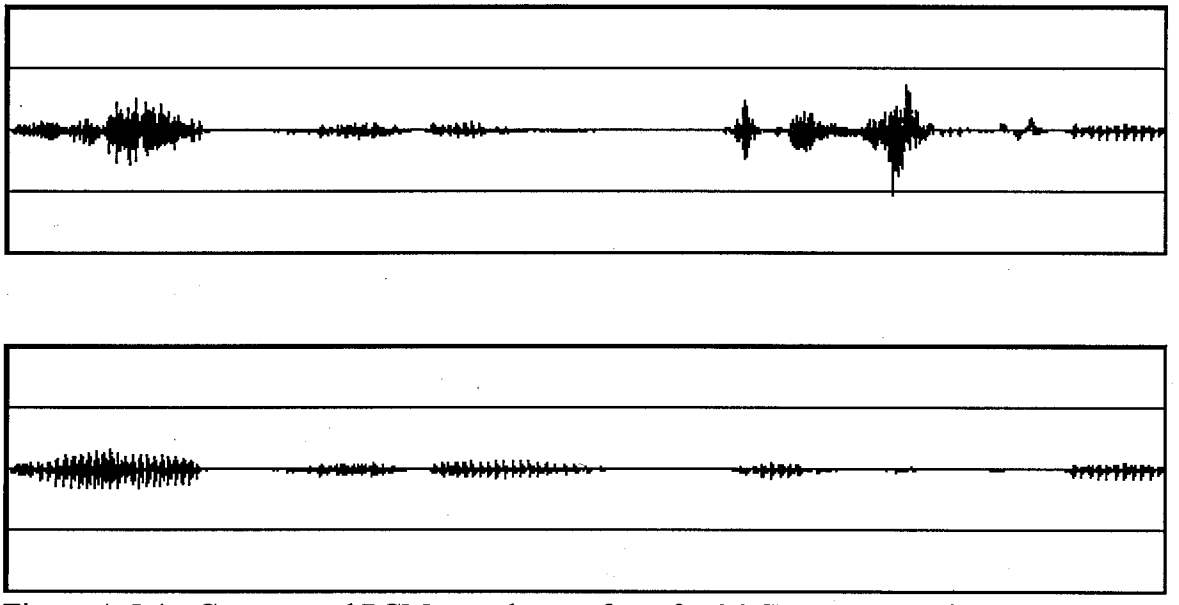

Figure A.5.4. Compressed PCM speech waveform for 8-FSK. Top waveform represents class 1.8 [SNR=40 dB, SIR=10 dB, SER=1.2e-1, BER=8.8e-2] and bottom waveform represents class 4.5[SNR=70 dB, SIR=40 dB, SER=4.1e-3, BER=3.2e-3].

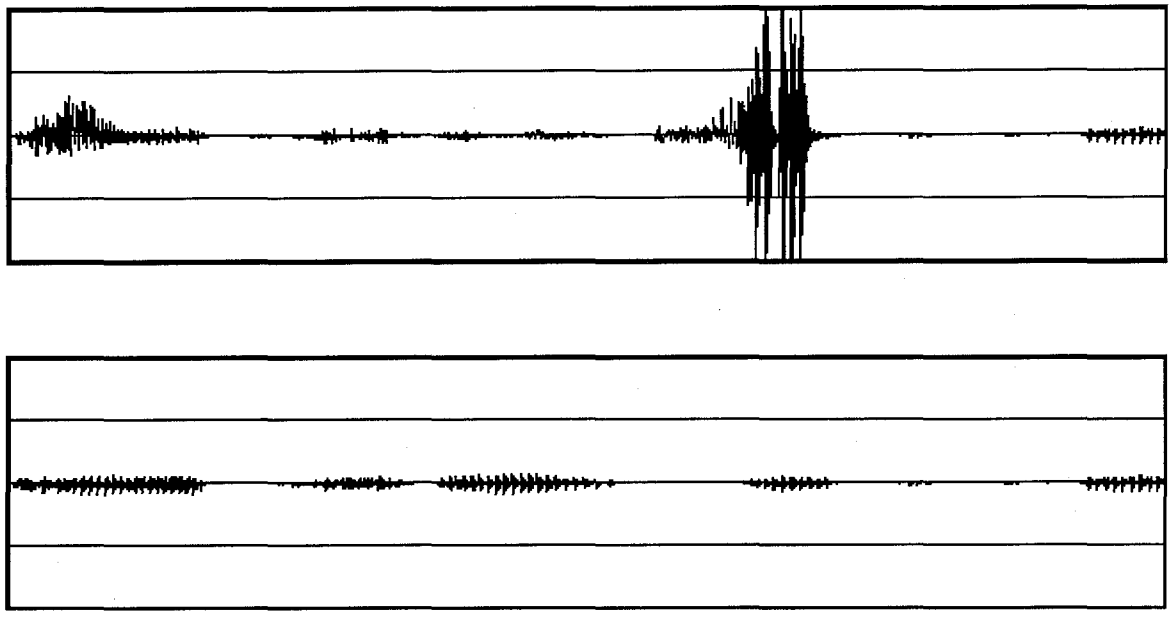

Figure A.5.5. Compressed PCM speech waveform for 2-DPSK. Top waveform represents class 2.0 [SNR=30 dB, SIR=10 dB, BER=5.1e-2] and bottom waveform represents class 5.0 [SNR=80 dB, SIR=40 dB, BER=4.0e-3].

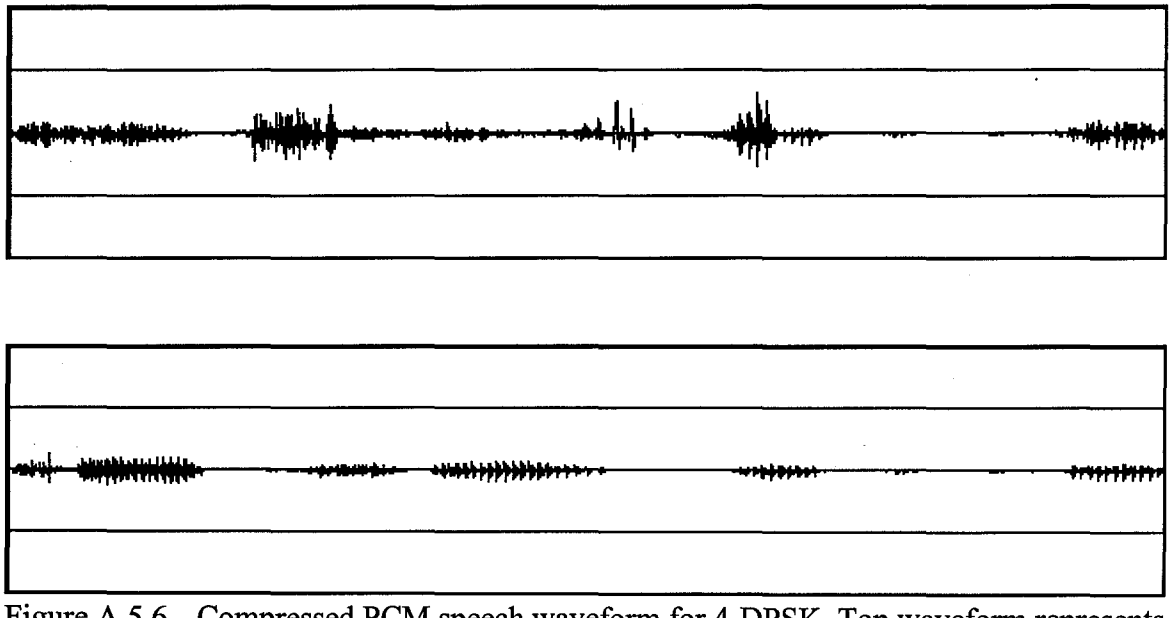

Figure A.5.6. Compressed PCM speech waveform for 4-DPSK. Top waveform represents class 1.5 [SNR=50 dB, SIR=10 dB, SER=1.7e-1, BER=1.2e-1] and bottom waveform represents class 4.5 [SNR=80 dB, SIR=50 dB, SER=1.2e-3, BER=1.3e-3].

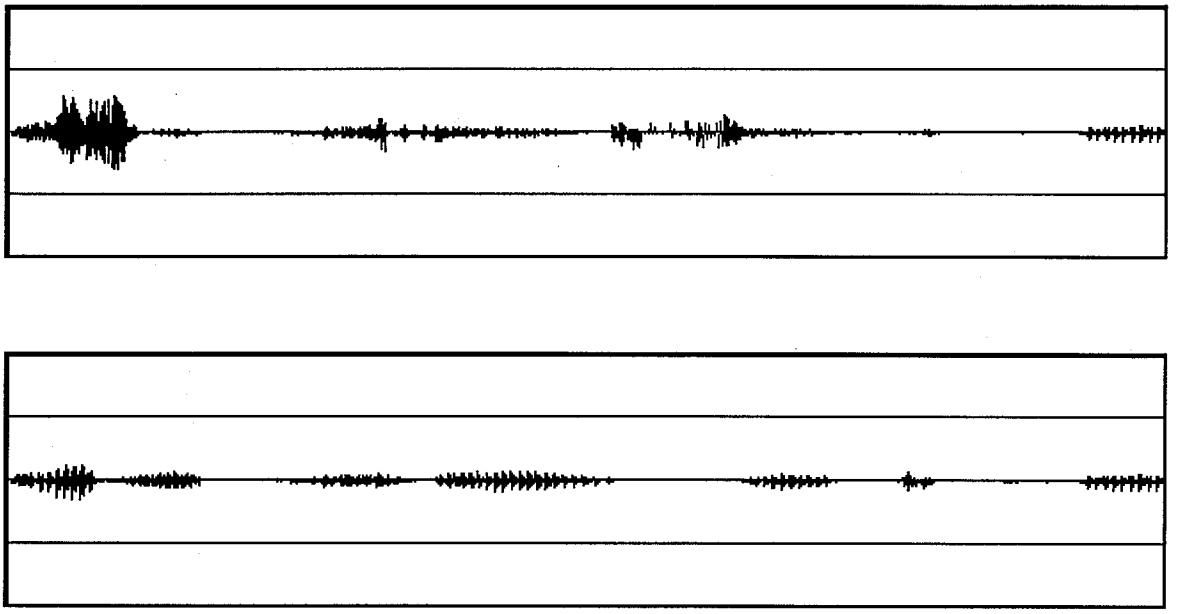

Figure A.5.7. Compressed PCM speech waveform for 8-DPSK. Top waveform represents class 1.8 [SNR=40 dB, SIR=20 dB, SER=8.8e-2, BER=6.8e-2] and bottom waveform represents class 4.0 [SNR=60 dB, SIR=40 dB, SER=5.5e-3, BER=5.9e-3].

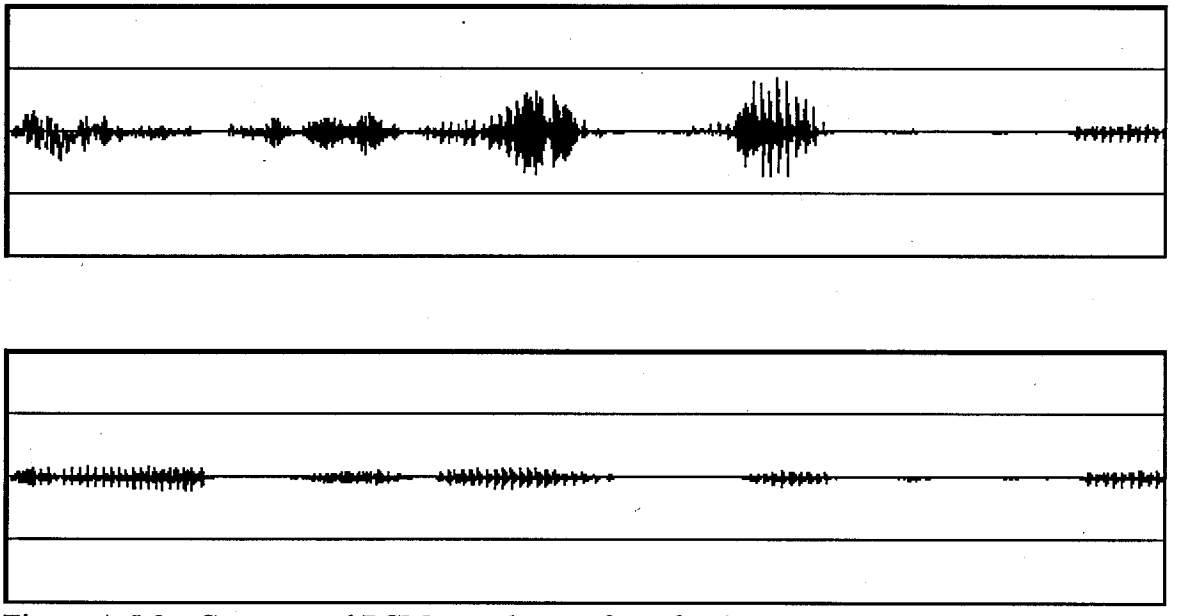

Figure A.5.8. Compressed PCM speech waveform for 6-tone, 2-FSK VFCT. Top waveform represents class 2.0 [SNR=30 dB, SIR=30 dB, BER=7.4e-2] and bottom waveform represents class 3.0 [SNR=80 dB, SIR=50 dB, BER=1.7e-2].

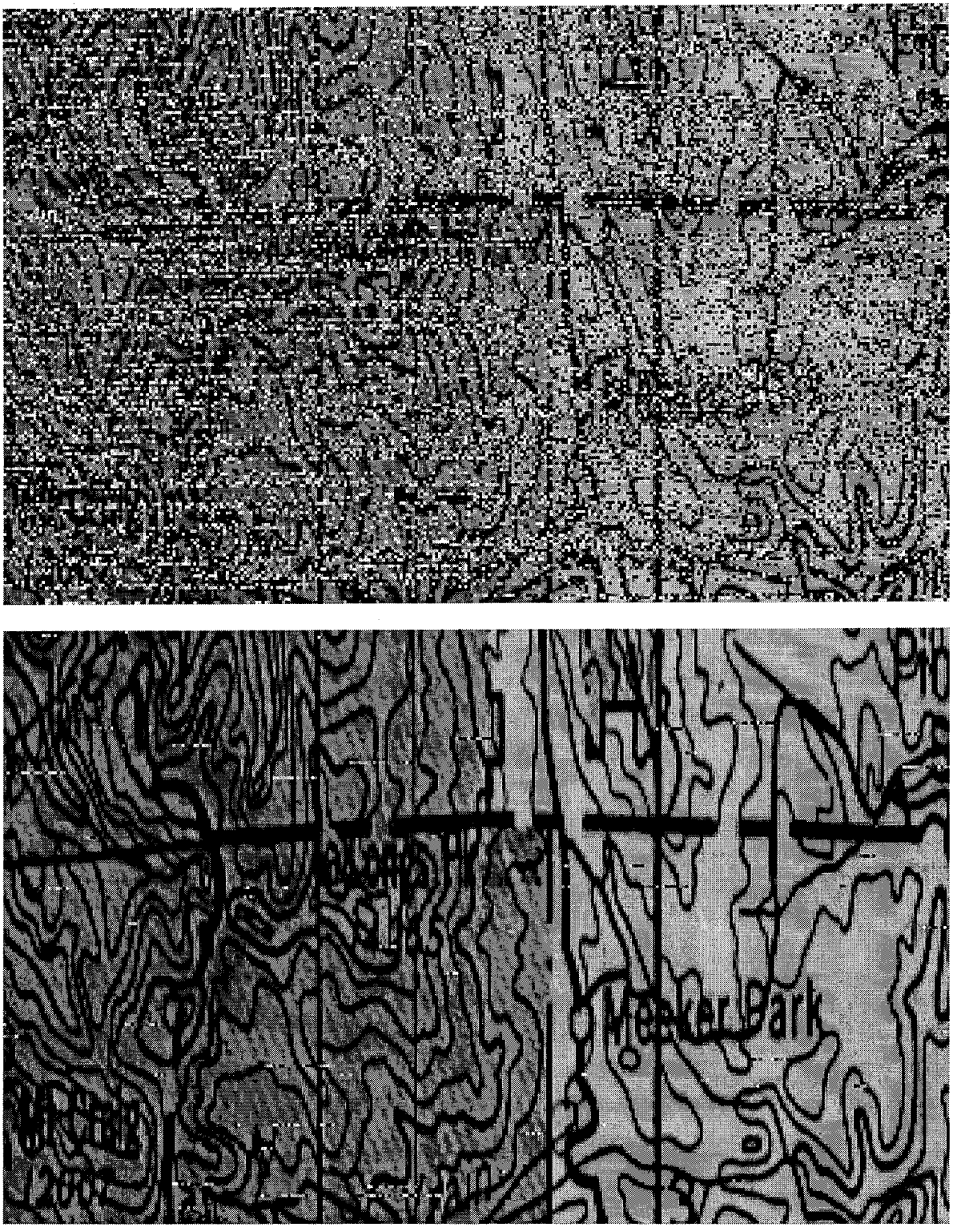

Figure A.6.1. PCM image for 2-FSK. Top image represents class 2.0 [SNR=20 dB, SIR=10 dB, BER=1.7e-1] and bottom image represents class 4.5 [SNR=80 dB, SIR=50 dB, BER=3.6e-3].

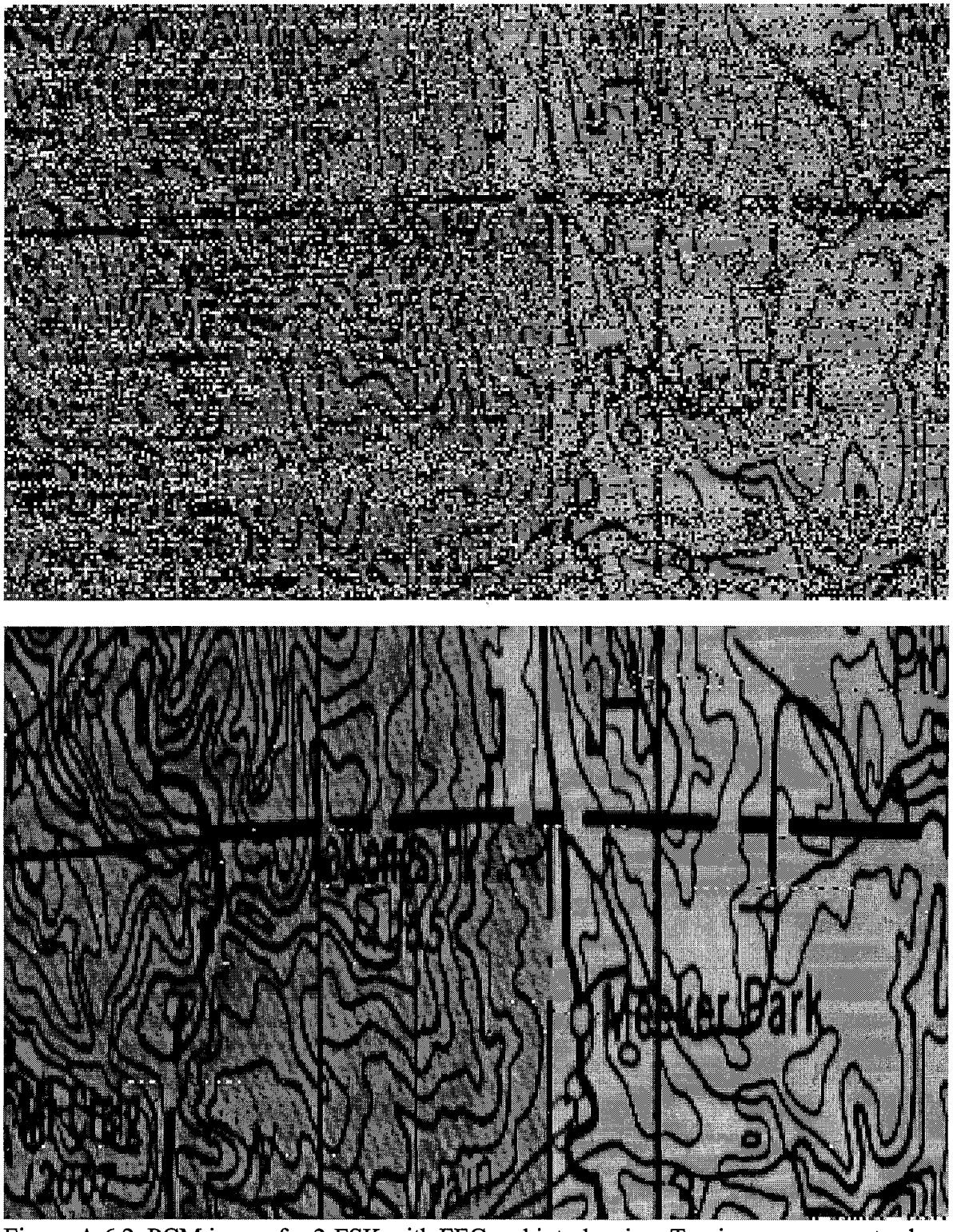

Figure A.6.2. PCM image for 2-FSK with FEC and interleaving. Top image represents class 2.0 [SNR=20 dB, SIR=5 dB, BER=2.0e-1] and bottom image represents class 5.0 [SNR=80 dB, SIR=30 dB, BER=1.2e-3].

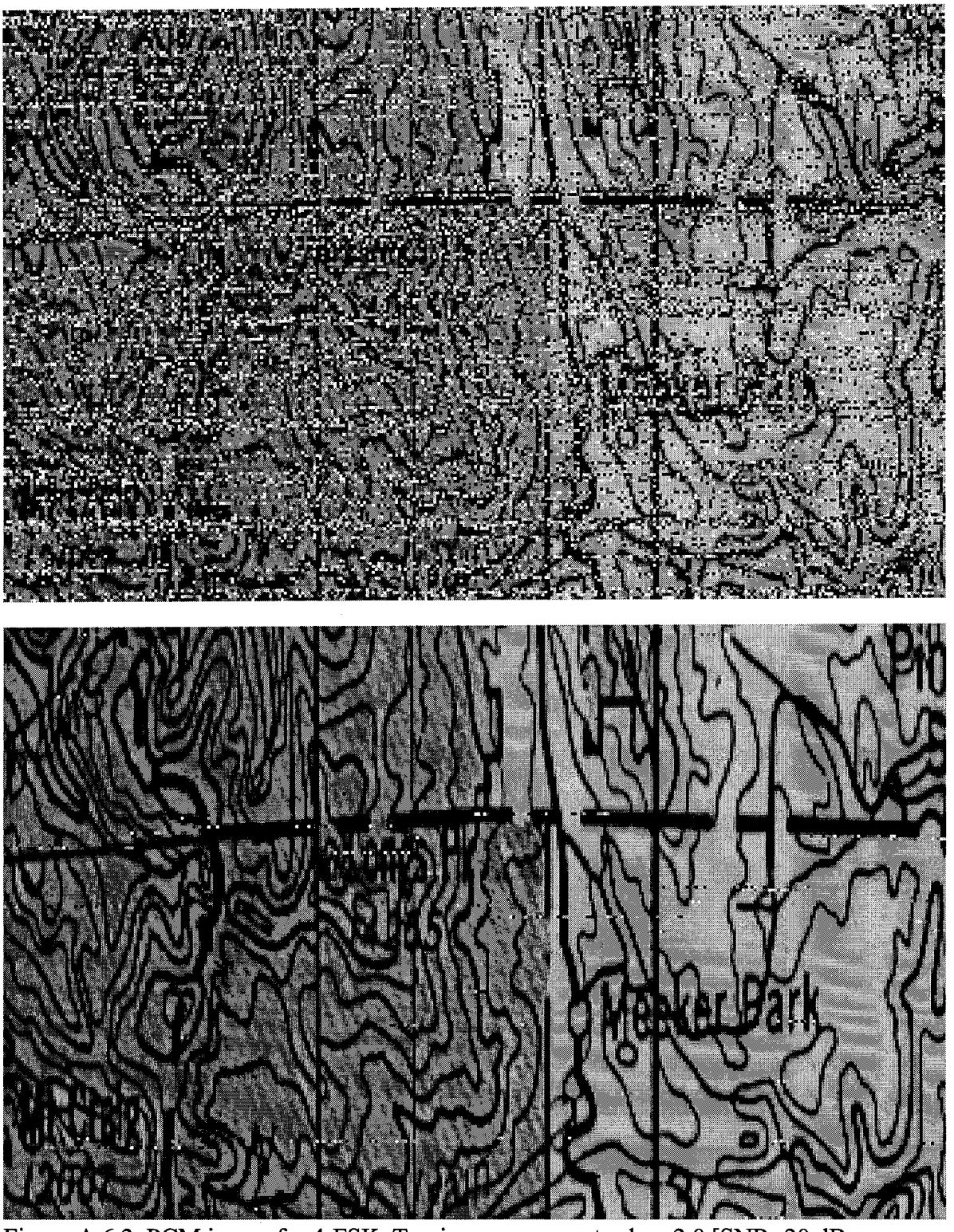

Figure A.6.3. PCM image for 4-FSK. Top image represents class 2.0 [SNR=20 dB, SIR=20 dB, BER=1.6e-1] and bottom image represents class 5.0 [SNR=80 dB, SIR=50 dB, SER=4.2e-3, BER=2.2e-3].

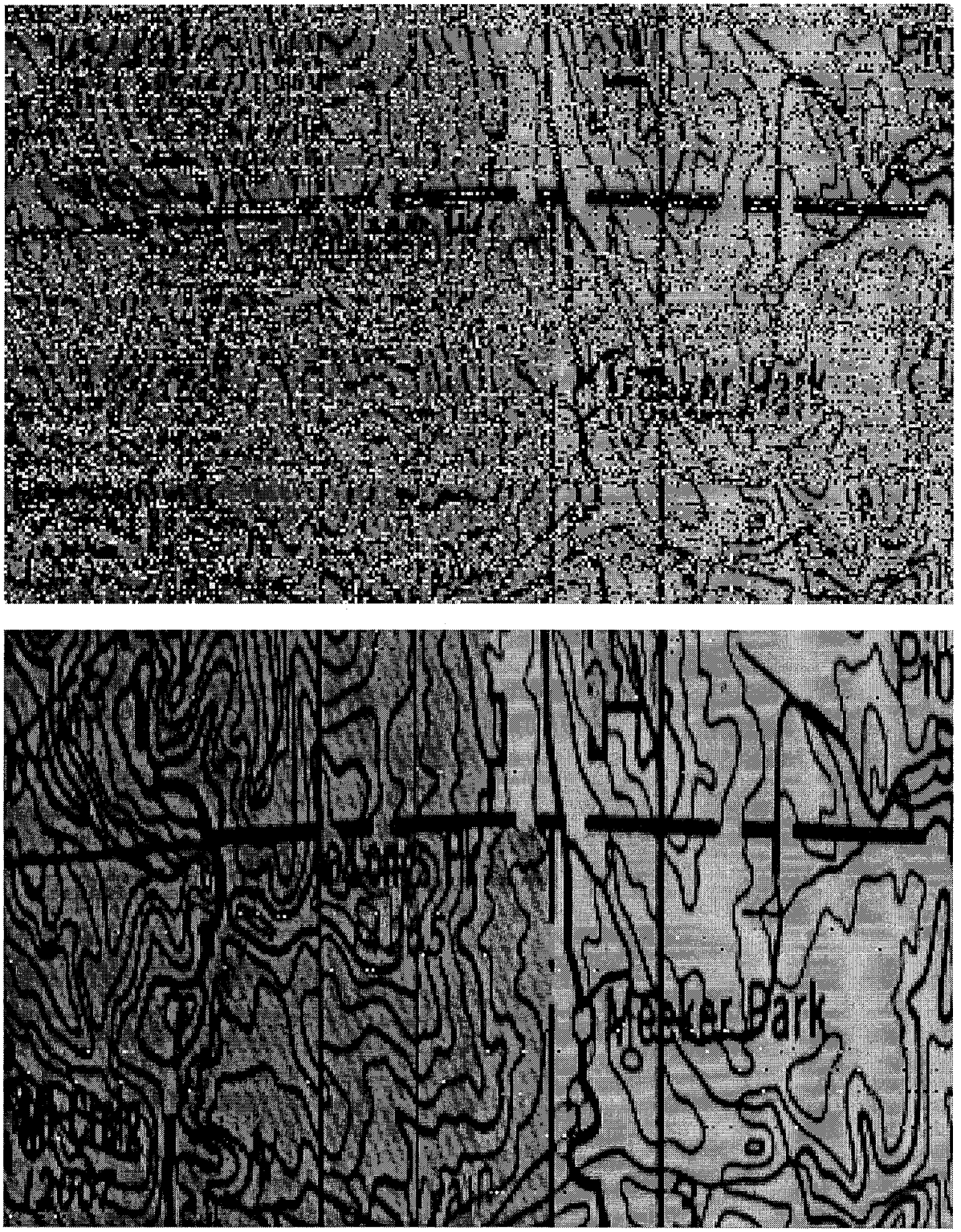

Figure A.6.4. PCM image for 8-FSK. Top image represents class 2.0 [SNR=20 dB, SIR=20 dB, SER=3.1e-1, BER=1.6e-1] and bottom image represents class 5.0 [SNR=70 dB, SIR=40 dB, SER=4.1e-3, BER=1.6e-3].

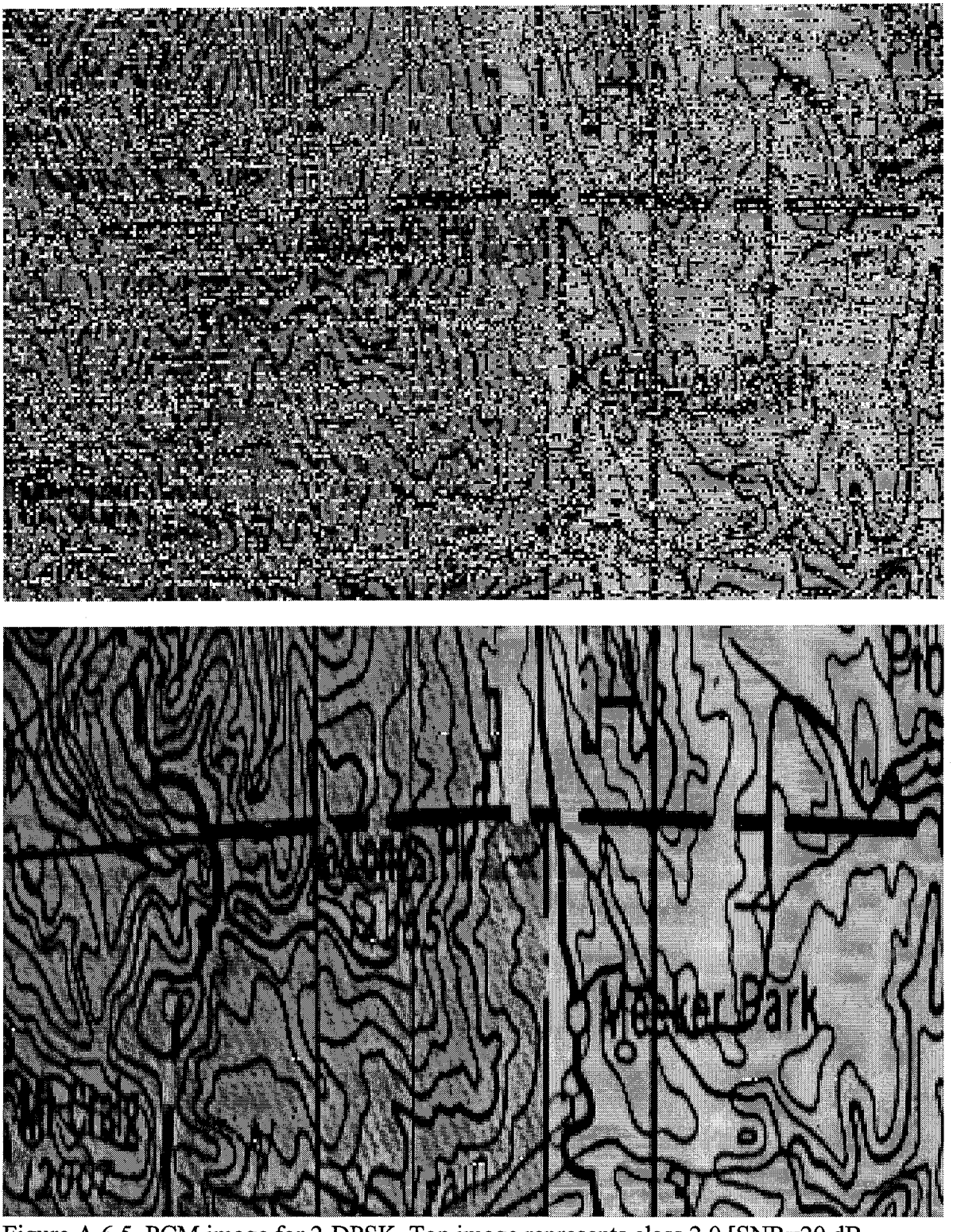

Figure A.6.5. PCM image for 2-DPSK. Top image represents class 2.0 [SNR=20 dB, SIR=5 dB, BER=1.9e-1] and bottom image represents class 5.0 [SNR=80 dB, SIR=60 dB, BER=4.0e-4].

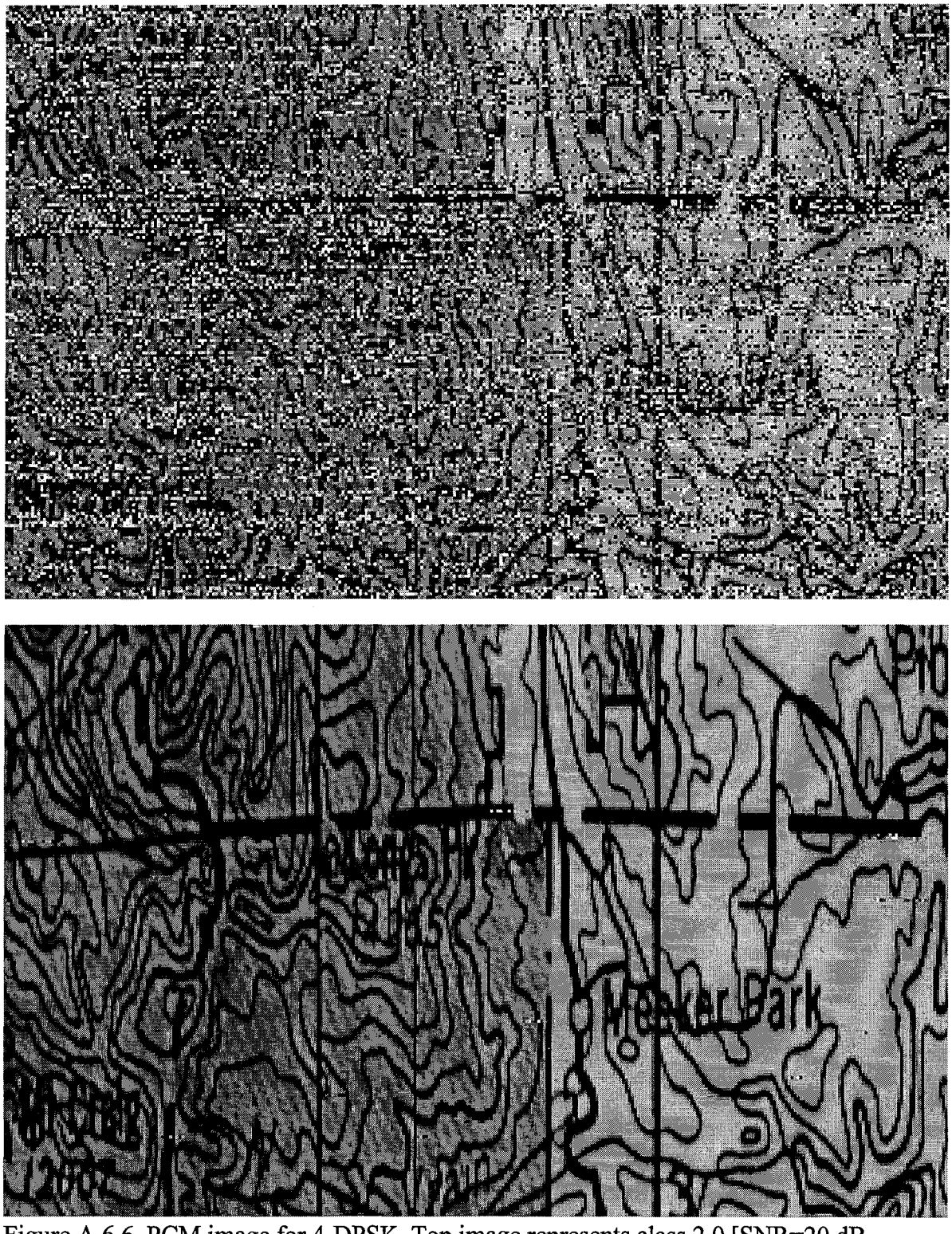

Figure A.6.6. PCM image for 4-DPSK. Top image represents class 2.0 [SNR=20 dB, SIR=10 dB, SER=3.1e-1, BER=2.2e-1] and bottom image represents class 5.0 [SNR=80 dB, SIR=50 dB, SER=1.3e-3, BER=8.0e-4].

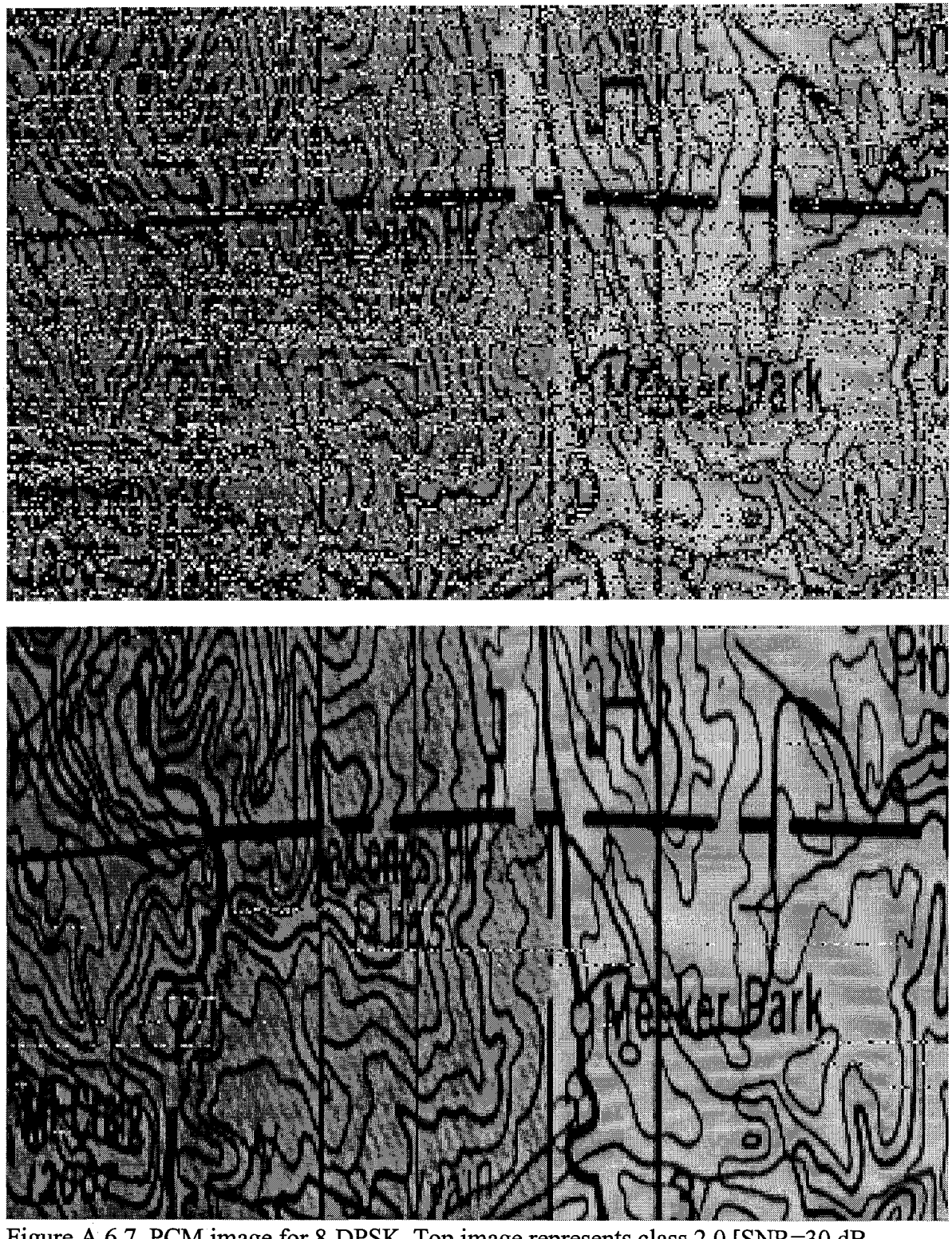

Figure A.6.7. PCM image for 8-DPSK. Top image represents class 2.0 [SNR=30 dB, SIR=15 dB, SER=2.6e-1, BER=1.4e-1] and bottom image represents class 5.0 [SNR=80 dB, SIR=50 dB, SER=5.5e-3, BER=2.7e-3].

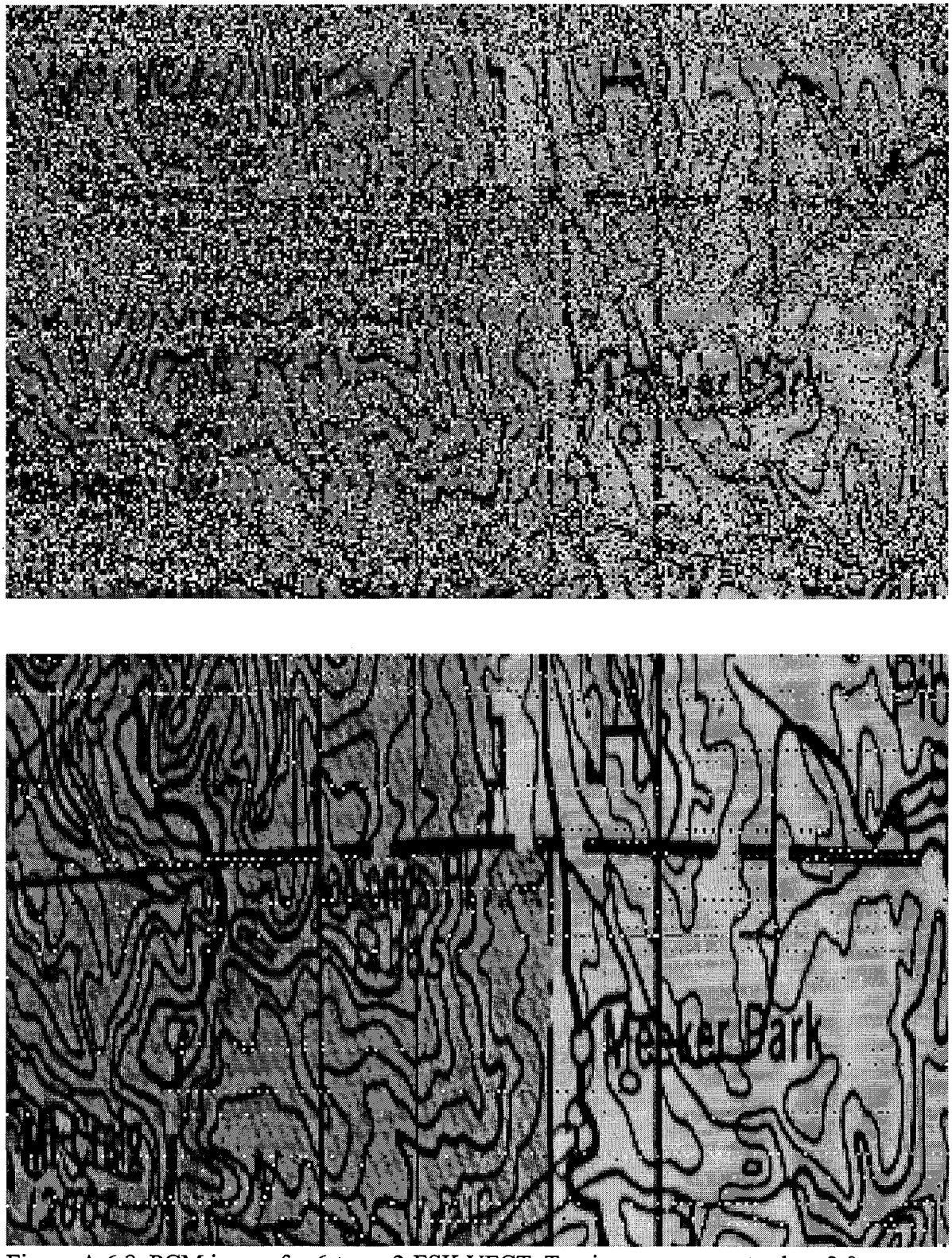

Figure A.6.8. PCM image for 6-tone, 2-FSK VFCT. Top image represents class 2.0 [SNR=20 dB, SIR=0 dB, BER=2.0e-1] and bottom image represents class 4.5 [SNR=80 dB, SIR=20 dB, BER=8.4e-3].

FORM NTIA-29
(4-80)

U.S. DEPARTMENT OF COMMERCE
NAT'L. TELECOMMUNICATIONS AND INFORMATION ADMINISTRATION

BIBLIOGRAPHIC DATA SHEET

	1. PUBLICATION NO.	2. Gov't Accession No.	3. Recipient's Accession No.

4. TITLE AND SUBTITLE
Radio Link Performance Prediction via Software Simulation

5. Publication Date

6. Performing Organization Code
NTIA/ITS

7. AUTHOR(S) E.A. Quincy, R.J. Achatz, M.G. Cotton, M.P. Roadifier, J.M. Ratzloff

9. Project/Task/Work Unit No.

8. PERFORMING ORGANIZATION NAME AND ADDRESS
NTIA/ITS
325 Broadway
Boulder, CO 80303-3328

10. Contract/Grant No.

11. Sponsoring Organization Name and Address
NTIA
1401 Constitution Ave, NW
Washington, DC 20230

12. Type of Report and Period Covered

13.

14. SUPPLEMENTARY NOTES

15. ABSTRACT *(A 200-word or less factual summary of most significant information. If document includes a significant bibliography or literature survey, mention it here.)*

The subjective quality of speech and image information, transmitted over a high frequency radio link impaired with varying levels of interference, has been evaluated using software simulation. The high frequency radio link was also degraded by frequency-selective multipath and non-Gaussian noise. During radio link signal simulation an error sequence, determined from a comparison of transmitted and received bits, was collected. Next digitized speech and image information was distorted by the error sequence. Last, the quality of the distorted speech and image information was subjectively evaluated. This process was repeated for a large number of interference conditions. The same process can be used to show how multipath and non-Gaussian noise affects speech and image quality. Other wireless applications such as personal communications service and wireless local area networks can be analyzed in the same way using radio channel measurements and models made by the Institute for Telecommunication Sciences.

16. Key Words *(Alphabetical order, separated by semicolons)*

Keywords: Digital modulation, radio link, radio channel, multipath, non-Gaussian noise, interference, bit error, speech coding, image coding, speech quality, image quality, software simulation.

17. AVAILABILITY STATEMENT	18. Security Class. *(This report)*	20. Number of pages
☐ UNLIMITED.		69
☐ FOR OFFICIAL DISTRIBUTION.	19. Security Class. *(This page)*	21. Price:

*USGPO 1999-0-573-020/40154